Model Independent Extraction of New Physics from Hadronic Uncertainties in $B \to K^* \ell^+ \ell^-$ Decay

By

Diganta Das

PHYS10200804004

The Institute of Mathematical Sciences, Chennai

A thesis submitted to the
Board of Studies in Physical Sciences

In partial fulfillment of requirements
For the Degree of

DOCTOR OF PHILOSOPHY

of

HOMI BHABHA NATIONAL INSTITUTE

May, 2013

Homi Bhabha National Institute

Recommendations of the Viva Voce Board

As members of the Viva Voce Board, we certify that we have read the dissertation prepared by Diganta Das entitled "Model Independent Extraction of New Physics from Hadronic Uncertainties in $B \to K^* \ell^+ \ell^-$ Decay", and recommend that it maybe accepted as fulfilling the dissertation requirement for the Degree of Doctor of Philosophy.

_____ Date:
Chair-

_____ Date:
Convener/Guide-

_____ Date:
Member 1-

_____ Date:
Member 2-

_____ Date:
Member 3-

Final approval and acceptance of this dissertation is contingent upon the candidate's submission of the final copies of the dissertation to HBNI.

I hereby certify that I have read this dissertation prepared under my direction and recommend that it may be accepted as fulfilling the dissertation requirement.

Date:

Place: Guide

STATEMENT BY AUTHOR

This dissertation has been submitted in partial fulfillment of requirements for an advanced degree at Homi Bhabha National Institute (HBNI) and is deposited in the Library to be made available to borrowers under rules of the HBNI.

Brief quotations from this dissertation are allowable without special permission, provided that accurate acknowledgment of source is made. Requests for permission for extended quotation from or reproduction of this manuscript in whole or in part may be granted by the Competent Authority of HBNI when in his or her judgment the proposed use of the material is in the interests of scholarship. In all other instances, however, permission must be obtained from the author.

Diganta Das

DECLARATION

I, hereby declare that the investigation presented in the thesis has been carried out by me. The work is original and has not been submitted earlier as a whole or in part for a degree / diploma at this or any other Institution / University.

Diganta Das

ACKNOWLEDGEMENTS

I would like to thank my supervisor, Prof. Rahul Sinha, for his constant guidance and supervision. I thank him for the way he led me towards the completion of this thesis. His continuous encouragement at all levels of difficulties that appeared during the course of my PhD work inspired me to work hard. He interacted with me quite actively and freely. I am very fortunate to have received his sincere and affectionate guidance. He was always patient, and ensured that I understood every subtle point. And more than anything else, I am extremely grateful to him for his patience and understanding towards me.

I would like to thank Prof. B. Ananthanarayan for giving me the opportunity to work with him and numerous helps that I received from him. I have discussed a lot on several intricate physics issues and clarified my doubts, whenever it was required. Discussions with him are always very enlightening, be it a face-to-face discussion or over Google-chat. I have always find it inspiring how he presents his ideas with clarity. His methods of identifying and working through research problems and excellent collaborative skills have been exemplary to me for going ahead in the world of research. I have experienced very happy, enjoyable and friendly moments with him which I will cherish all my life

I consider myself extremely fortunate to get the opportunity to collaborate with to Prof. Irinel Caprini. It has been an excellent experience for me to come across her knowledge, deep insight to physics and rigorous way of thinking during the last years of my Ph.D.

I thank my dear friend Dr. I. Sentitemsu Imsong for a wonderful collaboration. He was always very supportive and helped me out whenever I faced any problem. It was a great pleasure to learn a lot of things from him.

I would like to convey my thanks to my collaborators Gauhar Abbas and Rupak Dutta.

I would like to thank my co-supervisor Prof. D. Indumathi for teaching me particle physics. I am also thankful to Prof. Balachandran Sathiapalan for teaching me a wonderful course on

quantum field theory.

Apart from my collaborators and teachers I had the opportunity to learn many topics on physics from Prof. M. V. N. Murthy, Prof. Rahul Basu, and Prof. S. Gopalakrishna and Nita Sinha. They have guided me with their thoughtful suggestions at different stages of my work.

I have always found immense learning opportunity at IMSc due to the presence of many fellow students and friends. Thanks to Tanumoy and Dibyakarupa and Soumya for always helping me out with various problems whenever I approached them and for giving me company. Thanks to Rusa for wonderful collaboration. Thanks to Jahanur for keeping up with my personal idiosyncrasies for all these years at 113.

The friends who have made my stay at IMSc so enjoyable are Abhra, Sudhir, Neeraj, Gaurav, Tuhin, Tanmoy, Ramchandra, KK. I thank Abhra, Gaurav, Sudhir, Tuhin, Neeraj for teaching me a thing or two with the racquet and always being there as my toughest opponent at the other side of the net.

SYNOPSIS

The phenomena of meson decay and meson anti-meson mixing provide an excellent laboratory to test the Standard Model (SM) predictions and for indirect searches of physics beyond the SM also known as New Physics (NP). The effective Hamiltonian of meson decay and mixing is described in terms of Wilson coefficients and dimension six four quark local operators. The Wilson coefficients include the short distance QCD correction effects to the local operators and are calculable in perturbation theory. The hadronic matrix elements of the four quark local operators between the initial and the final state meson are parametrized in terms of form factors. The form factors are non-perturbative hadronic quantities, and hence are poorly known. New Physics may contribute virtually to meson decay and mixing through loop diagrams like the box and the penguin diagrams. Indirect searches for NP involve comparison of theoretically calculated observables related to the decay or mixing, with precision measurements of the observables in experiments, and the observed discrepancies are referred to as NP signal. However, searches of NP are often hindered by hadronic uncertainties. In addition to the poor knowledge of form factors, the significant part of hadronic uncertainties constitutes of 'non-factorizable' effects. In this thesis using the semi-leptonic decay $B \to K^* \ell^+ \ell^-$ we have shown how NP signal can be extracted to all orders in α_s in perturbation theory, including 'non-factorizable' corrections at leading order in Λ_{QCD}/m_b in heavy quark expansion. We have also derived relations between various hadronic form factor ratios and observables independent of any Wilson coefficients, which enable us to tests these ratios in experiments.

The $B \to K^* \ell^+ \ell^-$ decay is regarded as a very important mode for new physics search. Several different experiments Belle, Babar, CDF and LHCb have studied this mode. These experiments have provided valuable data as a function of the dilepton invariant mass squared q^2 by studying uni-angular distributions. Each of these four experiments have measured the partial branching fraction in chosen q^2 bins by preforming a complete angular integration. By studying the angular distribution of the direction of the lepton in an appropriately chosen frame

these experiments have also measured the well known forward-backward asymmetry $A_{\rm FB}$ and the longitudinal polarization fraction F_L in terms of integrated dilepton invariant mass squared regions of q^2. The CDF and LHCb collaborations have in addition performed an angular study of the azimuthal angle defined as the angle between the planes formed by the leptons and the decay products of K^* i.e. K, π. Recently the LHCb has also measured the zero crossing point of the forward-backward asymmetry which is consistent with the standard model expectation. Future experimental studies by LHC-B and Belle II will enable the study of this mode with significantly larger statistics making possible the analysis with multi-angular distributions and the measurement of all the observables.

The thesis is based on the two papers mentioned below and is divided in six chapters. In Chapter 1 we have given a very brief introduction to the theoretical tools needed to study B physics. After a brief introduction of the standard model of electrowek interaction we have discussed the Yukawa Lagrangian which encodes the entire flavour structure of the standard model. The typical energy scale of B decay is ~ 5 GeV where as the standard model contains significantly higher energy scales like the mass of the top quarks and the mass of the W bosons. Therefore the phenomenology of B decays are described in an effective field theory approach called the Operator Product Expansion (OPE). In our work the hadronic estimates are based on the heavy quark symmetry which is discussed at the end of the chapter.

The theoretical framework of $B \to K^* \ell^+ \ell^-$ decay is described in Chapter 2. At the quark level the decay is given by $\bar{b} \to \bar{s} \ell^+ \ell^-$ flavour changing neutral current transition and the effective Hamiltonian is described in terms of three Wilson coefficients $C_7^{\rm eff}$, $C_9^{\rm eff}$ and C_{10} and six form factors $V(q^2), A_{1,2}(q^2), T_{1,2,3}(q^2)$. The values of these form factors are not accurately known due to hadronic uncertainties. In the limit of heavy quark mass $m_b \to \infty$ and large recoil of the K^* meson all the form factors can be expressed in terms of two soft form factors $\xi_\perp(q^2)$ and $\xi_\parallel(q^2)$ and there arise various symmetry relations between them. These symmetry relations however are broken due to radiative corrections and 'non-factorizable' corrections. Our key observation is that the ratios $V(q^2)/A_1(q^2)$ and $T_2(q^2)/T_1(q^2)$ are free from $\xi_\perp(q^2)$ and $\xi_\parallel(q^2)$ to all orders in α_s in perturbation theory including the 'non-factorizable' corrections and

at leading order Λ_{QCD}/m_b in heavy quark expansion . In the low recoil region of the K^* meson there arise additional symmetries which imply $V(q^2)/A_1(q^2) = T_2(q^2)/T_1(q^2)$.

In Chapter 3 we have described the angular distribution of $B \to K^*\ell^+\ell^-$ decay and we have shown how the multitude of observables can be extracted from the angular distribution. In the semileptonic decay $B(p) \to K^*(k)\ell^+(q_1)\ell^-(q_2)$ decay the light vector meson K^* decays resonantly to $K(k_1)\pi(k_2)$. The decay is described by four kinematic variables; lepton pair invariant mass squared $q^2 = (q_1 + q_2)^2$, the angle between the decay planes formed by $K\pi$ and $\ell^+\ell^-$ denoted by ϕ, the angle θ_l between ℓ^- and the $+z$ axis in which the K^* is moving and the angle θ_K that K makes with the $+z$ direction. There are six transversity amplitudes corresponding to each of three polarization states of K^* meson with two chirality of the leptonic current. These amplitudes are written as $\mathcal{A}^{L,R}_{0,\|,\perp}$ where $0, \|, \perp$ are the three polarization states of K^* and L, R correspond to the left and right chirality of the leptonic current. In our analysis we have assumed that the lepton mass is zero and we have also neglected the tiny CP violation. In addition to the branching fraction Γ_f, the angular distribution enables a multitude of observables to be extracted; these include the longitudinal helicity fraction F_L, perpendicular helicity fraction $F_\perp$, parallel helicity fraction $F_\|$, the forward-backward asymmetry $A_{\rm FB}$ and angular asymmetries A_4 and A_5. The three helicity fractions are related by $F_L + F_\perp + F_\| = 1$ resulting in six independent observables in the limit of vanishing lepton mass and CP violation.

In Chapter 4 we have developed a model independent framework to study new physics effects. We write the six transversity amplitudes $\mathcal{A}^{L,R}_\lambda$ in the most general form, in terms of form factors $\mathcal{F}_\lambda$ and $\widetilde{\mathcal{G}}_\lambda$ as $\mathcal{A}^{L,R}_\lambda = C_{L,R}\mathcal{F}_\lambda - \widetilde{\mathcal{G}}_\lambda$, where $C_{L,R} = C_9 \mp C_{10}$. Here the Wilson coefficient $C_9^{\rm eff}$ is replaced by C_9 once the higher order corrections are taken into account. The form factors $\mathcal{F}_\lambda$ and $\widetilde{\mathcal{G}}_\lambda$ are related to the well known form factors $V(q^2), A_{1,2}(q^2)$ and $T_{1,2,3}(q^2)$. At the leading order in Λ_{QCD}/m_b in the heavy quark expansion the Wilson coefficient $C_7^{\rm eff}$ can not be distinguished from the form factor $\widetilde{\mathcal{G}}_\lambda$ due to α_s corrections and 'non-factorizable' corrections. Hence there are eight theoretical parameters; the two Wilson coefficients C_9, C_{10} and six form factors and only six independent observables $\Gamma_f, F_L, F_\perp, A_{\rm FB}, A_4, A_5$. Using the six observables the six theoretical parameters can be expressed in terms of the observables if two

reliably evaluated theoretical quantities are taken as inputs. In Chapter 2 we have identified the ratios $\mathsf{P}_1 = \mathcal{F}_\perp/\mathcal{F}_\parallel$ and $\mathsf{P}'_1 = \widetilde{\mathcal{G}}_\perp/\widetilde{\mathcal{G}}_\parallel$ that are free from α_s corrections to all orders in perturbation theory including 'non-factorizable' corrections at leading order in Λ_{QCD}/m_b in heavy quark expansion. Taking P_1 and P'_1 as theoretically reliable inputs we have expressed the Wilson coefficients C_9 and C_{10} and $\widetilde{\mathcal{G}}_\parallel$ in terms of F_L, $F_\perp$, $A_{\rm FB}$ and form factor $\mathcal{F}_\parallel$ which enables us to measure these theoretical quantities in experiment. As discussed in the thesis these solutions have very important implications on the correlations of different observables. Though the expressions of C_9 and C_{10} are not completely free from hadronic uncertainties due to the presence of form factor $\mathcal{F}_\parallel$ in the solutions, their ratio $R = C_9/C_{10}$ is free from any form factor and can be measured experimentally. The ratio R is known up to next-to-next-leading-logarithmic (NNLL) order. If the ratio R is taken as input, then there arise a important constraint between observables $A_{\rm FB}$ and F_L; $-3(1-F_L)T_-/4 \le A_{\rm FB} \le 3(1-F_L)T_+/4$ where, $T_\pm \approx 1$. The forward backward asymmetry $A_{\rm FB}$ is expressed in terms of helicity fractions F_L, $F_\perp$ and the ratios P_1 and P'_1, enabling measurement of $A_{\rm FB}$ in terms of helicity fractions only. Moreover we have derived stringent constraint between the helicity fractions F_L and $F_\perp$ based on the fact that $A_{\rm FB}$ is real.

In the limit of no *CP* violation all the Wilson coefficients are real. This leads to various constraints among observables such as $4F_\parallel F_\perp \ge (16/9)A_{\rm FB}^2$. We have derived three such relations. These relations are solely in terms of observables and do not involve any form factors and Wilson coefficients. Hence the violation of these relations will be clean signals of new physics.

There exist two additional sets of solutions of the Wilson coefficients involving other observables and require the introduction of four additional form factor ratios as inputs; $\mathsf{P}_2 = \mathcal{F}_\perp/\mathcal{F}_0$, $\mathsf{P}'_2 = \widetilde{\mathcal{G}}_\perp/\widetilde{\mathcal{G}}_0$, $\mathsf{P}_3 = \mathcal{F}_\perp/(\mathcal{F}_\parallel + \mathcal{F}_0)$ and $\mathsf{P}'_3 = \widetilde{\mathcal{G}}_\perp/(\widetilde{\mathcal{G}}_\parallel + \widetilde{\mathcal{G}}_\parallel)$. These ratios of form factors are not theoretically reliably calculated since they depend on soft form factors $\xi_\perp(q^2)$ and $\xi_\parallel(q^2)$. We have expressed these four ratios in terms theoretically reliably calculated ratios P_1 and P'_1 and observables. In addition we have also shown that the form factors ratio P_1 can be expressed as $\mathsf{P}_1 = -\sqrt{F_\perp}/\sqrt{F_\parallel}$ at the zero crossing point of the forward backward

asymmetry $A_{\rm FB}$. We have presented two more relations that relate P_2 and P_3 also in terms of observables at the zero crossing points A_5 and $A_{\rm FB} + \sqrt{2}A_5$ respectively. The three sets of solutions imply a very important relation between the observables; $A_4 = (8A_5A_{\rm FB}/9\pi F_\perp) + \sqrt{2}\Big(\sqrt{F_LF_\perp - (8/9)A_5^2}\,\sqrt{F_\parallel F_\perp - (4/9)A_{\rm FB}^2}\Big)/\pi F_\perp$. We end the chapter by discussing the low energy approximation of various relations. We have shown that these relations can be used to test the low energy approximation of form factor calculations.

In Chapter 5 we have presented a numerical analysis in comparing it with the current experimental data on the $B \to K^*\ell^+\ell^-$ mode. We have also compared our approach with the theoretical approach available in the literature. The conclusion is given in Chapter 6.

In this thesis we have presented various relations among observables without involving any form factors and Wilson coefficients The violation of these relations will be a clean signals of new physics. In addition we have derived various relations between ratios of form factors and observables that are free from any Wilson coefficients.

Refereed Journal Publications.

- **Parametrization-free determination of the shape parameters for the pion electromagnetic form factor.**

  B. Ananthanarayan, I. Caprini, Diganta Das, I. Sentitemsu Imsong.

  Eur. Phys. J. C , 73:2520 (2013).

  arXiv:1302.6373 [hep-ph]

- **Model independent bounds on the modulus of the pion form factor on the unitarity cut below the $\omega\pi$ threshold**

  B. Ananthanarayan, I. Caprini, Diganta Das, I. Sentitemsu Imsong.

  Eur. Phys. J. **72**, *2192 (2012).*

  arXiv:1209.0379 [hep-ph]

- **Consistency tests of AMPCALCULATOR and chiral amplitudes in $SU(3)$ Chiral Perturbation Theory: A tutorial based approach.**

  B. Ananthanarayan, Diganta Das, I. Sentitemsu Imsong.

  Eur. Phys. J. A **48**, *140 (2012).*

  arXiv:1207.2956 [hep-ph]

- **New Physics Effects and Hadronic Form Factor Uncertainties in $B \to K^* \ell^+ \ell^-$.**

  Diganta Das, Rahul Sinha.

  Phys. Rev. D **86**, *056006 (2012).*

  arXiv:1205.1438 [hep-ph]

- **Tadpole cancellation in top-quark condensation.**

  Diganta Das, Kosuke Odagiri.

  Phys. Rev. D **86**, *055019 (2012).*

  arXiv:1201.3968 [hep-ph]

- **Measuring the Magnitude of the Fourth-Generation CKM4 Matrix Element $V_{t'b'}$.**

  Diganta Das, David London, Rahul Sinha, Abner Soffer.

Phys. Rev. D **82**, *093019 (2010).*

arXiv:1008.4925 [hep-ph]

Preprint.

- **Isolating New Physics Effects from Hadronic Form Factor Uncertainties in $B \to K^* \ell^+ \ell^-$.**

  Diganta Das, Rahul Sinha.

  arXiv:1202.5105 [hep-ph]

The thesis is based on the following papers.

- **New Physics Effects and Hadronic Form Factor Uncertainties in $B \to K^* \ell^+ \ell^-$.**

  Diganta Das, Rahul Sinha.

  Phys. Rev. D **86**, *056006 (2012).*

  arXiv:1205.1438 [hep-ph]

- **Isolating New Physics Effects from Hadronic Form Factor Uncertainties in $B \to K^* \ell^+ \ell^-$.**

  Diganta Das, Rahul Sinha.

  arXiv:1202.5105 [hep-ph]

Contents

List of Figures

List of Tables

Chapter 1

Introduction

1.1 The Standard Model of Electroweak Interaction.

The standard model of electroweak interaction is a $SU(2)\otimes U(1)_Y$ [1, 2, 3, 4] gauge theory which successfully describes weak and the electromagnectic interaction in a unified framework. The particle spectrum of the standard model comprises of three generations of quarks and leptons collectively called the fermions. The left handed leptons and quarks are arranged in a $SU(2)$ doublets as,

$$\begin{pmatrix} \nu_e \\ e^- \end{pmatrix}_L \quad \begin{pmatrix} \nu_\mu \\ \mu^- \end{pmatrix}_L \quad \begin{pmatrix} \nu_\tau \\ \tau^- \end{pmatrix}_L \tag{1.1}$$

$$\begin{pmatrix} u' \\ d' \end{pmatrix}_L \quad \begin{pmatrix} c' \\ s' \end{pmatrix}_L \quad \begin{pmatrix} t' \\ b' \end{pmatrix}_L . \tag{1.2}$$

and the right handed quarks and leptons are arranged in singlets of $SU(2)$ as,

$$e_R^-,\ \mu_R^-,\ \tau_R^-,\ (\bar{\nu_e})_R,\ (\bar{\nu_\mu})_R,\ (\bar{\nu_\tau})_R \tag{1.3}$$

$$u'_R,\ c'_R,\ t'_R,\ d'_R,\ s'_R,\ b'_R \tag{1.4}$$

Such organization of quarks and leptons under $SU(2)$ automatically takes care of the parity violation in nature [5, 6, 7, 8]. The mediators of the electroweak interaction are the four

massless gauge bosons $W^1_\mu, W^2_\mu, W^3_\mu$ and B_μ which correspond to the four generators of the $SU(2) \otimes U(1)_Y$ group. The gauge bosons acquire masses through the mechanism of spontaneous symmetry breaking [9, 10, 11, 12] that breaks the $SU(2) \otimes U(1)_Y$ symmetry to $U(1)_Q$ symmetry. The outcome of the spontaneous symmetry breaking is a neutral scalar particle called the Higgs. After spontaneous symmetry breaking the three massive gauge bosons of weak interaction are W^+, W^-, Z and the massless gauge boson of electromagnetic interaction is γ. They weak-hypercharge Y is related to the electric charge Q by $Q = I_3 + Y/2$, where I_3 is the third component of isospin. In (1.2) and (1.4) the primes indicate that the quarks are massless. The quarks and the leptons become massive due their interaction with the Higgs field. The part of the Lagrangian that describes this interaction is called the Yukawa Lagrangian. In Sec. 1.2 we have discussed the Yukawa Lagrangian for quarks in great details.

The interaction part of the standard model Lagrangian for quarks and leptons is written as,

$$\mathcal{L}_{int} = \mathcal{L}_{CC} + \mathcal{L}_{NC},$$

where the subscript $\mathcal{L}_{CC}$ describes the charged current interactions and $\mathcal{L}_{NC}$ describes the neutral current interaction of quarks with the gauge bosons. The $\mathcal{L}_{CC}$ and $\mathcal{L}_{NC}$ can be written as,

$$\mathcal{L}_{CC} = \frac{g_2}{2\sqrt{2}}(J^+_\mu W^{+\mu} + J^-_\mu W^{-\mu}) \tag{1.5}$$

$$\mathcal{L}_{NC} = eJ^{em}_\mu + \frac{g_2}{2\cos\theta_W} J^0_\mu Z^\mu \tag{1.6}$$

where, e is the electric charge, g is the $SU(2)$ gauge coupling, θ_W is the Weinberg angle. The currents $J^\pm_\mu$, J^{em}_μ and J^0_μ are written in terms of massless quarks and lepton fields as,

$$\begin{aligned} J^+_\mu &= \frac{1}{2}\bar{u'}\gamma_\mu(1-\gamma_5)d' + \frac{1}{2}\bar{c'}\gamma_\mu(1-\gamma_5)s' + \frac{1}{2}\bar{t'}\gamma_\mu(1-\gamma_5)b' \\ &+ \frac{1}{2}\bar{\nu_e}\gamma_\mu(1-\gamma_5)e + \frac{1}{2}\bar{\nu_\mu}\gamma_\mu(1-\gamma_5)\mu + \frac{1}{2}\bar{\nu_\tau}\gamma_\mu(1-\gamma_5)\tau \end{aligned} \tag{1.7}$$

$$J^{em}_\mu = \sum_f q_f \bar{f}\gamma_\mu f, \tag{1.8}$$

$$
\begin{aligned}
J^0_\mu &= \sum_f \bar{f}\gamma_\mu(v_f - I^f_3\gamma_5)f, \quad \text{with} \\
v_f &= I^f_3 - 2q_f \sin^\theta_W .
\end{aligned}
\tag{1.9}
$$

Here f denotes the fermions, q_f is the charge of the fermion in the units of electric charge e, I^f_3 is the third component of isospin of fermion f.

1.2 Flavour Physics.

In the previous section we have introduced six flavours of quarks and leptons each of which are arranged in three generations. Flavour physics in general describes the interactions between these different generations of quarks and leptons. Within the standard model, the parameters of the flavour physics are the masses of six quarks and six leptons, three quark mixing angles and a phase and three lepton mixing angles and a phase. It is the Yukawa Lagrangian that completely fix the flavour structure of the standard model. We will discuss only the Yukawa Lagrangian for the quarks. In (1.2) and (1.4) the quarks fields are written in the interaction basis which means they are massless. The Lagrangian that give masses to the quarks and leptons is called the Yukawa Lagrangian $\mathcal{L}_{Yukawa}$. The Yukawa Lagrangian for the quarks is written as,

$$
\mathcal{L}_{Yukawa} = m^{ij}_{(d)}(\bar{u}'_i, d'_i)_L \begin{pmatrix} \phi^+ \\ \phi^0 \end{pmatrix} d_{jR} + m^{ij}_{(u)}(\bar{u}'_i, d'_i)_L \begin{pmatrix} -\bar{\phi}^0 \\ \phi^- \end{pmatrix} u_{jR} + \text{h.c}, \tag{1.10}
$$

Here, $i, j = 1, 2, 3$ correspond to the three generations of quarks. The matrices $m^{ij}_{u/d}$ are the coupling of the i'th and j'th quarks of the up or down type. Here we have introduced the Higgs fields,

$$
\phi = \begin{pmatrix} \phi^+ \\ \phi^0 \end{pmatrix}, \qquad \phi_c = \begin{pmatrix} -\bar{\phi}^0 \\ \phi^- \end{pmatrix}
$$

The spontaneous symmetry breaking occur when the ϕ^0 acquire a vacuum expectation value v:

$$\phi = \frac{1}{\sqrt{2}}\begin{pmatrix} 0 \\ v+\eta \end{pmatrix}, \qquad \phi_c = -\frac{1}{\sqrt{2}}\begin{pmatrix} v+\eta \\ 0 \end{pmatrix}$$

where, η is the fluctuation around the minimum v. After the spontaneous symmetry breaking the Yukawa Lagrangian reads as,

$$\mathcal{L}_{Yukawa} = \frac{v}{\sqrt{2}}\left(\overline{u}_L^i h_{(u)}^{ij} \overline{u}_R^j + \overline{d}_L^{\prime i} h_{(d)}^{ij} \overline{d}_R^{\prime j}\right) + \text{h.c.} \tag{1.11}$$

From the above Lagrangian the mass terms of the quarks can be written as,

$$M_{(u)}^{ij} = \frac{v}{\sqrt{2}} h_{(u)}^{ij}, \qquad M_{(d)}^{ij} = \frac{v}{\sqrt{2}} h_{(d)}^{ij} \tag{1.12}$$

The mass matrices $M_{(u)}^{ij}$ and $M_{(d)}^{ij}$ are neither symmetric nor Hermitian and also not necessarily diagonal. These can be diagonalized using four bi-unitary matrices $U_{L,R}$ and $D_{L,R}$ as,

$$\mathcal{M}_{(u)} = U_L^+ M_{(u)} U_R, \qquad \mathcal{M}_{(d)} = U_L^+ M_{(d)} U_R$$

The mass eigenstates can now be related to the interaction eigenstates as,

$$u_{L,R}^i = (U_{L,R}^+)^{ij} u_{L,R}^{\prime j} \tag{1.13}$$

$$d_{L,R}^i = (D_{L,R}^+)^{ij} d_{L,R}^{\prime j} \tag{1.14}$$

In terms of the mass eigenstates the charge currents become

$$j_\mu^+ = \overline{u}_L^i V^{ij} d_L^j \tag{1.15}$$

where, $V = U_L^+ D_L$ is called the Cabbibo–Kobayashi-Maskawa (CKM) matrix [13, 14, 4]. By construction the CKM matrix is unitary, since the matrices $U_{L,R}$ and $D_{L,R}$ are unitary. This

imply that,

$$\sum_j V_{ij} V_{jk}^* = \delta_{ik}$$

The unitarity relation that is particularly important for B decays is written as,

$$V_{ud} V_{ub}^* + V_{cd} V_{cb}^* + V_{td} V_{tb}^* = 0 \tag{1.16}$$

In this relation the CKM matrix elements V_{ub}, V_{cb} and V_{td} are under extensive study at present. It represents a triangle in the complex plane which has three sides of magnitudes $|V_{ud}V_{ub}^*|$, $|V_{cd}V_{cb}^*|$, $|V_{td}V_{tb}^*|$ and three angles α, β and γ which are defined as [15],

$$\alpha = \arg\Big(-\frac{V_{td}V_{tb}^*}{V_{ud}V_{ub}^*}\Big) \tag{1.17}$$

$$\beta = \arg\Big(-\frac{V_{cd}V_{cb}^*}{V_{td}V_{td}^*}\Big) \tag{1.18}$$

$$\gamma = \arg\Big(-\frac{V_{ud}V_{ub}^*}{V_{cd}V_{cb}^*}\Big) \tag{1.19}$$

The sum of these three angles is $\alpha + \beta + \gamma = 180°$. The CKM matrix V can be parametrized in different ways. The standard parametrization used by the Particle Data Group is [16]

$$V = \begin{pmatrix} c_{12}c_{13} & s_{12}c_{13} & s_{13}e^{-i\delta_{13}} \\ -s_{12}c_{23} - c_{12}s_{23}s_{13}e^{i\delta_{13}} & c_{12}c_{23} - s_{12}s_{23}s_{13}e^{i\delta_{13}} & s_{23}c_{13} \\ s_{12}s_{23} - c_{12}c_{23}s_{13}e^{i\delta_{13}} & -c_{12}s_{23} - s_{12}c_{23}s_{13}e^{i\delta_{13}} & c_{23}c_{13} \end{pmatrix}, \tag{1.20}$$

Here $s_{ij} = \sin\theta_{ij}$, $c_{ij} = \cos\theta_{ij}$ and δ is the CP violating phase. The term $s_{13} \sim O(10^{-3})$ and $s_{12} \sim O(10^{-2})$ and c_{13} and c_{23} are ≈ 1. Experimentally it is found that $s_{13} << s_{23} << s_{12} << 1$. Based on this hierarchy there exist another parametrization that is often used in B physics known as Wolfenstein parametrization, which exploits the aforementioned experimental information. The

CKM elements are expanded in small parameter $\lambda = |V_{us}| = 0.22$. We can define [17, 18, 19],

$$\begin{aligned} s_{12} &= \lambda = \frac{|V_{us}|}{\sqrt{|V_{ud}|^2 + |V_{us}|^2}}, \quad s_{23} = A\lambda^2 = \lambda\left|\frac{V_{cb}}{V_{us}}\right| \\ s_{13}e^{i\delta} &= V_{ub}^* = A\lambda^3(\rho + i\eta) = \frac{A\lambda^3(\bar{\rho} + i\bar{\eta})\sqrt{1 - A^2\lambda^4}}{\sqrt{1-\lambda^2}[1 - A^2\lambda^4(\bar{\rho} + i\bar{\eta})]} \end{aligned} \tag{1.21}$$

With the above relations it is ensured that $\bar{\rho} + i\bar{\eta} = -(V_{ud}V_{ub}^*/V_{cd}V_{cb}^*)$ is independent of phase convention. The unitarity relation is valid to all orders in λ if the CKM matrix is written in terms of $\lambda, A, \bar{\rho}$ and $\bar{\eta}$. Alternatively, the CKM matrix can also be parametrized in terms of A, λ, ρ, η as,

$$V = \begin{pmatrix} 1 - \frac{1}{2}\lambda^2 & \lambda & A\lambda^3(\rho - i\eta) \\ -\lambda & 1 - \frac{1}{2}\lambda^2 & A\lambda^2 \\ A\lambda^3(1 - \rho - i\eta) & -A\lambda^2 & 1 \end{pmatrix} + O(\lambda^4) \tag{1.22}$$

where, $\bar{\rho} = \rho(1 - \lambda^2/2 + \cdots)$ and $\bar{\eta} = \eta(1 - \lambda^2/2 + \cdots)$. It should be noted that in the above parametrization, known as Wolfenstein parametrization the the real part of the unitarity relation is restored up to order λ^3, and the imaginary part of the unitarity relation is restored up to order λ^5.

1.3 *B* physics in pursuit of New Physics.

Flavour physics has great potential to discover new physics beyond the standard model before new physics particles can be directly produced in colliders. There are many examples of such discoveries from the past. The existence of the charm quark was predicted by observing the smallness of the ratio $\Gamma(K_L \to \mu^+\mu^-)/\Gamma(K^+ \to \mu^+\nu)$ in the K meson decay and the value of ϵ_K led to the prediction of the third generation of quarks. The mass of the charm quark was predicted from the size of the $K_L - K_S$ mass differences $\Delta m_K = M_{K_L} - M_{K_S}$ and similarly the mass difference of the two B meson eigenstates Δm_B led to the successful prediction of the top mass. Flavour physics has thus played significant role in construction of the standard model. There are reasons to believe that the standard model is not the ultimate theory of nature and there are

physics beyond the standard model, referred to as new physics. In addition to the well known gauge hierarchy problem and naturalness problem [20, 21, 22, 23] of the standard model, there are motivations to search for physics beyond the standard model. For examples the amount of CP violation needed to explain the observed baryon asymmetry in the universe is less than what the CKM framework predicts. It therefore needs extra sources of CP violation that can only come from new physics. The observation of neutrino mass and oscillation is not accommodated in the standard model and needs physics beyond the standard model for explanation. At present there are several examples in flavor physics where the experimental data in various meson decay and mixing are not consistent with the standard model expectation. New physics models can be constructed to explain such discrepancies. Recently the D0 Collaboration observed [24] the semileptonic decays of B_s mesons and measured the like-sign dimuon charge asymmetry $A^b_{sl} = (-0.787 \pm 0.172(stat) + \pm 0.093(syst))$. The standard model predicts [25] $A^b_{sl} = (-0.028^{+0.005}_{-0.006})\%$. The experimental value deviates from theoretical calculations by 3.9σ standard deviations. On the other hand the A^b_{sl} depends on "wrong charge" asymmetries a^q_{sl} (where q is d or s quark). The recent measurements of $a^s_{sl} = (-1.08 \pm 0.72 \pm 0.17)\%$ by D0 [26] and $a^s_{sl} = (-0.24 \pm 0.54 \pm 0.33)\%$ by LHCb [27] are in agreement with the standard model expectation. This can be explained by physics beyond the standard model. Another example is from the charm sector. Based on the first observations by of $D^0 - \bar{D}^0$ oscillation by BaBar [28], Bell [29], the Heavy Flavor Averaging Group (HFAG) [30] has excluded the null hypothesis of mixing parameters $x = \Delta M/\Gamma$ and $y = \Delta\Gamma/2\Gamma$ at 10σ and presentss global averages $x = (6.5^{+1.8}_{-1.9}) \times 10^{-3}$ and $y = (7.4 \pm 1.2) \times 10^{-3}$.

In the past mainly the K system was studied to explore the physics of the quark flavour sector. Thanks to the efforts by Babar at SLAC, Belle at KEK and LHCb at CERN, the B mesons are now produced abundantly and is used to explore the quark flavour sector as well as new physics. The CP violation has already been established in the B system in $B^0_d \to J/\Psi K_S$ decay by the Belle [31, 32, 33, 34] and Babar [35, 36, 37, 38] experiments. Both at the theoretical and the experimental front B physics is important as it give insight to physics at short distances. The recent results from B-factories and LHCb has greatly improved our knowledge about the flavour structure of the standard model. These results present a strongly constrained

picture of the flavour sector with only tiny deviation from the standard model. Recent examples from the flavour factories constraining the flavour sector are: consistency of isospin asymmetry in $B \to K^* \mu^+ \mu^-$ [39] with the standard model calculation [40], the reduced discrepancy between $B \to \tau\nu$ and $\sin 2\beta$ from Belle results [41], agreement of the semileptonic asymmetry a_s^l with the standard model in LHCb measurements [42] and the absence of a large $B_s \mu^+ \mu^-$ [43, 44, 45, 46, 47] which is expected in some beyond standard model extensions [48, 49, 50]. Some new tensions in the flavour sector has also been seen recently. For example, the isospin asymmetry in $B \to K\mu^+\mu^-$ measured by LHCb [39] deviates from standard model by 4.4σ, and there are some deviations in the branching ratio of $B \to D^{(*)}\tau\nu$ [51, 52]. Precision B physics study such as the CP violation, rare decays and flavour changing neutral current processes will give access to the flavour physics at the short distances. The reason why short distance physics can be best studied in B decays or mixing is due to the heavy mass of the b quark. Inside the B meson the b quark is bound to a light quark by strong dynamics which poses the biggest difficulty to extract short distance information from B systems. The reason being that the strong dynamics can only be fully understood in a non-perturbative framework of field theory calculations which is yet to exist. This thesis partly give some answers to untangle new physics effects from the non-perturbative strong dynamics. There exists various theoretical tolls and techniques to study B system. In the following and subsequent sections we will discuss some of the techniques that are relevant for the study of B decay.

1.4 Operator Product Expansion.

The typical energy scale of meson decay and mixing are of the order of few GeV. For B decay it is $\sim$ 5GeV. On the other hand the standard model contains significantly higher energy scales like the mass of the top quark and the mass of the W boson. The description for meson decay and mixing therefore is provided by an effective field theory approach known as the Operator Product Expansion [53, 54, 55]. In this approach the products of charged current operators are expanded in a series of local six dimension four quark operators, and the contributions of each

of these operators are weighted by effective coupling known as the Wilson coefficients. Such expansions in local operators are possible since the typical momentum transfer k to the final state in weak decays of mesons is much smaller than the mass of the W bosons, $k << M_W^2$. Let us consider the non-local action functional

$$\mathcal{S} = \int d^4x \left(\mathcal{L}_{kin}^q + \mathcal{L}_{kin}^W + \mathcal{L}_{int} \right) \tag{1.23}$$

where, $\mathcal{L}_{kin}^q$ is the kinetic part of the quarks, and

$$\mathcal{L}_{kin}^W = -\frac{1}{4}\left(\partial_\mu W_\nu^+ - \partial_\nu W_\mu^-\right)\left(\partial^\mu W^{+\nu} - \partial^\nu W^{-\mu}\right) + M_W^2 W_\mu^+ W^{-\mu}. \tag{1.24}$$

$$\mathcal{L}_{int} = \frac{g_2}{2\sqrt{2}}\left(J_\mu^+ W^{+\mu} + J_\mu^- W^{-\mu}\right) \tag{1.25}$$

The charged currents J_μ^+ and J_μ^- can be written in terms of massive quark fields $U = (u, c, t)$ and $D = (d, s, b)$ as,

$$J_\mu^+ = V_{UD}\overline{U}\gamma_\mu(1 - \gamma_5)D, \quad J_\mu^- = (J_\mu^+)^\dagger$$

In the path-integral formalism, the generating functional for the Green function can be written as

$$\begin{aligned} Z[J] \sim & \int [\mathcal{D}W^+][\mathcal{D}W^-] exp\Big[i \int d^4x\, d^4y\, W_\mu(x) D^{\mu\nu}(xy) W_\nu^-(y) \\ & + i\frac{g}{2\sqrt{2}} \int d^4x (J_\mu^+ W^{+\mu} + J_\mu^- W^{-\mu}) \Big] \end{aligned} \tag{1.26}$$

where the operator $D^{\mu\nu}(x, y)$ is defined as,

$$D^{\mu\nu}(x, y) = \delta^4(x - y)\Big[g_{\mu\nu}(\partial^2 + M_W^2) - \partial_\mu \partial_\nu \Big]$$

After doing the Gaussian integral in Eq. (1.26) one can write,

$$Z[J] \sim exp\Big[-i \int d^4x\, d^4y\, \frac{g^2}{8}\, J^-_\mu(x)\, \Delta^{\mu\nu}(x,y)\, J^+_\nu(y) \Big]$$

where the W propagator $\Delta^{\mu\nu}(x,y)$ is defined in the unitary gauge as,

$$\Delta^{\mu\nu}(x,y) = -\int \frac{d^4k}{(2\pi)^4}\, \frac{1}{k^2 - M_W^2} (g^{\mu\nu} - \frac{k^\mu k^\nu}{M_W^2})\, e^{-ik.(x-y)}$$

The propagator $\Delta^{\mu\nu}(x,y)$ can be expanded in series in the increasing powers of $1/M_W^2$ so that the product of two nonlocal charged current interaction can be expanded in a series of dimension six four quark local operators denoted by Q. For example, in case of $b \to c\bar{u}d$ decay $Q = \bar{c}\gamma^\mu(1 - \gamma_5)b\bar{d}\gamma_\mu(1-\gamma_5)u$. This procedure is formally known as the Operator Product Expansion (OPE). The effective Hamiltonian corresponding to the first term of the expansion can be written as,

$$\mathcal{L}^{eff}_{int} = -\frac{G_F}{\sqrt{2}} V_{CKM} Q \tag{1.27}$$

where, V_{CKM} is the CKM matrix.

1.5 Low-Energy Effective Hamiltonian.

The dimension six four quark operators Q in the effctive Lagrangian (1.27) receive short distance quantum choromodynamics(QCD) corrections which are calculable in the perturbation theory. The radiative corrections are of the order $\alpha_s(\mu)\ln(M_W/\mu)$, where the $\mu \sim 5$ GeV in the case of b decay. The n-loop contribution of the radiative correction is $[\alpha_s(\mu)\ln(M_W/\mu)]^n$. Even if the $\alpha_s(\mu)$ is calculated at a very higher scale μ, the term $\alpha_s(\mu)\ln(M_W/\mu)$ is of the order unity, so that the overall n-loop contribution is very high and need to be summed up. This is achieved through the method of *renormalization group* (RG). The radiative corrections induce new operators with different quark structure and the subsequent RG evolution leads to mixing between them. It should be noted that the normalization scale dependence μ should cancel for

all physical prediction. Since the operators has scale dependence μ, the above is achieved by multiplicative factors called the Wilson coefficients. The Wilson coefficients $C(\mu)$ defined at the scale $\mu = M_W$ include all of the short distance corrections to the local operators. These can be calculated in the perturbation theory up to desired order in the strong coupling constant α_s. Using a renormalization group-improved perturbation theory, the Wilson coefficients are evolved up to $\mu \sim 5$GeV. The end result is that the effctive Hamiltonian (1.27) is finally written as,

$$\mathcal{H}_{eff} = \frac{G_F}{\sqrt{2}} \sum_i V^i_{CKM} C_i(\mu) Q_i(\mu) \tag{1.28}$$

An amplitude for initial B meson decay to final states F can be written as,

$$\mathcal{A}(B \to F) = \frac{G_F}{\sqrt{2}} \sum_i V^i_{CKM} C_i(\mu) \langle F| Q_i(\mu) |B\rangle \tag{1.29}$$

The amplitude written in this way separates the problem of calculating the amplitude in two parts. The first part is the calculation of the short distance Wilson coefficients $C_i(\mu)$ and the second part is the calculations of the long distance hadronic matrix elements $\langle F| Q_i(\mu) |B\rangle$. The hadronic matrix elements are usually parametrized by form factors. Since form factors carry all the long distance information these are non-perturbative hadronic quantities and hence are not reliably calculated. This is referred to as the the hadronic uncertainties. A significant part of the hadronic uncertainties also constitutes of “non-factorizable” corrections to the matrix elements of purely hadronic operators. In B meson decay, due to the heavy mass of the b quark there arises various symmetry relations between the form factors which are referred to as the heavy quark symmetries. These symmetry relations can be exploited to cancel hadronic uncertainties in ratios of form factors. In the next section we have discussed the heavy quark symmetry.

1.6 Heavy Quark Symmetry.

Inside the B meson, the heavy b quark is surrounded by light quarks and gluons bound together by complex strong interaction dynamics. The b quark mass is grater than $\Lambda_{\rm QCD} \sim 0.2$ GeV. On

the other hand all the light degrees of freedom interact with the heavy quark with soft gluon exchanges of the order $\sim \Lambda_{\rm QCD}$. These light degrees of freedom are therefore blind to flavour and spin of the heavy quark. This is called the heavy quark symmetry. This symmetry can be understood in the framework of heavy quark effective theory. The heavy spin and flavour symmetry is not manifest in the strong interaction Lagrangian in the limit when the quark mass becomes infinity. The effective field theory in which the spin and flavour symmetry is implemented in the limit of infinite quark mass is known as the heavy quark effective field theory. The starting point of constructing heavy quark effective theory is to consider a hadron with a single heavy quark m_Q traveling with velocity v so that the on-shell momentum is $p = m_Q v$. It interacts with the light degrees of freedom with the residual momentum. Hence the momentum of the off-shell heavy quark is $p = m_Q v + k$ [56] where residual momentum $k \sim \Lambda_{\rm QCD}$. We start by writing the Dirac Lagrangian as,

$$\mathcal{L} = \bar{Q}(x)(i\not{D} - m_Q)Q(x) \tag{1.30}$$

where $Q(x)$ is the heavy quark field and $D_\mu = \partial_\mu + igA_\mu$. In the limit of heavy quark mass, the propagator for the quark can be written as [57],

$$i\frac{\not{p} + m_Q}{p^2 - m_Q^2 + i\epsilon} = \frac{1 + \not{v}}{2v.k + i\epsilon} \tag{1.31}$$

The Lagrangian that give rise to the above propagator can be constructed by decomposing the original quark field $Q(x)$ into a velocity dependent field $Q_v(x)$ and a residual field $\mathcal{Q}_v(x)$as,

$$Q_v(x) = e^{im_Q v.x}\frac{1 + \not{v}}{2}Q(x), \quad \mathcal{Q}_v(x) = e^{im_Q v.x}\frac{1 - \not{v}}{2}Q(x).$$

Hence the original quark field can be written as,

$$Q(x) = e^{-im_Q v.x}\Big(Q_v(x) + \mathcal{Q}_v(x)\Big).$$

Substituting (1.32) in the Dirac Lagrangian (1.30) we get the Dirac Lagrangian in terms of heavy quark field $Q_v(x)$ as,

$$\mathcal{L} = \bar{Q}_v(x)\left(iv.D\right)Q_v(x). \tag{1.32}$$

Here we have neglected the part of the Lagrangian with $Q_v(x)$ which is suppressed by powers of $\Lambda_{\mathrm{QCD}}/m_Q$. This Lagrangian has spin and flavour symmetry. From the standpoint of heavy quark effective theory, the heavy to light transition matrix elements are simplified. Inside the meson the heavy quark travels with velocity v. The action of the weak current that causes the heavy to light transition changes the velocity from v to v'. Due to this change the light degrees of freedom arrange themselves so that the heavy meson now travel with the velocity v'. Because of the heavy flavour symmetry the transition current will be universal function of v and v'. These functions are usually denoted by $\xi(v.v')$ which are called the Isgur-Wise [58, 59] form factor or the soft form factor.

Chapter 2

Theoretical Framework of $B \to K^* \ell^+ \ell^-$ decay.

In this chapter we describe the theoretical framework to calculate the amplitude of $B \to K^* \ell^+ \ell^-$ decay. The B meson is a pseudoscalar meson that constitutes of a heavy b quark and a light u or d quark. The b quark decays to s quark and $\ell^+ \ell^-$ pair. The s quark forms the light vector meson K^* which results in our final state. Since flavour changing neutral current is not present in the standard model, the $b \to s \ell^+ \ell^-$ transition occurs via loop diagrams. The decay is described in terms of a effective Hamiltonian which is written in terms of Wilson coefficients and dimension six local four quark operators. The hadronic matrix elements of the local operators in the $B \to K^*$ transition are evaluated at $\mu \sim m_b$ and are parametrized in terms of form factors. The form factors carry the non-perturbative long distance information and therefore their values are not accurately calculated. In searches for new physics, the theoretical challenge of our poor knowledge of form factors can be overcome by exploiting the symmetry relations among the form factors arising at large recoil (low q^2) and low recoil (high q^2) regions of the K^* mesons. In Sec.2.3 and Sec.2.4 we discuss the parametrization of the form factors respectively at large and low recoil limit. We also discuss the symmetry relations among the form factors in these limits.

2.1 The Effective Hamiltonian for $B \to K^* \ell^+ \ell^-$ decay.

At the quark level the exclusive $B \to K^*(k)\ell^+(q_1)\ell^-$ decay is governed by $b \to s\ell^+\ell^-$ flavour changing neutral current transition. The lowest order Feynman diagrams are box diagrams and γ and Z penguin diagrams. The lowest order Feynman diagrams are shown in Fig. 2.1. The most general effective short distance effective Hamiltonian for $b \to s\ell^+\ell^-$ transition can be written as [60, 61, 62],

$$\mathcal{H}_{\text{eff}} = -\frac{G_F}{\sqrt{2}} V_{tb} V_{ts}^* \sum_{i=1}^{10} \Big[C_i(\mu)\, O_i(\mu) + C_i'(\mu)\, O_i'(\mu) \Big] \tag{2.1}$$

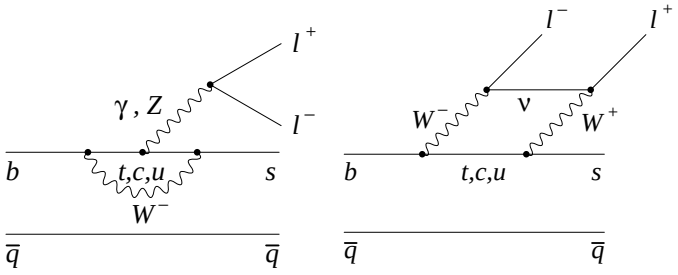

Figure 2.1: Some lowest order Feynman diagrams for $b \to sl^+l^-$ transition.

The primed operators are the one that arise in various new physics models, but are highly suppressed in the standard model. The un-primed operators $O_{i<6}$ also vanish in the standard model. In standard model the three operators that appear in the short distance Hamiltonian are,

$$O_7 = m_b(\bar{s}\sigma_{\mu\nu}P_R b)F^{\mu\nu} \tag{2.2}$$

$$O_9 = (\bar{s}\gamma_\mu P_L b)(\bar{\ell}\gamma^\mu \ell) \tag{2.3}$$

$$O_{10} = (\bar{s}\gamma_\mu P_L b)(\bar{\ell}\gamma^\mu\gamma^5 \ell) \tag{2.4}$$

where, $P_{L,R} = \frac{(1\mp\gamma_5)}{2}$ and $m_b = m_b(\mu)$ is the running quark mass evaluated in the $\overline{\text{MS}}$ scheme. The Wilson coefficients corresponding to these operators are denoted by C_7, C_9 and C_{10} respectively. Before we write down the Hamiltonian, few comments are in order regarding the Wilson coefficients. As mentioned in the previous chapter, the Wilson coefficients are calculated in the

perturbation theory up to desired order in the strong coupling constant $\alpha_s(\mu_W)$ at the matching scale $\mu_W = m_W$. The perturbation expansion reads as,

$$C_i(\mu_W) = C_i^{(0)}(\mu_W) + \frac{\alpha_s}{4\pi} C_i^{(1)}(\mu_W) + \frac{\alpha_s^2}{16\pi^2} C_i^{(2)}(\mu_W) + O(\alpha_s^3). \tag{2.5}$$

Using the normalization group equation, the coefficients are evolved to a scale $\mu = m_b = 4.8\text{GeV}$. For a leading-logarithmic (LL) result, one has to retain only the lowest order terms $C_i^{(0)}(\mu_W)$, and for next-to-leading-logarithmic result up to $C_i^{(1)}(\mu_W)$ is to be kept. In this work we mention next-to- next-to-leading-logarithmic (NNLL) results that are calculated in Refs. [63, 64, 65, 66, 67]. The NNLL calculations require matching at two-loop. In the renormalization group, the two-loop accuracy require anomalous dimension matrix up to three-loop accuracy [68, 69, 70]. The 10×10 anomalous dimension matrix mixes different operators. For example, the O_9 operator mix with $O_{1\ldots6}$. Due to such mixing it is found, that different Wilson coefficients always appear in certain combinations. The Wilson coefficients $C_{7,9}$ are thus replaced by effective Wilson coefficients $C_{7,9}^{\text{eff}}$. These are defined below,

$$\begin{aligned} C_7^{\text{eff}} &= \frac{4\pi}{\alpha_s} C_7 - \frac{1}{3} - \frac{4}{9} C_4 - \frac{20}{3} C_5 - \frac{80}{9} C_6 \\ C_9^{\text{eff}} &= \frac{4\pi}{\alpha_s} C_9 + Y(q^2), \end{aligned}$$

where the function $Y(q^2)$ is given by [60, 71, 72, 73]

$$\begin{aligned} Y(q^2) = {} & h(q^2, m_c)\left(\frac{4}{3}C_1 + C_2 + 6C_3 + 60C_5\right) \\ & -\frac{1}{2}h(q^2, m_b)\left(7C_3 + \frac{4}{3}C_4 + 76C_5 + \frac{64}{3}C_6\right) \\ & -\frac{1}{2}h(q^2, 0)\left(C_3 + \frac{4}{3}C_4 + 16C_5 + \frac{64}{3}C_6\right) \\ & +\frac{4}{3}C_3 + \frac{64}{9}C_5 + \frac{64}{27}C_6. \end{aligned}$$

The function $h(q^2, m_q)$ reads as:

$$\begin{aligned} h(q^2, m_q) &= -\frac{4}{9}\left(\ln\frac{m_q^2}{\mu^2} - \frac{2}{3} - y\right) - \frac{4}{9}(2+y)\sqrt{|y-1|} \\ &\times\left[\Theta(1-y)\left(\ln\frac{1+\sqrt{1-y}}{\sqrt{y}} - i\frac{\pi}{2}\right)\right. \\ &\left.+\Theta(y-1)\arctan\frac{1}{\sqrt{y-1}}\right], \end{aligned}$$

with y defined as $y = 4m_q^2/q^2$, and we have neglected the small weak phase. The standard model values of the Wilson coefficients used in this work are calculated at the next-to-next-to-leading logarithmic (NNLL) accuracy [63] and are given by,

$$C_7^{\text{eff}} = -0.304, \quad C_9^{\text{eff}} = 4.211 + Y(q^2), \quad C_{10} = -4.103.$$

The effective short distance Hamiltonian for $b \to s\ell^+\ell^-$ transition is well understood and given by: [62, 71, 74, 75]

$$\begin{aligned} \mathcal{H}_{\text{eff}} &= \frac{G_F\alpha}{\sqrt{2}\pi}V_{tb}V_{ts}^*\Big[C_9^{\text{eff}}(\bar{s}\gamma_\mu P_L b)\bar{\ell}\gamma^\mu\ell + C_{10}(\bar{s}\gamma_\mu P_L b)\bar{\ell}\gamma^\mu\gamma_5\ell \\ &- \frac{2C_7^{\text{eff}}}{q^2}\bar{s}i\sigma_{\mu\nu}q^\nu(m_b P_R + m_s P_L)b\bar{\ell}\gamma^\mu\ell\Big], \end{aligned} \tag{2.6}$$

with $q_\nu = q_{1\nu} + q_{2\nu}$, where $q_{1\nu}$ and $q_{2\nu}$ are momentum of the leptons and q^2 is the dilepton invariant mass squared.

2.2 Parametrization of Hadronic Matrix elements.

The decay under consideration occurs in two steps. First the B meson decays to K^* meson and lepton pairs, and subsequently K^* decays to $K\pi$ resonantly. The amplitude of $B \to K^*(k)(\to K(k_1)\pi(k_2))\ell^+(q_1)\ell^-(q_2)$ decay is written as,

$$\mathcal{M} = \frac{G_F\alpha}{\sqrt{2}\pi}V_{tb}V_{ts}^*\Big\{\Big[C_9^{\text{eff}}\langle K\pi|\bar{s}\gamma^\mu P_L b|\bar{B}\rangle(\bar{l}\gamma_\mu l) + C_{10}\langle K\pi|\bar{s}\gamma^\mu P_L b|\bar{B}\rangle(\bar{l}\gamma_\mu\gamma_5 l)$$

$$- \quad \frac{2C_7^{\rm eff} m_b}{q^2}\langle K\pi|\bar{s}i\sigma_{\mu\nu}q^\nu P_R b|\bar{B}\rangle(\bar{l}\gamma^\mu l)\Big\}\Big]. \tag{2.7}$$

Throughout the analysis to follow we will use the following notations,

$$q = q_1 + q_2, \;\; K = k_1 - k_2, \;\; Q = q_1 - q_2, \;\; k = k_1 + k_2.$$

The B to $K\pi$ hadronic matrix elements of the local quark bilinear operators $\bar{s}i\sigma_{\mu\nu}q^\nu m_b P_R b$ and $\bar{s}\gamma_\mu P_L b$ are calculated by first calculating the hadronic matrix elements for the $B \to K^*$ transition and then considering the subsequent decay of K^* to $K\pi$. The $B \to K^*$ hadronic matrix elements of the local quark bilinear operators $\bar{s}\gamma_\mu P_L b$ and $\bar{s}i\sigma_{\mu\nu}q^\nu m_b P_R b$ can be parametrized in terms of six q^2-dependent QCD form factors $V(q^2), A_{1,2}(q^2), T_{1,2,3}(q^2)$ as,

$$\begin{aligned}
\Big\langle \bar{K^*}(k)\Big|\bar{s}\gamma_\mu(1-\gamma_5)b\Big|\bar{B}(p)\Big\rangle &= -i\epsilon_\mu(m_B + m_{K^*})A_1(q^2) + p_\mu(\epsilon^*.q)\frac{2\,A_2(q^2)}{m_B + m_{K^*}} \\
&\quad + i\epsilon_{\mu\nu\rho\sigma}\epsilon^{*\nu}p^\rho k^\sigma \frac{2\,V(q^2)}{m_B + m_{K^*}} \qquad (2.8) \\
\Big\langle \bar{K^*}(k)\Big|\bar{s}\sigma_{\mu\nu}q^\nu(1+\gamma_5)b\Big|\bar{B}(p)\Big\rangle &= i\epsilon_{\mu\nu\rho\sigma}\epsilon^{*\nu}p^\rho k^\sigma 2\,T_1(q^2) + T_2(q^2)[\epsilon^*_\mu(m_B^2 - m_{K^*}^2) - 2\,(\epsilon^*.q)p_\mu] \\
&\quad -(\epsilon^*.q)\,q^2\frac{2\,T_3(q^2)}{m_B^2 - m_{K^*}^2}\,p_\mu\,, \qquad (2.9)
\end{aligned}$$

where, $q_\nu = p_\nu - k_\nu$. We have assumed that the lepton mass is zero. We have dropped the terms proportional to q_μ since the terms $q_\mu\bar{\ell}\gamma^\mu\gamma_5\ell$ and $q_\mu\bar{\ell}\gamma^\mu\ell$ do not contribute in the limit of vanishing lepton mass. The $B \to K\pi$ hadronic matrix elements can be calculated from the $B \to K^*$ hadronic matrix defined above. The $K^* \to K\pi$ effective Hamiltonian $\mathcal{H}$ can be written as

$$\mathcal{H} = g_{K^*K\pi}(k_1 - k_2).\epsilon^*$$

where, $g_{K^*K\pi}$ is the coupling of K^* to $K\pi$ and ϵ^* is the polarization of the K^*. Since the K^* decays to $K\pi$ resonantly, we assume narrow-width approximation in the propagator. Denoting

the K^* width as Γ_{K^*}, in the limit $m_{K^*} >> \Gamma_{K^*}$ we can write the propagator as,

$$\frac{1}{(k^2 - m_{K^*})^2 + m_{K^*}^2\Gamma_{K^*}^2} \longrightarrow \frac{\pi}{m_{K^*}\Gamma_{K^*}}\delta(k^2 - m_{K^*}^2)$$

The width Γ_{K^*} can be written as,

$$\Gamma_{K^*} = \frac{g_{K^*K\pi}}{48\pi} m_{K^*}\beta^3$$

where $g_{K^*K\pi}$ is the coupling of K^* to $K\pi$ and,

$$\beta = \frac{1}{m_{K^*}}\Big[m_{K^*}^4 + m_K^4 + m_\pi^4 - 2(m_{K^*}^2 m_K^2 + m_K^2 m_\pi^2 + m_{K^*}^2 m_\pi^2)\Big]^{1/2}$$

We can write the $B \to K^*$ transition hadronic matrix elements as,

$$\left\langle \bar{K^*}\middle| J_\mu \middle|\bar{B}\right\rangle = \epsilon^{*\nu} A_{\mu\nu}.$$

where $A_{\mu\nu}$ contains the $B \to K^*$ form factors. In terms of $A_{\mu\nu}$ the $B \to K\pi$ hadronic matrix elements can be written as,

$$\left\langle \bar{K}\pi\middle| J_\mu \middle|\bar{B}\right\rangle = -\frac{48\pi^2}{\beta^3 m_{K^*}}\delta(k^2 - m_{K^*}^2)\Big[K^\nu - \frac{m_K^2 - m_\pi^2}{k^2}k^\nu\Big]A_{\mu\nu} \tag{2.10}$$

The $B \to K^*\ell^+\ell^-$ decay has been studied by various authors. For example, in Refs. [76] the mode have been studied using light-cone hadron distribution amplitudes [78, 79, 80, 81, 82, 83] combined with QCD sum rules on the light cone [84, 85]. In Refs. [86] the mode was studied using naive factorization and QCD sum rules on the light cone. In in Refs. [73, 87, 88] it has been studied in the heavy quark limit using QCD factorization[89, 90, 91]. Soft-collinear effective theory [92, 93, 94, 95, 96] that is valid for small q^2 (large recoil of K^*) has been used to study the decay in Ref. [97]. In Ref.[98] the mode has been studied in a model independent approach in the low recoil using an operator product expansion in $1/Q$, where $Q = (m_b, \sqrt{q^2})$. In all these methods of parametrization of the hadronic matrix elements, the

theoretical uncertainties amounts to about 30% of the branching ratio.

2.3 Form factors at Large Recoil Limit of K^*.

The six form factors $V(q^2)$, $A_{1,2}(q^2)$ and $T_{1,2,3}(q^2)$ parametrizing the $B \to K^*$ hadronic matrix are non-perturbative quantities and therefore are not reliably calculated. At present the QCD sum rule on the light-cone technique [84] offers the most precise values of these form factors and it has been applied to the $B \to K^*$ transition in Ref. [76, 77]. Though the lattice calculations are also very promising, all the six form factors are not calculated as yet. Therefore in this work we do not rely on the numerical values of the form factors to extract new physics signals. We observe that the hadronic uncertainties coming from poor estimate of form factors and non-factorizable corrections cancel in ratios of form factors. These ratios can be taken as reliable theoretical inputs in the searches of clean signal of new physics. In the low q^2 region of the $B \to K^*$ transition, the light meson carries a very large energy E_{K^*}. The initial B meson carries the heavy quark b and since the momentum transfer q^2 to the lepton in the $b \to s$ transition is small the heavy quark symmetry [58, 59, 99] is applicable in this limit. The heavy quark symmetry is implemented in the Heavy Quark Effective Theory (HQET) [58, 59] Lagrangian. In HQET it is assumed that inside the B meson the mass of the b quark $m_b \to \infty$ and all the light degrees of freedom interact with it via soft exchanges of the the order $\Lambda_{\rm QCD}$. If the hard gluon exchanges are neglected then the six form factors can be expressed in terms of only two universal functions known as Isgur-Wise functions [58, 59], also known as soft form factors $\xi_\perp(q^2)$ and $\xi_\parallel(q^2)$. These two soft form factors correspond to the transverse and longitudinal polarization states of the K^* meson respectively. For our future numerical analysis, we chose the following parametrization [73] of $\xi_\perp(q^2)$ and $\xi_\parallel(q^2)$ at large recoil limit,

$$\begin{aligned}
\xi_\perp(q^2) &= \xi_\perp(0)\left(\frac{1}{1-q^2/m_B^2}\right)^2 \\
\xi_\parallel(q^2) &= \xi_\parallel(0)\left(\frac{1}{1-q^2/m_B^2}\right)^3
\end{aligned}$$

where $\xi_\perp(0) = 0.266 \pm 0.032$ and $\xi_\parallel(0) = 0.118 \pm 0.008$ [71]. The expressions of $V(q^2)$, $A_{1,2}(q^2)$ and $T_{1,2,3}(q^2)$ in terms of $\xi_\perp(q^2)$ and $\xi_\parallel(q^2)$ lead to various symmetry relations between the form factors [100]. Neglecting the corrections to be discussed later, the expressions of $V(q^2)$, $A_{1,2}(q^2)$ and $T_{1,2,3}(q^2)$ read as,

$$A_1(q^2) = \frac{2E_{K^*}}{m_B + m_{K^*}}\xi_\perp(E_{K^*}) \tag{2.11}$$

$$A_2(q^2) = \frac{m_B}{m_B - m_{K^*}}[\xi_\perp(E_{K^*}) - \xi_\parallel(E_{K^*})] \tag{2.12}$$

$$V(q^2) = \frac{m_B + m_{K^*}}{m_B}\xi_\perp(E_{K^*}) \tag{2.13}$$

$$T_1(q^2) = \xi_\perp(E_{K^*}) \tag{2.14}$$

$$T_2(q^2) = \frac{2E_{K^*}}{m_B}\xi_\perp(E_{K^*}) \tag{2.15}$$

$$T_3(q^2) = \xi_\perp(E_{K^*}) - \xi_\parallel(E_{K^*}), \tag{2.16}$$

where, E_{K^*} is the energy of the K^* meson,

$$E_{K^*} = \frac{m_B^2 + m_{K^*}^2 - q^2}{2m_B}. \tag{2.17}$$

Large recoil means when $E_{K^*} \sim O(m_b)$. Though the form factors $A_1(q^2)$, $V(q^2)$ and $T_1(q^2)$, $T_2(q^2)$ dependent on the soft form factors which however cancel in the following ratios,

$$\frac{V(q^2)}{A_1(q^2)} = \frac{(m_B + m_{K^*})^2}{2E_{K^*}m_B}, \tag{2.18}$$

$$\frac{T_2(q^2)}{T_1(q^2)} = \frac{2E_{K^*}}{m_B}. \tag{2.19}$$

The form factors $V(q^2)$, $A_{1,2}(q^2)$ and $T_{1,2,3}(q^2)$ receive perturbative [100] corrections in the powers of strong coupling α_s. In Ref. [101] the perturbative corrections were calculated. The form factor $V(q^2)$ do not receive any perturbative corrections and the corrections to $A_1(q^2)$ vanishes at α_s. Hence the left hand side of the Eq. (2.18) remains unchanged at leading order in α_s. The same is true for the ratio $T_2(q^2)/T_1(q^2)$. The corrections at order α_s to the form factors

$T_1(q^2)$ and $T_2(q^2)$ are [101],

$$\begin{aligned} T_1(q^2) &= \xi_\perp\Big(1+\frac{\alpha_s C_F}{4\pi}\Big[\ln\frac{m_b^2}{\mu^2}-L\Big]\Big)+\frac{\alpha_s C_F}{4\pi}\Delta T_1 \\ T_2(q^2) &= \frac{2E_{K^*}}{m_B}\xi_\perp\Big(1+\frac{\alpha_s C_F}{4\pi}\Big[\ln\frac{m_b^2}{\mu^2}-L\Big]\Big)+\frac{\alpha_s C_F}{4\pi}\Delta T_2 \end{aligned}$$

where,

$$L = -\frac{2E_{K^*}}{m_B-2E_{K^*}}\ln\frac{2E_{K^*}}{m_B}, \quad \text{and} \quad \frac{\Delta T_1}{\Delta T_2}=\frac{m_B}{2E_{K^*}}$$

Substituting these in to Eq. (2.19) it can be seen that the ratio $T_2(q^2)/T_1(q^2)$ is unchanged at leading order in α_s. It is shown in Refs. [101, 102] that, *at leading order in* $\Lambda_{\rm QCD}/m_b$, *the form factor ratios* $V(q^2)/A_1(q^2)$ *and* $T_2(q^2)/T_1(q^2)$ *are independent of perturbative corrections to all orders in* α_s. For the $V(q^2)/A_1(q^2)$ ratio, this can be understood more physically by considering the helicity amplitudes $H_\pm$,

$$H_{\pm1} \propto \left(V \mp \frac{(m_B+m_{K^*})^2}{2m_B E_{K^*}}A_1\right) \tag{2.20}$$

In the limit $m_B \to \infty$, $E_{K^*} \to \infty$ and $m_s \to 0$, the s-quark is created from b decay in the $-1/2$ helicity state. Hence the K^* helicity states can only be -1 or 0, but not +1. So $H_+ = 0$ to all orders in perturbation theory. Hence *at leading order in* $\Lambda_{\rm QCD}/m_b$, *the* $V(q^2)/A_1(q^2)$ *ratio is free from perturbative correction to all orders in* α_s. For the $T_2(q^2)/T_1(q^2)$ ratio, in addition to the perturbative corrections, at leading order in $\Lambda_{\rm QCD}/m_b$ a significant part of the hadronic uncertainties come from the "non-factorizable" [73] corrections. The "non-factorizable" corrections do not correspond to the form factors. These corrections arise when virtual photons are connected to the purely hadronic operators O_1 to O_6 and chromomagnetic-dipole operator O_8. These are calculated in Ref. [73] at leading order in $\Lambda_{\rm QCD}/m_b$ for $B \to K^*$ transitions, and can be incorporated by the following transformations [103],

$$\begin{aligned} C_7^{\rm eff}T_i &\to \mathcal{T}_i, \\ C_9^{\rm eff} &\to C_9, \end{aligned}$$

where the Wilson Coefficients are taken at the next-to-next-to leading order, and the $\mathcal{T}_i$ are defined as,

$$\mathcal{T}_1 = \mathcal{T}_\perp, \quad \mathcal{T}_2 = \frac{2E_{K^*}}{m_B}\mathcal{T}_\perp, \quad \mathcal{T}_3 = \mathcal{T}_\perp + \mathcal{T}_\parallel \tag{2.21}$$

The complete expressions of $\mathcal{T}_{\perp,\parallel}$ are given in Ref. [73]. The important thing to observe is that the form factors $V(q^2)$, $A_1(q^2)$ are unaffected by the "non-factorizable" corrections and hence at leading order in $\Lambda_{\rm QCD}/m_b$, *the ratio Eq. (2.18) still remains unaffected by "non-factorizable" corrections to all orders in* α_s. Due to "non-factorizable" corrections the tensor form factors $T_1(q^2)$ and $T_2(q^2)$ are replaced by $\mathcal{T}_1$ and $\mathcal{T}_2$ respectively However their ratio is still free from perturbative corrections to all orders in α_s,

$$\frac{\mathcal{T}_1(q^2)}{\mathcal{T}_2(q^2)} = \frac{T_1(q^2)}{T_2(q^2)} = \frac{2E_{K^*}}{m_B}$$

In our future discussions on the searches of new physics we will take the ratios $V(q^2)/A_1(q^2)$ and $T_1(q^2)/T_2(q^2)$ as reliable theoretical inputs.

2.4 Form factor at Low Recoil Limit of K^*.

In the low recoil limit of the K^* meson, the perturbative and the "non-factorizable" corrections are negligible. A model independent description for the case of low recoil energy of the K^* in $B \to K^*\ell^+\ell^-$ decay was put forward by Grinstein and Pirjol [98] in the modified Heavy Quark Effective Theory framework. In this approach [98], "near the zero point $q^2 \approx (m_B - m_{K^*})^2$, the long distance contributions to $B \to K^*\ell^+\ell^-$ can be computed as short distance effect using simultaneous heavy quark and operator product expansion in $1/Q$ with $Q \approx \{m_b, \sqrt{q^2}\}$." In view of this the sub-leading m_{K^*}/m_B terms are neglected and non-factorizable corrections are ignored. An elaborate study of the predictions for $B \to K^*\ell^+\ell^-$ was undertaken in Ref. [104] where the next-to-leading order corrections from the charm quark mass m_c and strong coupling at $\mathcal{O}(m_c/Q^2, \alpha_s)$ were included. The result is a relation between the $B \to K^*\ell^+\ell^-$ form factors that reduces the number of independent hadronic form factors to only three, i.e., $V(q^2), A_1(q^2)$

and $A_2(q^2)$ can be expressed in terms of the form factors $T_1(q^2), T_2(q^2), T_3(q^2)$ as:

$$T_1(q^2) = \kappa V(q^2) \tag{2.22}$$

$$T_2(q^2) = \kappa A_1(q^2) \tag{2.23}$$

$$T_3(q^2) = \kappa A_2(q^2)\frac{m_B^2}{q^2} \tag{2.24}$$

where, the expression of κ is given in [104]. From the above relations we get,

$$\frac{T_1(q^2)}{T_2(q^2)} = \frac{V(q^2)}{A_1(q^2)} \tag{2.25}$$

These relations will be very significant in our future discussions. Finally we give the q^2 dependance of the six form factors $V(q^2), A_{1,2}(q^2), T_{1,2,3}(q^2)$ [105, 106] that can be extrapolated from their region of validity at large recoil to low recoil,

$$\begin{aligned}
V(q^2) &= \frac{r_1}{1-q^2/m_R^2} + \frac{r_2}{1-q^2/m_{\rm fit}^2} \\
A_1(q^2) &= \frac{r_2}{1-q^2/m_{\rm fit}^2} \\
A_2(q^2) &= \frac{r_1}{1-q^2/m_{\rm fit}^2} + \frac{r_2}{(1-q^2/m_{\rm fit}^2)^2} \\
T_1(q^2) &= \frac{r_1}{1-q^2/m_R^2} + \frac{r_2}{1-q^2/m_{\rm fit}^2} \\
T_2(q^2) &= \frac{r_2}{1-q^2/m_{\rm fit}^2} \\
T_3(q^2) &= \frac{m_B^2 - m_{K^*}}{q^2}(\tilde{T}_3(q^2) - T_2(q^2))
\end{aligned} \tag{2.26}$$

where $\tilde{T}_3$ has same parametrization as A_1. The parameters $r_1, r_2, m_R^2, m_{\rm fit}^2$ for each of the above form factors have been taken from [105, 106].

Chapter 3

Angular Distribution and Observables.

The $B \to K^* \ell^+ \ell^-$ decay is regarded as a very important mode for searches of new physics as it provides with a multitude of related observables. Several different experiments Belle [107], Babar [108, 109], CDF [110, 111, 112] and LHCb [113] have studied this mode. These experiments have provided valuable data as a function of the dilepton invariant mass squared and the various angles describing the distribution. Each of these four experiments have measured the partial branching fraction in chosen q^2 bins by preforming a complete angular integration. By studying the angular distribution of the direction of the lepton in an appropriately chosen frame, these experiments have also measured the well known forward-backward asymmetry $A_{\rm FB}$ and the longitudinal polarization fraction F_L in terms of integrated dilepton invariant mass squared regions of q^2. The CDF and LHCb collaborations have in addition performed an angular study of the azimuthal angle defined as the angle between the planes formed by the leptons and the decay products of K^* i.e. K, π. Recently the LHCb [114] has also measured the zero crossing point of the forward-backward asymmetry which is consistent with the standard model expectation. Future experimental studies by LHCb and Belle II will enable the study of this mode with significantly larger statistics making possible the analysis with multi-angular distributions and the measurement of all the observables. The decay is best described in the rest frame of B in terms of three angles and the dilepton invariant mass squared. In this chapter we have described the angular distribution of $B \to K^* \ell^+ \ell^-$ decay and have shown how the multitude

of observables [71, 74, 115] can be extracted from the angular distribution. In the limit of no CP violation and zero lepton mass, the observable extracted from the angular analysis can be expressed in terms of six real transversity amplitudes that correspond to the three states of polarizations of K^* and the left or right chirality of the leptonic current. The leptons are usually muons which can be detected easily at the LHC. The mode $B \to K^* e^+ e^-$ is discussed in Ref. [116].

3.1 Transversity amplitudes.

To introduce the transversity amplitudes in $B \to K^* \ell^+ \ell^-$ decay, we first consider the decay $B \to K^* V^*$ where the V^* is a resonant vector meson. Denoting the polarization vector of K^* and V^* as $\epsilon^{\mu}_{K^*}$ and ϵ^{μ}_{V} the $B \to K^* V^*$ amplitudes can be written as [117, 118],

$$\mathcal{M}^{(\lambda,\lambda')}(B \to K^* V^*) = \epsilon^{(\lambda)*\mu}_{K^*} M_{\mu\nu} \epsilon^{(\lambda')*\nu}_{V^*} \tag{3.1}$$

where $\lambda, \lambda' = +, -, 0$ are the three helicity states. If we consider that the B meson is at rest and the K^* and V^* decays back to back then the polarization states of the K^* and V^* are [117, 118],

$$\epsilon^{(\pm)*\mu}_{K^*} = (0, 1, \pm i, 0)/\sqrt{2} \tag{3.2}$$

$$\epsilon^{(0)*\mu}_{K^*} = (k_z, 0, 0, k_0)/m_{K^*} \tag{3.3}$$

$$\epsilon^{(\pm)*\mu}_{V^*} = (0, 1, \pm i, 0)/\sqrt{2} \tag{3.4}$$

$$\epsilon^{(0)*\mu}_{V^*} = (-q_z, 0, 0, -q_0)/\sqrt{q^2} \tag{3.5}$$

where, $k^\mu = (k_0, 0, k_z)$, $q^\mu = (q_0, 0, q_z)$ and $k_z = -q_z$. The orthonormality and completeness relations can be written [117, 118] as,

$$\epsilon^{(\lambda)*\mu}_{V^*} \epsilon^{(\lambda')*}_{V^*\mu} = g_{\lambda\lambda'} \tag{3.6}$$

$$\sum_{\lambda\lambda'} \epsilon^{(\lambda)*\mu}_{V^*} \epsilon^{(\lambda')*\nu}_{V^*} g_{\lambda\lambda'} = g^{\mu\nu} \tag{3.7}$$

$$\epsilon^{(\lambda)*\mu}_{K^*}\ \epsilon^{(\lambda')*}_{K^*\mu} = -\delta_{\lambda\lambda'} \tag{3.8}$$

$$\sum_{\lambda\lambda'} \epsilon^{(\lambda)*\mu}_{K^*}\ \epsilon^{(\lambda')*\nu}_{K^*}\delta_{\lambda\lambda'} = -g^{\mu\nu} + \frac{k^\mu k^\nu}{m_{K^*}} \tag{3.9}$$

Considering the subsequent decay of V^* to $\ell^+\ell^-$ pair, we can further write the amplitudes as,

$$\begin{aligned}\mathcal{M}^{(\lambda,\lambda')}(B\to K^*V^*(\to \ell^+\ell^-)) &= \epsilon^{(\lambda)*\mu}_{K^*}\ M^L_{\mu\nu}\ \sum_{\lambda',\eta}\epsilon^{(\lambda')*\nu}_{V^*}\epsilon^{(\eta)*\alpha}_{V^*} g_{\lambda'\eta}[\bar{\ell}\gamma_\alpha P_L \ell] \\ &+ \epsilon^{(\lambda)*\mu}_{K^*}\ M^R_{\mu\nu}\ \sum_{\lambda',\eta}\epsilon^{(\lambda')*\nu}_{V^*}\epsilon^{(\eta)*\alpha}_{V^*} g_{\lambda'\eta}[\bar{\ell}\gamma_\alpha P_R \ell],\end{aligned} \tag{3.10}$$

where, $\eta = +,-,0$. From Eq. (3.10) we can introduce the six helicity amplitudes by taking $\lambda' = \lambda$ as,

$$H^L_\lambda = -\epsilon^{(\lambda)*\mu}_{K^*}\epsilon^{(\lambda)*\nu}_{V^*}M^L_{\mu\nu} \tag{3.11}$$

$$H^R_\lambda = -\epsilon^{(\lambda)*\mu}_{K^*}\epsilon^{(\lambda)*\nu}_{V^*}M^R_{\mu\nu} \tag{3.12}$$

The six transversity amplitude can be constructed from Eq. (3.11) and Eq. (3.12) as,

$$\mathcal{A}^{L,R}_{\perp,\parallel} = \frac{1}{\sqrt{2}}(H^{L,R}_+ \mp H^{L,R}_-) \tag{3.13}$$

$$\mathcal{A}^{L,R}_0 = H^{L,R}_0. \tag{3.14}$$

Considering a B meson at rest decaying back-to-back in to K^* and a $\ell^+\ell^-$ pair, the above formulation can be generalized to write the explicit expressions of six transversity amplitudes as,

$$\mathcal{A}^{L,R}_\perp = N\sqrt{2}\sqrt{\lambda(m_B^2, m_{K^*}^2, q^2)}\Big[\Big[(C_9^{\rm eff} \mp C_{10}^{\rm eff})\Big]\frac{V(q^2)}{m_B + m_{K^*}} + \frac{2m_b}{q^2}C_7^{\rm eff}T_1(q^2)\Big], \tag{3.15}$$

$$\mathcal{A}^{L,R}_\parallel = -N\sqrt{2}(m_B^2 - m_{K^*}^2)\Big[\Big[(C_9^{\rm eff} \mp C_{10}^{\rm eff})\Big]\frac{A_1(q^2)}{m_B - m_{K^*}} + \frac{2m_b}{q^2}C_7^{\rm eff}T_2(q^2)\Big], \tag{3.16}$$

$$\begin{aligned}\mathcal{A}^{L,R}_0 &= -\frac{N}{2m_{K^*}\sqrt{q^2}}\Big(\Big[(C_9^{\rm eff} \mp C_{10}^{\rm eff})\Big]\times\Big[(m_B^2 - m_{K^*}^2 - q^2)(m_B + m_{K^*})A_1(q^2) \\ &- \lambda(m_B^2, m_{K^*}^2, q^2)\frac{A_2(q^2)}{m_B + m_{K^*}}\Big] + 2m_b C_7^{\rm eff}\Big[(m_B^2 + 3m_{K^*}^2 - q^2)T_2(q^2) \\ &- \frac{\lambda(m_B^2, m_{K^*}^2, q^2)}{m_B^2 - m_{K^*}^2}T_3(q^2)\Big]\Big)\end{aligned} \tag{3.17}$$

where, $\perp, \|, 0$ are the helicity of K^* and L, R are the chirality of lepton and the normalization factor N is given

$$N = V_{tb}V_{ts}^* \left[\frac{G_F^2 \alpha^2}{3 \cdot 2^{10} \pi^5 m_B^3} q^2 \sqrt{\lambda(m_B^2, m_{K^*}^2, q^2)} \right]^{1/2}, \tag{3.18}$$

with $\lambda(m_B^2, m_{K^*}^2, q^2) = m_B^4 + m_{K^*}^4 + q^4 - 2(m_B^2 m_{K^*}^2 + m_{K^*}^2 q^2 + m_B^2 q^2)$. We note that the helicity amplitudes $\mathcal{A}_{\perp,\|,0}^{L,R}$ are functions of q^2, for simplicity we have suppressed the explicit dependence on q^2. In these expressions we have neglected the lepton mass and also the tiny CP violation [74] that arise in the standard model. Hence helicity amplitudes $\mathcal{A}_{\perp,\|,0}^{L,R}$ are all real.

3.2 Angular Distributions.

The $B \to K^* \ell^+ \ell^-$ angular analysis is studied in the helicty frame shown in Fig. 3.1. In this frame the B meson is at rest, and the K^* and the $\ell^+\ell^-$ decay back-to-back. The momentum of the K^* is taken along the positive z-axis. In its rest frame the K^* decays back-to-back into a K and a π. The angle between the K and the z axis is θ_K where as θ_ℓ is the angle between ℓ^- and the $+z$ axis. The decay can be completely described by four independent kinematic variables: the lepton pair invariant mass squared $q^2 = (q_1 + q_2)^2$, the angle ϕ between the decay planes formed by the $\ell^+\ell^-$ and $K\pi$, and the angles θ_K and θ_ℓ. In this frame the differential decay distribution can be written as [74],

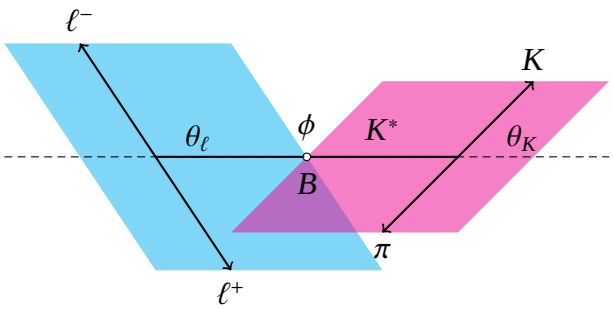

Figure 3.1: The helicity frame for $B \to K^*(k)(\to K(k_1)\pi(k_2))\ell^-(q_1)\ell^+(q_2)$ decay.

$$\frac{d^4\Gamma(B \to K^* \ell^+ \ell^-)}{dq^2\, d\cos\theta_\ell\, d\cos\theta_K\, d\phi} = I(q^2, \theta_\ell, \theta_K, \phi) \tag{3.19}$$

where, we can write,

$$\begin{aligned} I(q^2,\theta_\ell,\theta_K,\phi) &= \frac{9}{32\pi}\Big[I_1^s\sin^2\theta_K + I_1^c\cos^2\theta_K + (I_2^s\sin^2\theta_K + I_2^c\cos^2\theta_K)\cos 2\theta_\ell + \\ &+ I_3\sin^2\theta_K\sin^2\theta_\ell\cos 2\phi + I_4\sin 2\theta_K\sin 2\theta_\ell\cos\phi + I_5\sin 2\theta_K\sin\theta_\ell\cos\phi + \\ &+ I_6^s\sin^2\theta_K\cos\theta_\ell + I_7\sin 2\theta_K\sin\theta_\ell\sin\phi + I_8\sin 2\theta_K\sin 2\theta_\ell\sin\phi \\ &+ I_9\sin^2\theta_K\sin^2\theta_\ell\sin 2\phi\Big]. \end{aligned} \tag{3.20}$$

The angular coefficients I are function of q^2. For notational simplicity we will suppress the q^2 throughout. The explicit expressions of I's in terms of the transversity amplitudes can be written as,

$$\begin{aligned} I_1^s &= \frac{3}{4}\Big[|\mathcal{A}_\perp^L|^2 + |\mathcal{A}_\parallel^L|^2 + (L\to R)\Big], \\ I_1^c &= \Big[|\mathcal{A}_0^L|^2 + (L\to R)\Big], \\ I_2^s &= \frac{1}{4}\Big[|\mathcal{A}_\perp^L|^2 + |\mathcal{A}_\parallel^L|^2 + (L\to R)\Big], \\ I_2^c &= -\Big[|\mathcal{A}_0^L|^2 + (L\to R)\Big], \\ I_3 &= \frac{1}{2}\Big[|\mathcal{A}_\perp^L|^2 - |\mathcal{A}_\parallel^L|^2 + (L\to R)\Big], \\ I_4 &= \frac{1}{\sqrt{2}}\Big[\mathrm{Re}(\mathcal{A}_0^L\mathcal{A}_\parallel^{L^*}) + (L\to R)\Big], \\ I_5 &= \sqrt{2}\Big[\mathrm{Re}(\mathcal{A}_0^L\mathcal{A}_\perp^{L^*}) - (L\to R)\Big] \\ I_6^s &= 2\Big[\mathrm{Re}(\mathcal{A}_\parallel^L\mathcal{A}_\perp^{L^*}) - (L\to R)\Big], \\ I_7 &= \sqrt{2}\Big[\mathrm{Im}(\mathcal{A}_0^L\mathcal{A}_\parallel^{L^*}) - (L\to R)\Big], \\ I_8 &= \frac{1}{\sqrt{2}}\Big[\mathrm{Im}(\mathcal{A}_0^L\mathcal{A}_\perp^{L^*}) + (L\to R)\Big], \\ I_9 &= \Big[\mathrm{Im}(\mathcal{A}_\parallel^{L^*}\mathcal{A}_\perp^L) + (L\to R)\Big]. \end{aligned} \tag{3.21}$$

In the absence of CP violation, $I_{7,8,9} = 0$ and the conjugate decay mode $\overline{B}\to \overline{K}^*(k)(\to K(k_1)\pi(k_2))\ell^-(q_1)\ell^+(q_2)$ has identical distribution as above except for the fact that $I_{5,6,8,9}\to -I_{5,6,8,9}$ which results from the switch in sign in the amplitude $\mathcal{A}_\perp$. Substituting the expressions

Eqs. (3.21) in Eq. (3.20) we get,

$$
\begin{aligned}
I(q^2,\theta_\ell,\theta_K,\phi) &= \frac{9}{16\pi}\Bigg[\frac{(|\mathcal{A}_\perp^L|^2+|\mathcal{A}_\perp^R|^2+|\mathcal{A}_\parallel^L|^2+|\mathcal{A}_\parallel^R|^2)}{4}\sin^2\theta_K(1+\cos^2\theta_\ell) \\
&+ (|\mathcal{A}_0^L|^2+|\mathcal{A}_0^R|^2)\cos^2\theta_K\sin^2\theta_\ell \\
&+ \frac{(|\mathcal{A}_\perp^L|^2+|\mathcal{A}_\perp^R|^2-|\mathcal{A}_\parallel^L|^2-|\mathcal{A}_\parallel^R|^2)}{4}\cos 2\phi\sin^2\theta_K\sin^2\theta_\ell \\
&+ \mathrm{Re}(\mathcal{A}_\parallel^L\mathcal{A}_\perp^{L^*}-\mathcal{A}_\parallel^R\mathcal{A}_\perp^{R^*})\cos\theta_\ell\sin^2\theta_K \\
&+ \frac{\mathrm{Re}(\mathcal{A}_0^L\mathcal{A}_\perp^{L^*}-\mathcal{A}_0^R\mathcal{A}_\perp^{R^*})}{\sqrt{2}}\cos\phi\sin\theta_\ell\sin(2\theta_K) \\
&+ \frac{\mathrm{Re}(\mathcal{A}_0^L\mathcal{A}_\parallel^{L^*}+\mathcal{A}_0^R\mathcal{A}_\parallel^{R^*})}{2\sqrt{2}}\cos\phi\sin(2\theta_\ell)\sin(2\theta_K)\Bigg]. \qquad (3.22)
\end{aligned}
$$

Integrating over $\cos\theta_K$, $\cos\theta_\ell$, and ϕ results in the differential decay rate with respect to the invariant lepton mass, which is given by the sum of the modulus squared of all the transversity amplitudes at the same invariant lepton mass:

$$
\frac{d\Gamma}{dq^2} = \sum_{\lambda=0,\parallel,\perp}(|\mathcal{A}_\lambda^L|^2+|\mathcal{A}_\lambda^R|^2) \qquad (3.23)
$$

From Eq. (3.22) we see that from a complete study of the angular distribution will allow us to measure six observables. Among these are the three helicity fractions which are defined as,

$$
F_L = \frac{|\mathcal{A}_0^L|^2+|\mathcal{A}_0^R|^2}{\Gamma_f}, \qquad (3.24)
$$

$$
F_\parallel = \frac{|\mathcal{A}_\parallel^L|^2+|\mathcal{A}_\parallel^R|^2}{\Gamma_f}, \qquad (3.25)
$$

$$
F_\perp = \frac{|\mathcal{A}_\perp^L|^2+|\mathcal{A}_\perp^R|^2}{\Gamma_f}, \qquad (3.26)
$$

where, $\Gamma_f \equiv \sum_\lambda(|\mathcal{A}_\lambda^L|^2+|\mathcal{A}_\lambda^R|^2)$. The helicity fractions sums up to unity, $F_L+F_\parallel+F_\perp=1$. The well known forward-backward asymmetry $A_{\rm FB}$ is defined as,

$$
A_{\rm FB} = \frac{\Big[\int_0^1 - \int_{-1}^0\Big]d\cos\theta_\ell\frac{d^2(\Gamma+\bar{\Gamma})}{dq^2 d\cos\theta_\ell}}{\int_{-1}^1 d\cos\theta_\ell\frac{d^2(\Gamma+\bar{\Gamma})}{dq^2 d\cos\theta_\ell}}, \qquad (3.27)
$$

It can be expressed in terms of the transversity amplitudes as,

$$A_{\rm FB} \;=\; \frac{3}{2}\frac{{\rm Re}\Big[\mathcal{A}_\parallel^L\mathcal{A}_\perp^L - \mathcal{A}_\parallel^R\mathcal{A}_\perp^R\Big]}{\Gamma_f}. \tag{3.28}$$

The observables can be extracted from a fit to angular distribution. A complete angular analysis requires much larger data set than is currently analyzed, hence angular distributions in terms of only one angular variable have been studied. The angular distribution as a function of q^2 and $\cos\theta_\ell$ with ϕ and $\cos\theta_K$ integrated out is given by:

$$\frac{d^2\Gamma}{dq^2 d\cos\theta_\ell} = \Gamma\Big[A_{\rm FB}\cos\theta_\ell + \frac{3}{8}(1-F_L)\,(1+\cos^2\theta_\ell) + \frac{3}{4}F_L(1-\cos^2\theta_\ell)\Big]\,. \tag{3.29}$$

Angular analysis in terms of $\cos\theta_\ell$ enables the measurement of both F_L the longitudinal helicity fraction and the forward–backward asymmetry $A_{\rm FB}$. The other helicity fractions $F_\perp$ or $F_\parallel$ can be measured from the angular distributions as well but it is believed that one need to perform a full angular analysis. It is, however, easy to see that a combination of F_L and $F_\perp$ can be measured if the angular distribution in terms of ϕ is studied. The angular distribution in ϕ is given by:

$$\frac{d^2\Gamma}{dq^2 d\phi} = \frac{\Gamma}{2\pi}\Big[1 - \frac{1-F_L-2F_\perp}{2}\cos 2\phi + I_9\sin 2\phi\Big]. \tag{3.30}$$

The distribution in ϕ allows us to measure $1-F_L-2F_\perp$. If F_L is measured independently one can obtain $F_\perp$. The distribution also allows us to measure I_9, which is immeasurably small in the standard model [115], and assumed to be zero in our study. Recently the angular analysis in ϕ has been studied [112, 114] by CDF and LHCb collaborations. In the next section we will show that $1-F_L-2F_\perp$ is also small in the standard model as a consequence of heavy quark effective theory. We will conclude in subsequent section that the angular distribution will be almost constant for $q^2 \approx 0$, with small variation in $\cos\phi$ at large q^2. There is yet another technique to measure $F_\perp$ which involves studying angular distributions in terms of only one angular variable. However, this approach requires independent analysis in the transversity frame defined with J/ψ at rest. In this frame the lepton makes an angle $\theta_{\rm tr}$ with the z-axis. The

expression for the differential decay rate as a function of $\cos\theta_{\rm tr}$ is given by:

$$\frac{d\Gamma}{dq^2 d\cos\theta_{\rm tr}} = \Gamma\Big[\frac{3}{8}(1-F_\perp)(1+\cos^2\theta_{\rm tr}) + \frac{3}{4}F_\perp(1-\cos^2\theta_{\rm tr})\Big] \tag{3.31}$$

Clearly, $F_\perp$ the perpendicular polarization fraction can be measured from a fit to $\cos\theta_{\rm tr}$ in the transversity frame. The errors in F_L and $F_\perp$ measured in this fashion will be correlated and the correlation will have to be taken care of. Two other angular observables A_4 and A_5 are defined as,

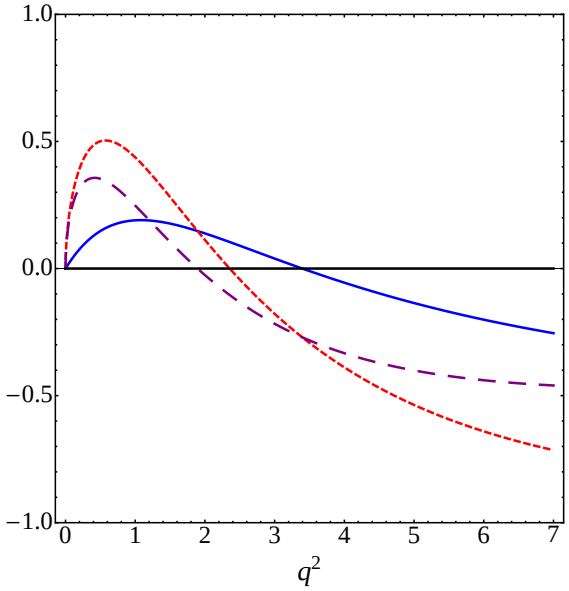

Figure 3.2: Using heavy-to-light form factor at large recoil (see Sec. (2.3)) the normalized angular asymmetries $A_{\rm FB}$ (solid line in red), A_5 (long dashed line in purple) and $A_{\rm FB} + \sqrt{2}A_5$ (short dashed line red) are plotted as a function of q^2. The higher order corrections to the form factors are neglected and all the inputs are taken at their central values. This figure is just to indicate the zero crossing behavior of the angular observables.

$$A_4 = \frac{\int_{D_{LR}} d\phi \int_D d\cos\theta_K \int_D d\cos\theta_\ell \frac{d^4(\Gamma-\bar{\Gamma})}{dq^2 d^3\Omega}}{\int_0^{2\pi} d\phi \int_{-1}^1 d\cos\theta_K \int_{-1}^1 d\cos\theta_\ell \frac{d^4(\Gamma+\bar{\Gamma})}{dq^2 d^3\Omega}} \tag{3.32}$$

$$A_5 = \frac{\int_{-1}^1 d\cos\theta_\ell \int_{D_{LR}} d\phi \int_D d\cos\theta_K \frac{d^4(\Gamma+\bar{\Gamma})}{dq^2 d^3\Omega}}{\int_{-1}^1 d\cos\theta_\ell \int_0^{2\pi} d\phi \int_{-1}^1 d\cos\theta_K \frac{d^4(\Gamma+\bar{\Gamma})}{dq^2 d^3\Omega}} \tag{3.33}$$

where, $\int_D \equiv \int_0^1 - \int_{-1}^0$ and $\int_{D_{LR}} \equiv \int_{\pi/2}^{3\pi/2} - \int_{-\pi/2}^{\pi/2}$. In terms of the transversity amplitudes A_4 and A_5 can be written as,

$$A_4 = \frac{\sqrt{2}}{\pi}\frac{\mathrm{Re}(\mathcal{A}_0^L\mathcal{A}_\parallel^{L*}) + \mathrm{Re}(\mathcal{A}_0^R\mathcal{A}_\parallel^{R*})}{\Gamma_f}, \tag{3.34}$$

$$A_5 = \frac{3}{2\sqrt{2}}\frac{\mathrm{Re}(\mathcal{A}_0^L\mathcal{A}_\perp^{L} - \mathcal{A}_0^R\mathcal{A}_\perp^{R})}{\Gamma_f} \tag{3.35}$$

The importance of the zero crossing point $A_{\rm FB}$ [86] which is sensitive to new physics is very well known. We notice that the observables A_5 and $A_{\rm FB} + \sqrt{2}A_5$ also has similar zero crossing behavior. In Fig.3.2 we have plotted the variation of $A_{\rm FB}$, A_5 and $A_{\rm FB} + \sqrt{2}A_5$ as a function of q^2. We have taken heavy to light form factors at large recoil. All the inputs are taken at their central values and higher order corrections to the form factors are neglected.

Chapter 4

Model Independent Extraction of New Physics

It is well known that the new physics can either be discovered by direct production of new particles at high energies or by indirect searches at high luminosity facilities where it can contribute virtually to loop processes. The most well known example of the latter kind is the muon magnetic moment. Unfortunately, even though muon is a lepton, hadronic contributions have to be estimated and turn out to be the limiting factor in the search for new physics. Indirect searches for new physics often involve precision measurement of a single quantity as in the case of muon magnetic moment. The single measurement is compared to a theoretical estimate that needs to be accurately calculated. There are however, certain decays which involve measurement of several related observables. The most well known example is the $B \to K^* \ell^+ \ell^-$ decay. The decay is described in terms of six transversity amplitudes that enable us to construct multitude of observables to be extracted from the angular distribution. In addition to the branching fractions Γ_f, there are six observables mentioned in the previous chapter: the longitudinal helicity fraction F_L, perpendicular helicity fraction $F_\perp$, parallel helicity fraction $F_\parallel$, the forward-backward helicity fraction $A_{\rm FB}$ and angular asymmetries A_4 and A_5. The three helicity fractions are constrained by $F_L + F_\parallel + F_\perp = 1$ resulting in six independent observables. Each of these observables can be written in terms of the six transversity amplitudes $\mathcal{A}^{L,R}_{0,\parallel,\perp}$. which are

written in Eq. (3.15) to (3.17) in terms of Wilson coefficients and hadronic form factors. Due to poor knowledge of form factors, the transversity amplitudes and the observables constructed therefrom are polluted by hadronic uncertainties.

In the search for new physics, it is therefore crucial to effectively separate the effect of new physics from hadronic uncertainties that can contribute to the decay. This has brought into focus the need for theoretically cleaner observables, i.e. observables that are relatively free from hadronic uncertainties. Construction of such observables has been attempted by various authors. For example the observable $A_T^{(2)}$ was constructed in Ref. [103] and $A_T^{(3,4,5)}$ was constructed in Ref.[88, 119]. At low-q^2, the observables $A_T^{(\mathrm{re,\,im})}$ [120] show new physics sensitivity and the high-q^2 analog of the same are $H_T^{(1,2,3,4,5)}$ [104]. These observables are constructed in such a way that the dependance of soft form factors cancel in ratios. *However such cancellations hold only at leading order in perturbation theory*. In the Refs. [121, 122] we have shown that the multitude of related observables obtained via an angular analysis in $B \to K^* \ell^+ \ell^-$ can provide many *"clean tests" of the new physics to all orders in* α_s. The hallmark of these "tests" is that several of them are independent of the universal form factors $\xi_\parallel$ and $\xi_\perp$ in heavy quark effective theory. Indeed, in the large recoil region considered in Refs. [121, 122], these relations are even more interesting as they are unaffected by corrections to all orders in α_s. *We will refer to such relations that are independent of universal form factors and are unaffected by corrections to all orders in* α_s *as "clean relations."* A variety of relations are derived, including relations between observables and form factors that are independent of Wilson coefficients. Such relations are inherently clean and important as they enable verification of hadronic estimates. We show how the form factor ratios can be measured directly from the ratios of helicity amplitudes measured at the zero crossings of asymmetries without any assumptions what so ever. Another achievement is the derivation of a relation between observables alone, based entirely on the assumption that the amplitudes have form given by the standard model, and is independent of form factors and Wilson coefficients. This relation would provide an unambiguous test of the standard model relying purely on observables. We also presented a clean expression for the "effective photon vertex" involving the same operator that also contributes to the process

$B \to K^*\gamma$. We emphasize that the amplitude for $B \to K^*\gamma$ involves the universal form factor $\xi_\parallel$ and is inherently not clean. It is hence some what surprising that the same vertex can be expressed independently of the universal form-factors in heavy quark effective theory in a way that is valid at order $1/m_b$ to all orders in α_s. While C_9 and C_{10} individually depend on form factors, we find that the expression for the ratio C_9/C_{10} is clean. Based purely on the signs of the form factors and the fact that the zero crossing of the forward backward asymmetry has been observed, we convincingly concluded that the signs of the Wilson coefficients are in agreement with Standard Model. We found that there exist three sets of equivalent solutions to each of the three Wilson coefficients involving different observables. However, only two of the sets are independent. It was shown that the allowed parameter space for observables is very tightly constrained in Standard Model, thereby providing clean signals of New Physics.

4.1 Notataion: Observables in terms of Form Factors.

As discussed in Chapter 2, the treatment of form factors depends largely on the recoil energy of the K^* meson or equivalently q^2. There are two distinct recoil regions where the form factors are treated differently. In the large recoil region, the next to leading order corrections including the factorizable and the non-factorizable corrections are parametrically included in the transversity amplitudes by the replacements $C_9^{\rm eff} \to C_9$ and $C_7^{\rm eff} T_i \to \mathcal{T}_i$ (see Sec. 2.3). Even at the leading order it is impossible to separate the Wilson coefficient $C_7^{\rm eff}$ from the form factors T_i and they are lumped together in to a single entity. In the low recoil region, the leading order corrections to the form factors are the non-perturbative effects up to and including terms suppressed by $\Lambda_{\rm QCD}/Q$, where $Q = \{m_b, \sqrt{q^2}\}$ and include next-to-leading order corrections from the charm quark mass m_c and the strong coupling at $O(m_c^2/Q^2, \alpha_s)$. Our motivation therefore is to present methods to extract new physics signals independently of the hadronic uncertainties. The idea is to write the transversity amplitudes in their most general form that is valid to all orders in α_s and

encompasses both factorizable and non-factorizable corrections to the form factors [121, 122],

$$\mathcal{A}_{\perp}^{L,R} = C_{L,R}\mathcal{F}_{\perp} - \widetilde{\mathcal{G}}_{\perp} \tag{4.1}$$

$$\mathcal{A}_{\parallel}^{L,R} = C_{L,R}\mathcal{F}_{\parallel} - \widetilde{\mathcal{G}}_{\parallel} \tag{4.2}$$

$$\mathcal{A}_{0}^{L,R} = C_{L,R}\mathcal{F}_{0} - \widetilde{\mathcal{G}}_{0} \tag{4.3}$$

At leading order $C_{L,R} = C_9^{\text{eff}} \mp C_{10}$. The form factors $\mathcal{F}_\lambda$ and $\widetilde{\mathcal{G}}_\lambda$ can be related to the form factors $V(q^2)$, $A_{1,2}(q^2)$ and $T_{1,2,3}(q^2)$ by comparing the Eqs. (3.15)– (3.17) with the Eqs. (4.1) – (4.3). Including higher order QCD corrections and "non-factorizable" corrections, $\mathcal{F}_\lambda$ and $\widetilde{\mathcal{G}}_\lambda$ can be written as [121, 122],

$$\widetilde{\mathcal{G}}_{\perp} = -N\sqrt{2\lambda(m_B^2, m_{K^*}^2, q^2)}\frac{2m_b}{q^2}C_7^{\text{eff}}T_1(q^2) + \cdots \tag{4.4}$$

$$\widetilde{\mathcal{G}}_{0} = \frac{Nm_b}{m_{K^*}\sqrt{q^2}}\Big[(m_B^2 + 3m_{K^*}^2 - q^2)C_7^{\text{eff}}T_2(q^2) - \lambda(m_B^2, m_{K^*}^2, q^2)\frac{C_7^{\text{eff}}T_3(q^2)}{m_B^2 - m_{K^*}^2}\Big] + \cdots. \tag{4.5}$$

$$\widetilde{\mathcal{G}}_{\parallel} = N\sqrt{2}(m_B^2 - m_{K^*}^2)\frac{2m_b}{q^2}C_7^{\text{eff}}T_2(q^2) + \cdots \tag{4.6}$$

$$\mathcal{F}_{\perp} = N\sqrt{2\lambda(m_B^2, m_{K^*}^2, q^2)}\,\frac{V(q^2)}{m_B + m_{K^*}} \tag{4.7}$$

$$\mathcal{F}_{\parallel} = -N\sqrt{2}(m_B + m_{K^*})A_1(q^2) \tag{4.8}$$

$$\mathcal{F}_{0} = \frac{-N}{2m_{K^*}\sqrt{q^2}}\Big[(m_B^2 - m_{K^*}^2 - q^2)(m_B + m_{K^*})A_1(q^2) - \lambda(m_B^2, m_{K^*}^2, q^2)\frac{A_2(q^2)}{m_B + m_{K^*}}\Big] \tag{4.9}$$

In the expressions of $\widetilde{\mathcal{G}}_\lambda$, the ellipses indicate the higher order QCD corrections as well as the non-factorizable corrections. At low recoil, the non-factorizable corrections are small and can be ignored. We can therefore write the form factors $\mathcal{G}_\lambda$ at low recoil as:

$$\widetilde{\mathcal{G}}_\lambda = C_7^{\text{eff}}\mathcal{G}_\lambda \tag{4.10}$$

So at low recoil, the Wilson coefficient C_7^{eff} can be separated from the form factor $\mathcal{G}_\lambda$. Using Eqs. (4.1) to (4.3) the observables F_L, $F_\parallel$, $F_\perp$, A_{FB}, A_4 and A_5 can be written in terms of the

Wilson coefficients and from factors as [121, 122],

$$
\begin{aligned}
F_L\Gamma_f &= 2(C_9^2+C_{10}^2)\mathcal{F}_0^2+2\widetilde{\mathcal{G}}_0^2-4C_9\mathcal{F}_0\widetilde{\mathcal{G}}_0 && (4.11)\\
F_\parallel\Gamma_f &= 2(C_9^2+C_{10}^2)\mathcal{F}_\parallel^2+2\widetilde{\mathcal{G}}_\parallel^2-4C_9\mathcal{F}_\parallel\widetilde{\mathcal{G}}_\parallel && (4.12)\\
F_\perp\Gamma_f &= 2(C_9^2+C_{10}^2)\mathcal{F}_\perp^2+2\widetilde{\mathcal{G}}_\perp^2-4C_9\mathcal{F}_\perp\widetilde{\mathcal{G}}_\perp && (4.13)\\
\frac{\pi A_4\Gamma_f}{2\sqrt{2}} &= \widetilde{\mathcal{G}}_\parallel\widetilde{\mathcal{G}}_0+(C_9^2+C_{10}^2)\mathcal{F}_0\mathcal{F}_\parallel-C_9(\mathcal{F}_\parallel\widetilde{\mathcal{G}}_0+\widetilde{\mathcal{G}}_\parallel\mathcal{F}_0) && (4.14)\\
\frac{\sqrt{2}A_5\Gamma_f}{3} &= C_{10}(\mathcal{F}_\perp\widetilde{\mathcal{G}}_0+\widetilde{\mathcal{G}}_\perp\mathcal{F}_0)-2C_9C_{10}\mathcal{F}_0\mathcal{F}_\perp && (4.15)\\
\frac{A_{FB}\Gamma_f}{3} &= C_{10}(\mathcal{F}_\parallel\widetilde{\mathcal{G}}_\perp+\mathcal{F}_\perp\widetilde{\mathcal{G}}_\parallel)-2C_9C_{10}\mathcal{F}_\parallel\mathcal{F}_\perp && (4.16)
\end{aligned}
$$

These are the the most general expressions of the observables in terms of form factors and Wilson coefficients. Our aim is to solve the theoretical parameters in terms of the observables and minimum number of inputs. Naively, we have nine theoretical parameters, the three Wilson coefficients C_7, C_9 and C_{10} and the six form factors $\mathcal{F}_0$, $\mathcal{F}_\parallel$, $\mathcal{F}_\perp$, $\widetilde{\mathcal{G}}_0$, $\widetilde{\mathcal{G}}_\parallel$ and $\widetilde{\mathcal{G}}_\perp$ describing the six observables Γ_f, F_L, $F_\perp$, A_4, A_5 and $A_{\rm FB}$. However at the large recoil region the Wilson coefficient $C_7^{\rm eff}$ can not be distinguished from the form factors $\widetilde{\mathcal{G}}_\lambda$. Hence we have only eight independent theoretical parameters: the two Wilson coefficients C_9 and C_{10} and six form factors $\mathcal{F}_0$, $\mathcal{F}_\parallel$, $\mathcal{F}_\perp$, $\widetilde{\mathcal{G}}_0$, $\widetilde{\mathcal{G}}_\parallel$ and $\widetilde{\mathcal{G}}_\perp$. It is obvious that with two theoretical inputs in addition to the observables we should in principle be able to solve for the remaining six theoretical parameters purely in terms of these two reliable inputs and observables.

There are three sets of solutions in terms of different combinations of observables. In our subsequent discussion we derive the first set of solutions. The other two solutions can be derived in the similar way. We simplify the Eqs. (4.12), (4.13) and (4.16) by introducing new variables,

$$
\begin{aligned}
r_\parallel &= \frac{\widetilde{\mathcal{G}}_\parallel}{\mathcal{F}_\parallel}-C_9, && (4.17)\\
r_\perp &= \frac{\widetilde{\mathcal{G}}_\perp}{\mathcal{F}_\perp}-C_9, && (4.18)
\end{aligned}
$$

In terms of $r_\parallel$ and $r_\perp$, we can express Eqs. (4.12), (4.13) as,

$$F_\parallel \Gamma_f = 2\mathcal{F}_\parallel^2 (r_\parallel^2 + C_{10}^2) \tag{4.19}$$

$$F_\perp \Gamma_f = 2\mathcal{F}_\perp^2 (r_\perp^2 + C_{10}^2) \tag{4.20}$$

$$A_{\rm FB} \Gamma_f = 3\mathcal{F}_\perp \mathcal{F}_\parallel C_{10} (r_\parallel + r_\perp). \tag{4.21}$$

To obtain the solutions of the Wilson coefficients in terms of observables, we rewrite the above equations as,

$$r_\parallel^2 + C_{10}^2 = \frac{F_\parallel \Gamma_f}{2\mathcal{F}_\parallel^2} \tag{4.22}$$

$$r_\perp^2 + C_{10}^2 = \frac{F_\perp \Gamma_f}{2\mathcal{F}_\perp^2} \tag{4.23}$$

$$2C_{10}(r_\parallel + r_\perp) = \frac{2}{3}\frac{A_{\rm FB}\Gamma_f}{\mathcal{F}_\perp \mathcal{F}_\parallel}. \tag{4.24}$$

With the help of these equations we can write,

$$\begin{aligned} \frac{F_\parallel F_\perp \Gamma_f^2}{4\mathcal{F}_\parallel^2 \mathcal{F}_\perp^2} &= (r_\parallel r_\perp - C_{10})^2 + C_{10}^2 (r_\parallel + r_\perp)^2 \\ &= (r_\parallel r_\perp - C_{10})^2 + \frac{A_{\rm FB}^2 \Gamma_f^2}{9\mathcal{F}_\parallel^2 \mathcal{F}_\perp^2} \end{aligned}$$

hence,

$$r_\parallel r_\perp - C_{10}^2 = \pm \frac{\Gamma_f}{2\mathcal{F}_\parallel \mathcal{F}_\perp} \sqrt{F_\parallel F_\perp - \frac{4A_{\rm FB}^2}{9}}. \tag{4.25}$$

Now we can express C_{10}^2 in terms of $r_\parallel^2$ using Eq. (4.22) or in terms of $r_\perp^2$ using Eq. (4.23) to re-express $2r_\parallel r_\perp - C_{10}^2$ as,

$$2r_\parallel r_\perp - 2C_{10}^2 = 2r_\parallel r_\perp - \left(\frac{F_\parallel \Gamma_f}{2\mathcal{F}_\parallel^2} - r_\parallel^2\right) - \left(\frac{F_\perp \Gamma_f}{2\mathcal{F}_\perp^2} - r_\perp^2\right)$$

$$= \left[(r_\parallel + r_\perp)^2 - \frac{F_\parallel \Gamma_f}{2\mathcal{F}_\parallel^2} - \frac{F_\perp \Gamma_f}{2\mathcal{F}_\perp^2}\right] \tag{4.26}$$

Equating Eqs. (4.25) and (4.26) we get,

$$\begin{aligned} r_\parallel + r_\perp &= \pm\left[\frac{F_\parallel \Gamma_f}{2\mathcal{F}_\parallel^2} + \frac{F_\perp \Gamma_f}{2\mathcal{F}_\perp^2} \pm \frac{\Gamma_f}{2\mathcal{F}_\parallel \mathcal{F}_\perp} Z_1\right]^{1/2} \\ &= \frac{\pm\sqrt{\Gamma_f}}{\sqrt{2}\mathcal{F}_\perp}\left[\mathsf{P}_1^2 F_\parallel + F_\perp \pm \mathsf{P}_1 Z_1\right]^{1/2} \end{aligned} \tag{4.27}$$

Here we have defined,

$$Z_1 = \sqrt{4F_\parallel F_\perp - \frac{16}{9}A_{\rm FB}^2} \tag{4.28}$$

$$\mathsf{P}_1 = \frac{\mathcal{F}_\perp}{\mathcal{F}_\parallel}, \tag{4.29}$$

The Eqs. (4.22) and (4.23) imply:

$$r_\parallel^2 - r_\perp^2 = \frac{F_\parallel \Gamma_f}{2\mathcal{F}_\parallel^2} - \frac{F_\perp \Gamma_f}{2\mathcal{F}_\perp^2}, \tag{4.30}$$

Using the expression of $r_\parallel + r_\perp$ from Eq.(4.27) we can write

$$\begin{aligned} r_\parallel - r_\perp &= \frac{1}{r_\parallel + r_\perp}\left[\frac{F_\parallel \Gamma_f}{2\mathcal{F}_\parallel^2} - \frac{F_\perp \Gamma_f}{2\mathcal{F}_\perp^2}\right] \\ &= \frac{\pm\sqrt{\Gamma_f}}{\sqrt{2}\mathcal{F}_\perp} \frac{\mathsf{P}_1^2 F_\parallel - F_\perp}{\left[\mathsf{P}_1^2 F_\parallel + F_\perp \pm \mathsf{P}_1 Z_1\right]^{1/2}} \end{aligned} \tag{4.31}$$

In addition to the overall sign ambiguity, there is a sign ambiguity in front of P_1 in both the equations Eqs. (4.27) and (4.31). From Eq. (4.21) we note that $r_\parallel + r_\perp$ is proportional to $A_{\rm FB}$ and hence it vanishes at the zero crossing point of $A_{\rm FB}$. At the zero crossing point of the forward-backward asymmetry we have from Eq. (4.27),

$$r_\parallel + r_\perp\Big|_{A_{\rm FB}=0} = \pm\frac{\sqrt{\Gamma_f}}{\sqrt{2}\mathcal{F}_\perp}\left(\sqrt{F_\perp} \pm \mathsf{P}_1 \sqrt{F_\parallel}\right) = 0 \tag{4.32}$$

The second equality on the right hand side is written from Eq. (4.21). Since P_1 is negative and the expression for $r_\parallel + r_\perp$ should be valid for all values of the observables, the right hand side could go to zero only if positive sign ambiguity is chosen in front of P_1. Up to overall sign ambiguity we can therefore write,

$$r_\parallel + r_\perp = \frac{\pm\sqrt{\Gamma_f}}{\sqrt{2}\mathcal{F}_\perp}\left[\mathsf{P}_1^2 F_\parallel + F_\perp + \mathsf{P}_1 Z_1\right]^{1/2} \tag{4.33}$$

$$r_\parallel - r_\perp = \frac{\pm\sqrt{\Gamma_f}}{\sqrt{2}\mathcal{F}_\perp}\frac{\mathsf{P}_1^2 F_\parallel - F_\perp}{\left[\mathsf{P}_1^2 F_\parallel + F_\perp \pm \mathsf{P}_1 Z_1\right]^{1/2}} \tag{4.34}$$

If we ignore the non-factorizable corrections to form factors and neglect the higher order corrections then at the leading order the Wilson coefficient $C_7^{\rm eff}$ can be distinguished from the form factors $\mathcal{G}_\lambda$. Then the condition $r_\parallel + r_\perp = 0$ gives us the familiar relation for the zero crossing of $A_{\rm FB}$. The definitions of $r_\parallel$ and $r_\perp$ straight forwardly imply that $A_{\rm FB} = 0$ at:

$$\begin{aligned}
2\,C_9 &= C_7^{\rm eff}\left(\frac{\mathcal{G}_\perp}{\mathcal{F}_\perp} + \frac{\mathcal{G}_\parallel}{\mathcal{F}_\parallel}\right), \\
&= -\frac{2m_b}{q^2}C_7\frac{T_1(q^2)}{V(q^2)}(m_B + m_{K^*}) \times \left(1 + \frac{(m_B - m_{K^*})}{(m_B + m_{K^*})}\frac{T_2(q^2)}{T_1(q^2)}\frac{V(q^2)}{A_1(q^2)}\right), \\
&= -\frac{4m_b}{q^2}C_7\frac{T_1(q^2)}{V(q^2)}(m_B + m_{K^*})\left(1 - \frac{m_{K^*}^2}{2m_B^2}\right), \\
&= -\frac{4m_b m_B}{q^2}C_7\left(1 - \frac{m_{K^*}^2}{2m_B^2}\right) + O(\alpha_s)\,.
\end{aligned} \tag{4.35}$$

This is a very well known relation of forward-backward asymmetry zero-crossing [86]. To obtain the last two lines we have used Eqns. (2.19) and (2.18). The $O(\alpha_s)$ dependence arises from the ratio $T_1(q^2)/V(q^2)$ which also depends on $\xi_\perp(q^2)$ [101].

The aforementioned second and the third set of solutions can be obtained by introducing two more variables r_0 and $r_\wedge$,

$$r_0 = \frac{\widetilde{\mathcal{G}}_0}{\mathcal{F}_0} - C_9, \tag{4.36}$$

$$r_\wedge = \frac{\widetilde{\mathcal{G}}_\parallel + \widetilde{\mathcal{G}}_0}{\mathcal{F}_\parallel + \mathcal{F}_0} - C_9. \tag{4.37}$$

The solutions are obtained by introducing the combination of variables $(F_L + F_\parallel + \sqrt{2}\pi A_4)$ and $(A_{\rm FB} + \sqrt{2}A_5)$. In terms of r_0 and $r_\wedge$ we can write the expressions of F_L, A_5, $(F_L + F_\parallel + \sqrt{2}\pi A_4)$ and $(A_{\rm FB} + \sqrt{2}A_5)$ as,

$$F_L\Gamma_f = 2\mathcal{F}_0^2(r_0^2 + C_{10}^2) \tag{4.38}$$

$$(F_L + F_\parallel + \sqrt{2}\pi A_4)\Gamma_f = 2(\mathcal{F}_0 + \mathcal{F}_\parallel)^2(r_\wedge^2 + C_{10}^2) \tag{4.39}$$

$$\sqrt{2}A_5\Gamma_f = 3\mathcal{F}_\perp\mathcal{F}_0 C_{10}(r_0 + r_\perp) \tag{4.40}$$

$$(A_{\rm FB} + \sqrt{2}A_5)\Gamma_f = 3\mathcal{F}_\perp(\mathcal{F}_0 + \mathcal{F}_\parallel)C_{10}(r_\wedge + r_\perp) \tag{4.41}$$

Similar to the Eqs. (4.33) and (4.34) we derive the expressions of $r_0 + r_\perp$, $r_0 - r_\perp$ and $r_\wedge + r_\perp$, $r_\wedge - r_\perp$. We write $r_0 + r_\perp$ as,

$$r_0 + r_\perp = \pm\frac{\sqrt{\Gamma_f}}{\sqrt{2}\mathcal{F}_\perp}\left(\mathsf{P}_2^2 F_L + F_\perp \pm \mathsf{P}_2 Z_2\right)^{1/2} \tag{4.42}$$

where we have defined

$$Z_2 = \sqrt{4F_L F_\perp - \frac{32}{9}A_5^2}, \tag{4.43}$$

$$\mathsf{P}_2 = \frac{\mathcal{F}_\perp}{\mathcal{F}_0} \tag{4.44}$$

In the equation Eq. (4.42) the sign ambiguity is removed by studying the behavior of $r_0 + r_\perp$ at the zero crossing point of the angular asymmetry A_5. The Eq. (4.40) imply that $r_0 + r_\perp = 0$ when $A_5 = 0$. On the other hand from Eq. (4.42) we can write,

$$r_0 + r_\perp\Big|_{A_5=0} = \pm\frac{\sqrt{\Gamma_f}}{\sqrt{2}\mathcal{F}_\perp}\left(\sqrt{F_\perp} \pm \mathsf{P}_2\sqrt{F_L}\right) = 0 \tag{4.45}$$

Since both $\sqrt{F_\perp}$ and $\sqrt{F_L}$ are positive and P_2 is negative the right hand side of the above can go to zero only if the positive sign ambiguity before P_2 is chosen. Hence after removing the

sign ambiguity we can write,

$$r_0 + r_\perp = \pm\frac{\sqrt{\Gamma_f}}{\sqrt{2}\mathcal{F}_\perp}\left(\mathsf{P}_2^2 F_L + F_\perp + \mathsf{P}_2 Z_2\right)^{1/2} \tag{4.46}$$

$$r_0 - r_\perp = \frac{\pm\sqrt{\Gamma_f}}{\sqrt{2}\mathcal{F}_\perp}\frac{\mathsf{P}_2^2 F_L - F_\perp}{\left[\mathsf{P}_2^2 F_L + F_\perp + \mathsf{P}_2 Z_2\right]^{1/2}} \tag{4.47}$$

where the expression of $r_0 - r_\perp$ is derived in the same way as Eq. (4.34). Finally we write down the solutions for $r_\wedge + r_\perp$ and $r_\wedge - r_\perp$,

$$r_\wedge + r_\perp = \pm\frac{\sqrt{\Gamma_f}}{\sqrt{2}\mathcal{F}_\perp}\left[\mathsf{P}_3^2(F_L + F_\parallel + \sqrt{2}\pi A_4) + F_\perp + \mathsf{P}_3 Z_3\right]^{1/2} \tag{4.48}$$

$$r_\wedge - r_\perp = \frac{\pm\sqrt{\Gamma_f}}{\sqrt{2}\mathcal{F}_\perp}\frac{\mathsf{P}_3^2(F_L + F_\parallel + \sqrt{2}\pi A_4) - F_\perp}{\left[\mathsf{P}_3^2(F_L + F_\parallel + \sqrt{2}\pi A_4) + F_\perp + \mathsf{P}_3 Z_3\right]^{1/2}} \tag{4.49}$$

where we have defined,

$$Z_3 = \sqrt{4(F_L + F_\parallel + \sqrt{2}\pi A_4)F_\perp - \frac{16}{9}(A_{\rm FB} + \sqrt{2}A_5)^2}. \tag{4.50}$$

$$\mathsf{P}_3 = \frac{\mathcal{F}_\perp}{\mathcal{F}_0 + \mathcal{F}_\parallel} \tag{4.51}$$

Once again we note that there appear a sign ambiguity before P_3 which has been removed by observing the behavior of $r_\wedge + r_\perp$ at the zero-crossing point of $A_{\rm FB} + \sqrt{2}A_5$. The form factor ratio P_3 defined above can be expressed in terms of previously defined P_1 and P_2 as,

$$\mathsf{P}_3 = \frac{\mathsf{P}_1\mathsf{P}_2}{\mathsf{P}_1 + \mathsf{P}_2} \tag{4.52}$$

In addition to the form factor ratios P_1, P_2 and P_3 we introduce three other form factors ratios P_1', P_2' and P_3' which will appear in our future discussions. These are defined as,

$$\mathsf{P}_1' = \frac{\widetilde{\mathcal{G}}_\perp}{\widetilde{\mathcal{G}}_\parallel}, \tag{4.53}$$

$$\mathsf{P}_2' = \frac{\widetilde{\mathcal{G}}_\perp}{\widetilde{\mathcal{G}}_0}, \tag{4.54}$$

$$\mathsf{P}'_3 \;=\; \frac{\widetilde{\mathcal{G}}_\perp}{\widetilde{\mathcal{G}}_\parallel + \widetilde{\mathcal{G}}_0} = \frac{\mathsf{P}'_1\mathsf{P}'_2}{\mathsf{P}'_1 + \mathsf{P}'_2}. \tag{4.55}$$

4.2 Form Factor Ratios.

In the subsequent sections we will derive the expressions of Wilson coefficients and "effective photon" vertex in terms of observables. The six form factor ratios P_1, P_2, P_3, P'_1, P'_2 and P'_3 in the previous section will be used as theoretical inputs. In this section we discuss the theoretical reliability of these form factor ratios at large and the low recoil regions of the K^* meson.

4.2.1 Form Factor Ratios at Large Recoil Region.

At large recoil the seven form factors can be expressed in terms of only two soft form factors $\xi_\perp(q^2)$ and $\xi_\parallel(q^2)$ (see Chapter 2). At leading order in $\Lambda_{\rm QCD}/m_b$ the form factors receive radiative corrections and "non-factorizable" corrections. In Chapter 2 we have shown that the ratios $V(q^2)/A_1(q^2)$ and $T_1(q^2)/T_2(q^2)$ are unaffected by higher order corrections at the large recoil region and are theoretically reliably calculated. Using Eqs. (2.18) and (2.22) the form factor ratios P_1 and P'_1 can be written as,

$$\mathsf{P}_1 \;=\; \frac{\mathcal{F}_\perp}{\mathcal{F}_\parallel} = -\frac{\sqrt{\lambda(m_B^2, m_{K^*}^2, q^2)}}{(m_B + m_{K^*})^2}\,\frac{V(q^2)}{A_1(q^2)} = \left[-\frac{\sqrt{\lambda(m_B^2, m_{K^*}^2, q^2)}}{2E_{K^*}m_B}\right], \tag{4.56}$$

$$\mathsf{P}'_1 \;=\; \frac{\widetilde{\mathcal{G}}_\perp}{\widetilde{\mathcal{G}}_\parallel} = -\frac{\sqrt{\lambda(m_B^2, m_{K^*}^2, q^2)}}{m_B^2 - m_{K^*}^2}\,\frac{\mathcal{T}_1}{\mathcal{T}_2} = \left[-\frac{\sqrt{\lambda(m_B^2, m_{K^*}^2, q^2)}\,m_B}{2E_{K^*}(m_B^2 - m_{K^*}^2)}\right]. \tag{4.57}$$

The form factor ratios P_1 and P'_1 are therefore negative and *independent of universal form factors $\xi_\parallel(q^2)$ and $\xi_\perp(q^2)$ to all orders in the strong coupling constant α_s in perturbation theory,* including "non-factorizable" corrections at leading order in $\Lambda_{\rm QCD}/m_b$ in the heavy quark expansion. The ratios P_1 and P'_1 therefore can used by as reliable theoretical inputs. The other form factor ratios $\mathsf{P}_{2,3}$ and $\mathsf{P}'_{2,3}$ are not independent of the soft form factors and hence are not regarded as theoretically clean inputs. In our subsequent discussions we will derive relations expressing $\mathsf{P}_{2,3}$ and $\mathsf{P}'_{2,3}$ in terms of P_1 and P'_1 and observables.

The expressions Eqs. (4.56) and (4.57) are valid for large recoil region where q^2 is small and are usually considered extremely accurate for q^2 between 1 GeV^2 and 6 GeV^2 [101]. The region $q^2 < 1$ GeV^2 is ignored to eliminate resonance contributions which might not only introduce uncertainties but also introduce complex contributions which we have assumed are absent. Unless otherwise stated, large recoil region would mean $0.10\text{GeV}^2 \leq q^2 \leq 12.86\text{GeV}^2$. We stress that once the non-factorizable corrections are taken into account, the Wilson coefficient C_7^{eff} can no longer be separated from the hadronic form factor. The C_7^{eff} and the the hadronic form factors are lumped together into an effective photon vertex $\widetilde{\mathcal{G}}_\lambda$, which as we will show, can be expressed in terms of observables and the form factors P_1 and P'_1. For our future numerical analysis we compile the values of P'_1 and $\mathcal{F}_\parallel$ at low recoil region in the Table. 4.1. The q^2 binning used in Table. 4.1 is the same as the one used by the LHCb experiments [113, 114].

GeV^2	0.10-2	2-4.3	4.3-8.68	10.09-12.86	1-6
P_1	-0.8924	-0.9286	-0.9034	-0.8337	-0.9259
P'_1	-0.9189	-0.9561	-0.9302	-0.8585	-0.9533
$\mathcal{F}_\parallel(10^{-12})$	-5.7667	-11.330	-17.4311	-25.8917	-11.8692

Table 4.1: The form factor ratios $\mathsf{P}_1, \mathsf{P}'_1$ and $\mathcal{F}_\parallel$ averaged over different q^2 bins at large recoil region.

4.2.2 Form Factor Ratios at Low Recoil Region.

In the low recoil limit the "non-factorizable" corrections and higher order corrections are ignorable. Hence we can write $\widetilde{\mathcal{G}}_\lambda = C_7^{\text{eff}}\mathcal{G}_\lambda$ for all $\lambda = \{0, \parallel, \perp\}$. The conditions in Eqs. (2.22) to (2.24) together with Eq. (4.4), on ignoring m_{K^*}/m_B terms, can be recast as,

$$\frac{\mathcal{G}_\parallel}{\mathcal{F}_\parallel} = \frac{\mathcal{G}_\perp}{\mathcal{F}_\perp} = \frac{\mathcal{G}_0}{\mathcal{F}_0} \equiv \hat{\kappa} = -\kappa\frac{2m_B m_b}{q^2}. \tag{4.58}$$

This implies

$$\mathsf{P}_1 = \mathsf{P}'_1, \qquad \mathsf{P}_2 = \mathsf{P}'_2, \qquad \mathsf{P}_3 = \mathsf{P}'_3 \tag{4.59}$$

and hence

$$r_{\parallel} = r_{\perp} = r_0 = r_{\wedge} \equiv r. \tag{4.60}$$

In the low recoil limit the form factor ratios P_1 and P'_1 are easily derived to be,

$$\mathsf{P}_1 \;=\; \mathsf{P}'_1 = \frac{-\sqrt{\lambda(m_B^2, m_{K^*}^2, q^2)}}{(m_B + m_{K^*})^2} \frac{V(q^2)}{A_1(q^2)}. \tag{4.61}$$

Note that in this limit the form factors are parametrized according to Eq. (2.26). The low-recoil approximation is expected to work well in region $14.18\text{GeV}^2 \leq q^2 \leq 19\text{GeV}^2$. Conventionally the low-recoil region is meant to imply this range of q^2. In the low recoil limit we need to take special care of the fact that $\mathsf{P}_1 = \mathsf{P}'_1$. For our future numerical analysis we compile the values of

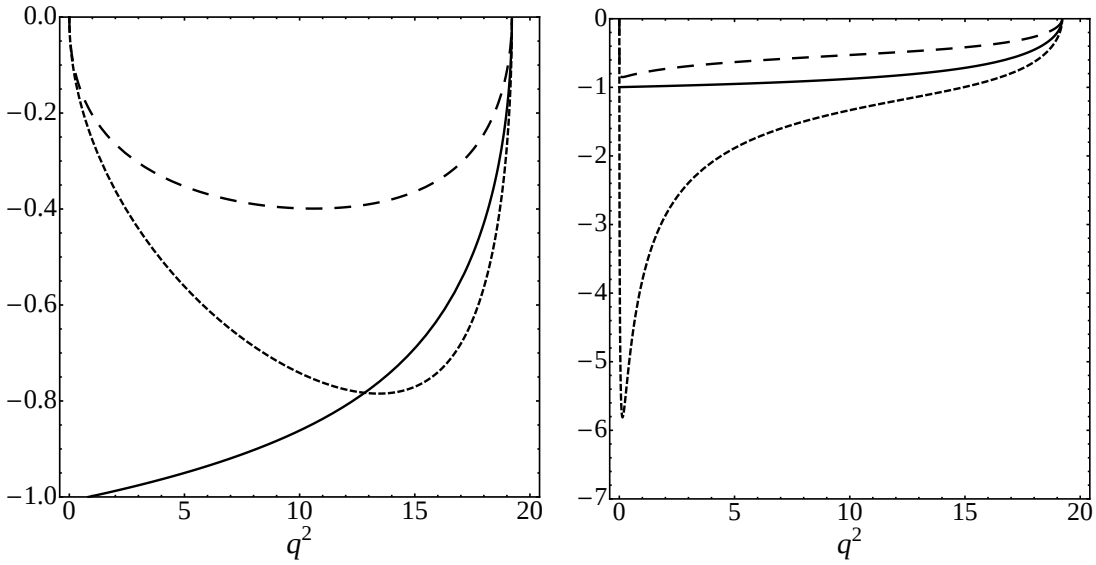

Figure 4.1: In the panel to the left the form factor ratios P_1 (solid curve), P_2 (short dashed) and P_3 (long dashed) are shown as functions of q^2. In the panel to the right we have plotted P'_1 (solid curve), P'_2 (short dashed) and P'_3 (long dashed) against q^2.

P'_1 and $\mathcal{F}_{\parallel}$ at low recoil region in the Table. 4.2. For comparison with the experimental results we calculate the values averaged over different dilepton mass squared q^2 bins. The q^2 binning used in Table. 4.2 is the same as the one used by the LHCb experiment [113, 114]. Also shown in the tables are the numerical values of the form factor $\mathcal{F}_{\parallel}$. In Fig. 4.1 we show the variation of form factor ratios $\mathsf{P}_{1,2,3}$ and $\mathsf{P}'_{1,2,3}$ as a function of q^2. The parametrization of $V(q^2)$, $A_{1,2,3}(q^2)$ and $T_{1,2}(q^2)$ are taken from Eq. (2.26). This parametrization is obtained from light cone sum

GeV^2	14.18-16	16-19
P_1	-0.6836	-0.4719
P'_1	-0.7093	-0.4952
$\mathcal{F}_{\parallel}(10^{-12})$	-27.8735	-25.0050

Table 4.2: The form factor ratios P_1, P'_1 and $\mathcal{F}_{\parallel}$ averaged over different q^2 bins at low recoil.

rules and valid at the low recoil region. Here these are extrapolated from their region of validity to large recoil region with physical pole. In the left panel of the figure the variation of P_1, P_2 and P_3 are shown respectively in solid, short-dashed and long-dashed lines. In the panel to the right P'_1, P'_2 and P'_3 are shown respectively in solid, short-dashed and long-dashed lines. The purpose of these figures is to show that all the six form factor ratios are negative in the region of interest.

4.3 Solution of Wilson coefficients in terms of observables.

In this section we derive the expressions of Wilson coefficients C_9, C_{10} and the "effective photon vertex". As previously mentioned, there are three sets of solutions. From Eqs. (4.24) and (4.33) we can express C_{10} in terms forward-backward asymmetry and helicity fractions $F_{\parallel}$ and $F_{\perp}$ as [121, 122],

$$C_{10} = \frac{\sqrt{\Gamma_f}}{\sqrt{2}\mathcal{F}_{\parallel}} \frac{2}{3} \frac{A_{\rm FB}}{\Big[\pm \sqrt{P_1^2 F_{\parallel} + F_{\perp} + P_1 Z_1} \Big]} \,. \tag{4.62}$$

The two theoretical inputs that are required to measure the value of C_{10} in experiments are P_1 and $\mathcal{F}_{\parallel}$. The Eq. (4.62) can be used to predict the values of C_{10} in different q^2 bins, using the values of the observables measured in experiments, and the two theoretical inputs P_1 and $\mathcal{F}_{\parallel}$. It should however be noted that due the presence of the form factor $\mathcal{F}_{\parallel}$, the predictions of C_{10} are not completely free from hadronic uncertainties.

The way the matrix element decomposition is defined in the heavy quark and large energy limit at next-to-leading logarithmic order [73], it does not allow us to factor out the Wilson coefficient $C_7^{\rm eff}$ from the hadronic form factors T_i. Hence, the solution of $C_7^{\rm eff}$ is not possible. However we can solve for the "effective photon vertex" $\widetilde{\mathcal{G}}_{\parallel}$. From the Eqs. (4.17) and (4.18) we

get,

$$\begin{aligned} r_\parallel - r_\perp &= \frac{\widetilde{\mathcal{G}}_\parallel}{\mathcal{F}_\parallel} - \frac{\widetilde{\mathcal{G}}_\perp}{\mathcal{F}_\perp} \\ &= \widetilde{\mathcal{G}}_\parallel \frac{\mathsf{P}_1 - \mathsf{P}_1'}{\mathcal{F}_\perp}. \end{aligned} \tag{4.63}$$

Using the expression of $r_\parallel - r_\perp$ from Eq. (4.34) in the above equation we get the expression of $\widetilde{\mathcal{G}}_\parallel$ in terms of observables as:

$$\widetilde{\mathcal{G}}_\parallel = \frac{\sqrt{\Gamma_f}}{\sqrt{2}} \frac{(\mathsf{P}_1^2 F_\parallel - F_\perp)}{\left[\pm (\mathsf{P}_1 - \mathsf{P}_1') \sqrt{\mathsf{P}_1^2 F_\parallel + F_\perp + \mathsf{P}_1 Z_1} \right]}. \tag{4.64}$$

Using Eqs. (4.17) and (4.18) we can write,

$$C_9 = \left[\frac{\widetilde{\mathcal{G}}_\parallel}{\mathcal{F}_\perp} (\mathsf{P}_1 + \mathsf{P}_1') - (r_\parallel + r_\perp) \right].$$

Using the expression of $\widetilde{\mathcal{G}}_\parallel$ from Eq. (4.64) in the above equation we get,

$$C_9 = \frac{\sqrt{\Gamma_f}}{\sqrt{2}\mathcal{F}_\parallel} \frac{(F_\parallel \mathsf{P}_1 \mathsf{P}_1' - F_\perp) - \frac{1}{2}(\mathsf{P}_1 - \mathsf{P}_1') Z_1}{\left[\pm (\mathsf{P}_1 - \mathsf{P}_1') \sqrt{\mathsf{P}_1^2 F_\parallel + F_\perp + \mathsf{P}_1 Z_1} \right]}. \tag{4.65}$$

The only hadronic inputs that enter in the expression of the effective photon vertex are the theoretically clean form factor ratios P_1 and P_1'. In the expression of C_9 there is a source of hadronic uncertainty that comes from $\mathcal{F}_\parallel$.

To derive the three expressions Eqs. (4.62), (4.65) and (4.64) we have removed the sign ambiguities in the solution by looking at the behavior of the solutions at the $A_{\rm FB}$ zero crossing points. All our solutions for the Wilson coefficients depend explicitly on the assumption that $A_{\rm FB} \neq 0$, hence, the Wilson coefficients and the effective photon vertex $\widetilde{\mathcal{G}}_\parallel$ can be determined at any q^2 except at the zero crossing of $A_{\rm FB}$. The denominator of $\widetilde{\mathcal{G}}_\parallel$ and C_9 depend on $\mathsf{P}_1 - \mathsf{P}_1'$ so their behaviors at the point $\mathsf{P}_1 \to \mathsf{P}_1'$ needs careful examination. Unlike the zeros of $A_{\rm FB}$, which can be experimentally determined and hence avoided, the crossing point for P_1 and P_1',

a priori, can only be determined based on calculations and hence may be uncertain. We note that in this limit we have $r_\parallel - r_\perp = 0$, where as in the limit $A_{\rm FB} = 0$ we had $r_\parallel + r_\perp = 0$. Naively, C_9 and $\widetilde{\mathcal{G}}_\parallel$ appear to be divergent in the limit $\mathsf{P}_1 \to \mathsf{P}'_1$, as can be seen from Eqs. (4.65) and (4.64) and indeed Eq. (4.34) cannot be used to determine the Wilson coefficients $C_7^{\rm eff}$ and C_9. However, it is easily seen that the Wilson coefficients are finite when $\mathsf{P}_1 \to \mathsf{P}'_1$. Consider the combination $\widetilde{\mathcal{G}}_\parallel - \mathcal{F}_\parallel C_9$, which is seen from Eqs. (4.64) and (4.65) to be manifestly finite in the limit $\mathsf{P}'_1 \to \mathsf{P}_1$:

$$\widetilde{\mathcal{G}}_\parallel - \mathcal{F}_\parallel C_9 = \sqrt{\frac{\Gamma_f}{2}} \frac{F_\parallel \mathsf{P}_1 + \frac{1}{2} Z_1}{\sqrt{\mathsf{P}_1^2 F_\parallel + F_\perp + \mathsf{P}_1 Z_1}}. \tag{4.66}$$

We will show that the combination $\widetilde{\mathcal{G}}_\parallel - \mathcal{F}_\parallel C_9$ can be determined and indeed if $\mathcal{F}_\parallel$ is assumed $\widetilde{\mathcal{G}}_\parallel$ and C_9 can be individually determined and are finite. So at low recoil limit only the Wilson coefficient C_{10} can be solved and one can not solve for C_9 and $\widetilde{\mathcal{G}}_\parallel$ or for that matter $C_7^{\rm eff}$.

We now derive the second set of solutions of Wilson coefficients C_9 and C_{10} and the effective photon vertex $\widetilde{\mathcal{G}}_0$. Using Eqs. (4.40) and (4.46) we can obtain the expression of C_{10} as,

$$C_{10} \;=\; \frac{\sqrt{\Gamma_f}}{\sqrt{2}\mathcal{F}_0} \frac{2}{3} \frac{\sqrt{2} A_5}{\Big[\pm \sqrt{\mathsf{P}_2^2 F_L + F_\perp + \mathsf{P}_2 Z_2} \Big]}. \tag{4.67}$$

The expression of $\widetilde{\mathcal{G}}_0$ is obtained by using the Eqs. (4.18), (4.36) and (4.47). In terms of observables F_L, $F_\perp$ and A_5 it read as,

$$\widetilde{\mathcal{G}}_0 \;=\; \frac{\sqrt{\Gamma_f}}{\sqrt{2}} \frac{(\mathsf{P}_2^2 F_L - F_\perp)}{\Big[\pm (\mathsf{P}_2 - \mathsf{P}'_2) \sqrt{\mathsf{P}_2^2 F_L + F_\perp + \mathsf{P}_2 Z_2} \Big]}. \tag{4.68}$$

The expression of $\widetilde{\mathcal{G}}_0$ can be obtained by using the Eqs. (4.18), (4.36) and (4.68) as,

$$C_9 \;=\; \frac{\sqrt{\Gamma_f}}{\sqrt{2}\mathcal{F}_0} \frac{(F_L \mathsf{P}_2 \mathsf{P}'_2 - F_\perp) - \frac{1}{2}(\mathsf{P}_2 - \mathsf{P}'_2) Z_2}{\Big[\pm (\mathsf{P}_2 - \mathsf{P}'_2) \sqrt{\mathsf{P}_2^2 F_L + F_\perp + \mathsf{P}_2 Z_2} \Big]}. \tag{4.69}$$

It can be noted that the second set of solutions, Eqs. (4.67), (4.68) and (4.69) can be obtained from the first set, Eqs. (4.62), (4.65) and (4.64) by the following replacements: $F_\parallel \to F_L$,

$A_{\rm FB} \to \sqrt{2}A_5$, $\mathcal{F}_\parallel \to \mathcal{F}_0$, $\widetilde{\mathcal{G}}_\parallel \to \widetilde{\mathcal{G}}_0$ (which also imply that $r_\parallel \to r_0$), $\mathsf{P}_1 \to \mathsf{P}_2$ and $\mathsf{P}'_1 \to \mathsf{P}'_2$.

In the third set of solutions we solve for C_{10}, C_9 and $\widetilde{\mathcal{G}}_\parallel + \widetilde{\mathcal{G}}_0$ in terms of $F_L, F_\perp, A_4$ and A_5. The expression of C_{10} can be obtained by using the Eqs. (4.41) and (4.48). It reads as,

$$C_{10} = \frac{\sqrt{\Gamma_f}}{\sqrt{2}(\mathcal{F}_0 + \mathcal{F}_\parallel)} \frac{2}{3} \frac{A_{FB} + \sqrt{2}A_5}{\left[\pm \sqrt{\mathsf{P}_3^2(F_L + F_\parallel + \sqrt{2}\pi A_4) + F_\perp + \mathsf{P}_3 Z_3} \right]}. \tag{4.70}$$

Using Eqs. (4.18), (4.37) and Eq. (4.49) we can express $\widetilde{\mathcal{G}}_\parallel + \widetilde{\mathcal{G}}_0$ as,

$$\widetilde{\mathcal{G}}_\parallel + \widetilde{\mathcal{G}}_0 = \frac{\sqrt{\Gamma_f}}{\sqrt{2}} \frac{\left(\mathsf{P}_3^2(F_L + F_\parallel + \sqrt{2}\pi A_4) - F_\perp\right)}{\left[\pm (\mathsf{P}_3 - \mathsf{P}'_3) \sqrt{\mathsf{P}_3^2(F_L + F_\parallel + \sqrt{2}\pi A_4) + F_\perp + \mathsf{P}_3 Z_3} \right]}. \tag{4.71}$$

The expression of C_9 can be obtained by using the expression of Eqs. (4.18), (4.37) and Eq. (4.71).

$$C_9 = \frac{\sqrt{\Gamma_f}}{\sqrt{2}(\mathcal{F}_0 + \mathcal{F}_\parallel)} \frac{\left((F_L + F_\parallel + \sqrt{2}\pi A_4)\mathsf{P}_3\mathsf{P}'_3 - F_\perp\right) - \frac{1}{2}(\mathsf{P}_3 - \mathsf{P}'_3)Z_3}{\left[\pm \sqrt{\mathsf{P}_3^2(F_L + F_\parallel + \sqrt{2}\pi A_4) + F_\perp + \mathsf{P}_3.Z_3} \right]}, \tag{4.72}$$

The expressions Eqs. (4.70), (4.71) and (4.72) can be obtained from the Eqs. (4.62), (4.65) and (4.64) by the replacements: $F_\parallel \to F_L + F_\parallel + \sqrt{2}\pi A_4$, $A_{\rm FB} \to A_{\rm FB} + \sqrt{2}A_5$, $\mathcal{F}_\parallel \to \mathcal{F}_\parallel + \mathcal{F}_0$, $\widetilde{\mathcal{G}}_\parallel \to \widetilde{\mathcal{G}}_\parallel + \widetilde{\mathcal{G}}_0$ (which also imply $r_\parallel \to r_\wedge$), $\mathsf{P}_1 \to \mathsf{P}_3$, $\mathsf{P}'_1 \to \mathsf{P}'_3$. The consequences of the solutions Eqs. (4.62), (4.64), (4.65), Eqs. (4.67), (4.68), (4.69) and Eqs. (4.70), (4.71), (4.72) are discussed in the subsequent sections.

4.4 Prediction of $F_\perp$.

The three sets of expressions of the Wilson coefficients and the effective photon vertices derived so far have many important consequences as far as the precision test of standard model and the searches of new physics are concerned. Since the expressions are in terms of experimentally measurable observables with minimum theoretical inputs, the Wilson coefficients and the effective photon vertices can be measured in the experiments. This would however require a full

angular analysis to measure all the observations. If on the other hand the C_{10} or C_9 are taken as theoretical inputs then the form factor $\mathcal{F}_\parallel$ can be measured using Eq. (4.62) and (4.65). As previously mentioned these two expression of the Wilson coefficients are not free from hadronic uncertainties due to the presence of the form factor $\mathcal{F}_\parallel$. However we can define their ratio R that is free from any hadronic uncertainties,

$$R \equiv \frac{C_9}{C_{10}} = \frac{2(F_\parallel \mathsf{P}_1 \mathsf{P}'_1 - F_\perp) - (\mathsf{P}_1 - \mathsf{P}'_1)Z_1}{\frac{4}{3}A_{FB}(\mathsf{P}_1 - \mathsf{P}'_1)} \,. \tag{4.73}$$

The expression above depends only on the forward-backward asymmetry $A_{\rm FB}$ and the helicity fractions $F_\parallel$ and $F_\perp$. The only theoretical inputs are the form factor ratios P_1 and P'_1, which in the heavy quark effective theory framework is calculated reliably. We note that since the longitudinal helicity fraction F_L has been measured and since since $F_L + F_\parallel + F_\perp = 1$, we can express $F_\parallel$ in terms of F_L and $F_\perp$. Actually it is possible to express all the expressions in terms of only two helicity fraction F_L and $F_\perp$. Eq. (4.73) can be used to experimentally test the ratio of C_9 and C_{10}. On the other hand if the ratio $R = C_9/C_{10}$ is known very accurately, $F_\perp$ can be predicted using Eq. (4.73) in terms of F_L and $A_{\rm FB}$ as [121, 122]:

$$F_\perp = \frac{-4RA_{\rm FB}(\mathsf{P}_1 - \mathsf{P}'_1)(1 + \mathsf{P}_1\mathsf{P}'_1) + 3(1 - F_L)(\mathsf{P}_1 + \mathsf{P}'_1)^2 - (\mathsf{P}_1 - \mathsf{P}'_1)\sqrt{T_\perp}}{6(1 + \mathsf{P}_1^2)(1 + \mathsf{P}_1'^2)} \tag{4.74}$$

where,

$$\begin{aligned} T_\perp &= 9(1 - F_L)^2(\mathsf{P}'_1 + \mathsf{P}_1)^2 - 24RA_{\rm FB}(1 - F_L)(\mathsf{P}_1 - \mathsf{P}'_1)(1 - \mathsf{P}_1\mathsf{P}'_1) \\ &- 16A_{\rm FB}^2[R^2(\mathsf{P}_1 - \mathsf{P}'_1)^2 + (1 + \mathsf{P}_1^2)(1 + \mathsf{P}_1'^2)] \end{aligned} \tag{4.75}$$

The sign of the term containing $\sqrt{T_\perp}$ could either be positive or negative. Of the two possible solutions for $F_\perp$, in Eq. (4.74) we have chosen the solution which gives the correct value of R obtained from Eq. (4.73). This solution corresponds to the one with the negative ambiguity as shown in Eq. (4.74). As can be seen from the Eq. (4.74), the transversity amplitude $F_\perp$ is expressed in terms of two observables F_L and $A_{\rm FB}$, and two form factor ratios P_1 and P'_1. Since

P_1 and P'_1 are known precisely, the predictions of $F_\perp$ from Eq. (4.74) are free from any hadronic uncertainties. Using the measured values of F_L and $A_{\rm FB}$ from Ref. [113] and [114] and $F_\perp$ we have tabulated the predicted values of $F_\perp$ in Tables 5.1 and 5.2 respectively. The ratio $R \equiv \frac{C_9}{C_{10}}$ can be also expressed in terms of other observables using Eqs. (4.67) and (4.69) as,

$$\frac{C_9}{C_{10}} = \frac{2(F_L \mathsf{P}_2 \mathsf{P}'_2 - F_\perp) - (\mathsf{P}_2 - \mathsf{P}'_2) Z_2}{\frac{4}{3}\sqrt{2} A_5 (\mathsf{P}_2 - \mathsf{P}'_2)}\,, \tag{4.76}$$

and a similar relation follows from Eqs. (4.70) and (4.72),

$$\frac{C_9}{C_{10}} = \frac{2((F_L + F_\parallel + \sqrt{2}\pi A_4)\mathsf{P}_3 \mathsf{P}'_3 - F_\perp) - (\mathsf{P}_3 - \mathsf{P}'_3) Z_3}{\frac{4}{3}(A_{\rm FB} + \sqrt{2} A_5)(\mathsf{P}_3 - \mathsf{P}'_3)}. \tag{4.77}$$

The theoretical inputs required to measure the ratio R from Eqs. (4.76) and (4.77) are the form factor ratios $\mathsf{P}_{2,3}$ and $\mathsf{P}'_{2,3}$ which are not completely free from theoretical uncertainties. We therefore do not use these equations to predict $F_\perp$ which also requires the measurements of the observables A_4 and A_5. These equations however will be useful however in future discussions.

4.5 The $F_L - A_{\rm FB}$ constraint.

The perpendicular helicity fraction $F_\perp$ predicted in Eq. (4.74) in terms forward-backward asymmetry $A_{\rm FB}$ and the longitudinal helcity fraction F_L consists of the term $T_\perp$. In the Eq. (4.75), $T_\perp$ is expressed in terms of $A_{\rm FB}$, F_L, R and P_1 and P'_1. Since the helicity fractions are physical quantities the term $T_\perp$ must be positive. The positivity of $T_\perp$ imposes constraints on the possible values for F_L and $A_{\rm FB}$ which cannot therefore be arbitrarily chosen. The requirement for real solution for $F_\perp$ hence implies a constraint on $A_{\rm FB}$ in terms of P_1, P'_1, R and observable F_L as [121, 122]:

$$\frac{-3(1-F_L)}{4}\, T_- \leq A_{FB} \leq \frac{3(1-F_L)}{4}\, T_+ \tag{4.78}$$

where, the expressions of $T_\pm$

$$T_\pm = \frac{(\mathsf{P}_1 + \mathsf{P}'_1)^2}{\sqrt{(1+\mathsf{P}_1^2)(1+\mathsf{P}_1'^2)}\sqrt{(\mathsf{P}_1+\mathsf{P}'_1)^2 + R^2(\mathsf{P}_1-\mathsf{P}'_1)^2} \mp (1-\mathsf{P}_1\mathsf{P}'_1)(\mathsf{P}_1-\mathsf{P}'_1)R} \tag{4.79}$$

It is easy to see that $T_\pm \approx 1$ when $\mathsf{P}_1 \approx \mathsf{P}_1{}' \approx -1$. Given the values of P_1 and $\mathsf{P}_1{}'$ from Table 4.1, we expect $T_\pm \approx 1$. The allowed domain for $A_{\rm FB}$ is hence almost free from R as long as $\mathsf{P}_1 \approx \mathsf{P}_1{}' \approx -1$. The allowed $F_L - A_{\rm FB}$ region predicted from the above equations is studied in details in Chapter 5.

4.6 The $F_L - F_\perp$ constraint.

The Eq. (4.73) can be inverted to express the forward-backward asymmetry $A_{\rm FB}$ in terms of the ratios P_1, P'_1 and R;

$$A_{\rm FB} = \frac{3\left(RX - \sqrt{Y(\mathsf{P}_1-\mathsf{P}'_1)^2(1+R^2) - X^2}\right)}{4(\mathsf{P}_1-\mathsf{P}'_1)(1+R^2)} \tag{4.80}$$

where,

$$\begin{aligned} X &= 2(F_\parallel \mathsf{P}_1\mathsf{P}'_1 - F_\perp) \\ Y &= 4F_\parallel F_\perp . \end{aligned}$$

Note that the Eq. (4.73) is quadratic in $A_{\rm FB}$, and should have resulted in a two-fold ambiguity in the solution. One easily confirms that only the solution with positive sign in front of the square root is valid. This is done by substituting the observables $F_\parallel$, $F_\perp$ in terms form-factors and the Wilson coefficients in the Eq. (4.80). The forward-backward asymmetry $A_{\rm FB}$ being a real quantity the right hand side of the Eq. (4.80) has to be real also. Hence the the radical in the left hand side of the Eq. (4.80) must be positive. This imply a constraint on the $F_L - F_\perp$

parameter space which is derived form the positivity argument of the radical [121, 122],

$$1 + \frac{\mathsf{P}_1^2 + \mathsf{P}_1'^2 + R^2(\mathsf{P}_1 - \mathsf{P}_1')^2 - (\mathsf{P}_1 - \mathsf{P}_1')\sqrt{R^2+1}\sqrt{R^2(\mathsf{P}_1 - \mathsf{P}_1')^2 + (\mathsf{P}_1' + \mathsf{P}_1)^2}}{2\mathsf{P}_1^2\mathsf{P}_1'^2} \leq \frac{1-F_L}{F_\perp} \leq 1 + \frac{\mathsf{P}_1^2 + \mathsf{P}_1'^2 + R^2(\mathsf{P}_1 - \mathsf{P}_1')^2 + (\mathsf{P}_1 - \mathsf{P}_1')\sqrt{R^2+1}\sqrt{R^2(\mathsf{P}_1 - \mathsf{P}_1')^2 + (\mathsf{P}_1' + \mathsf{P}_1)^2}}{2\mathsf{P}_1^2\mathsf{P}_1'^2} \tag{4.81}$$

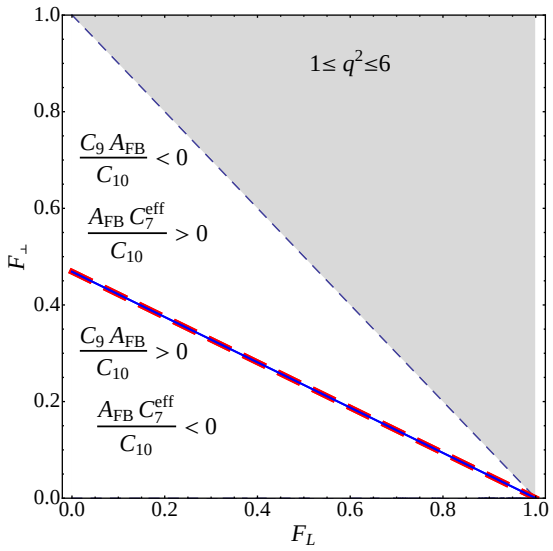

Figure 4.2: The constraints on $F_L - F_\perp$ parameter space arising from Eq. (4.81) is shown. The values of P_1 and P_1' are averaged over 1 GeV$^2 \leq q^2 \leq 6$ GeV^2. The allowed region for $R = -1$ is depicted by the diagonal thick solid (blue) line that predicts $F_\perp$ to lie in a very narrow region, well approximated by a line. The shaded region is forbidden by $F_L + F_\perp + F_\parallel = 1$. Thick dashed (red) line correspond to the solution of $F_\perp$ from Eq. (4.80) for $A_{FB} = 0$. This line divides the allowed domain into two regions fixing the sign of A_{FB} relative to C_9/C_{10} and C_7^{eff}/C_{10} as depicted in the figure(see Sec. 4.8).

In Figs. 4.2 and 4.4 the constraint implied by the above equations are shown in the large and low recoil region respectively. As mentioned in the figure captions, the values of P_1 and P_1' are averaged over the q^2 bins. The Eq. (4.81) implies very strict constraints on the $F_L - F_\perp$ parameter space. The constraint is sensitive to the value of the ratio R, however the sign of R is irrelevant. In the standard model the value of R is close to -1. In Figs. 4.2 and 4.4 we have made two choices of R; $R = -1$ and $R = -10$. For $R = -1$ the value of $F_\perp$ predicted by the

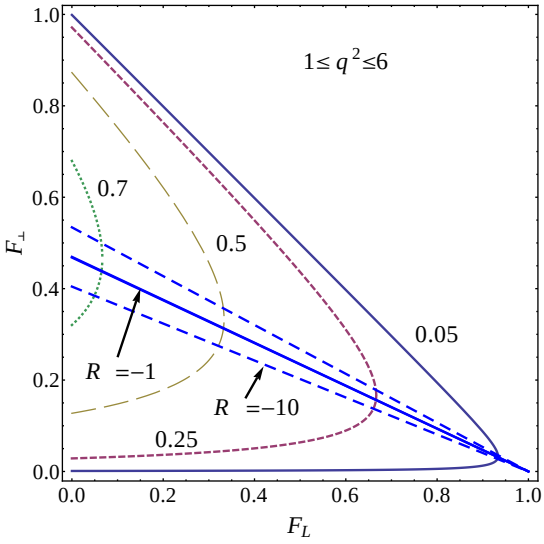

Figure 4.3: The allowed region for $R = -1$ is depicted by the diagonal thick solid (blue) line that predicts $F_\perp$ to lie in a very narrow region, well approximated by a line. The allowed $F_L - F_\perp$ region for $R = -10$ is constrained between the dashed (blue) lines. The additional curves in the figure correspond to the constraint on $F_L - F_\perp$ arising from $Z_1^2 > 0$ for different values of $A_{\rm FB}$: 0.05, 0.25, 0.5, 0.7, where all the regions to the left of these curves are allowed.

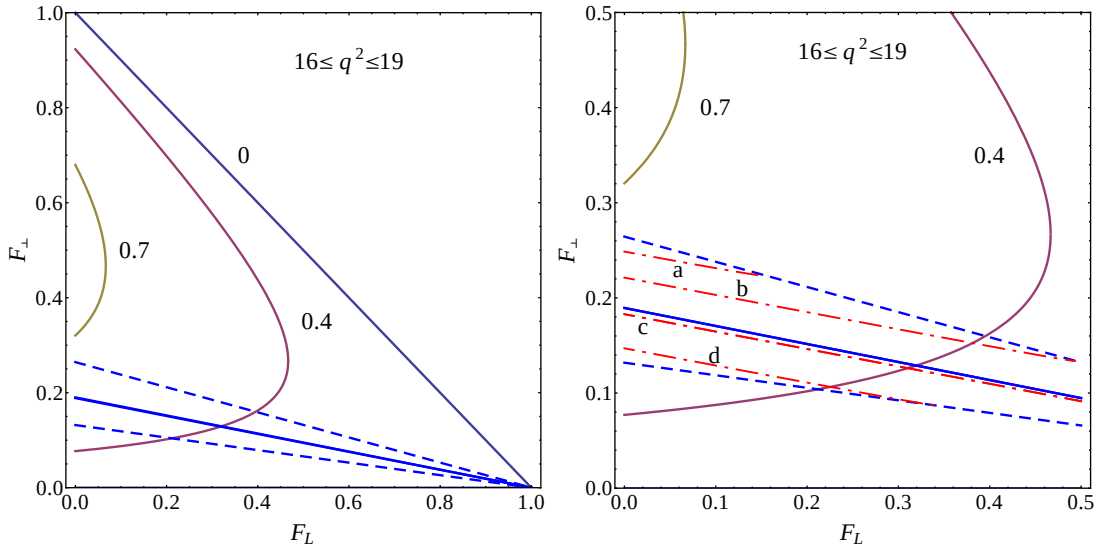

Figure 4.4: The same as in Fig. 4.3 except that P_1 and P_1' are averaged over 16 GeV$^2 \le q^2 \le$ 19 GeV^2. The figure to the right is the inset of the figure to the left. In this figure the solid and the dashed diagonal (blue) lines are the same as in the figure to the right. The dot-dash (red) lines labeled by "a,b,c,d" correspond to $A_{\rm FB} = 0.5, 0.3, 0, -0.3$ respectively for $R = -10$. The line "c" (for $A_{\rm FB} = 0$) divides the domain and corresponds to the thick dashed (red) line in Fig. 4.2. The $A_{\rm FB}$, F_L and $F_\perp$ must be consistent as shown by the dot-dash lines. For $R = -1$ similar lines exist for different value of $A_{\rm FB}$ but overlap with the solid blue line. Hence they are not depicted in the figure.

Eq. (4.81) is constrained to a very narrow region which can be approximated by a line. This is shown Figs. 4.2, 4.3 and 4.4, by the diagonal solid blue lines. The shaded region to the left of the dashed blue region is forbidden by the constraint $F_L + F_\perp + F_\parallel = 1$ and the thick dashed line in red corresponds to the solution of $F_\perp$ from Eq. (4.80). For a large value $R = -10$ the constraint is relaxed and the range of $F_\perp$ predicted by Eq. (4.81) is larger. This is depicted in Figs. 4.3 and 4.4 by two dashed (blue) lines. As will be discussed later there are additional constraints that come from the condition $Z_1^2 > 0$ which can be written as,

$$4(1 - F_L - F_\perp)F_\perp - \frac{16}{9}A_{\rm FB}^2 > 0$$

The constraints coming from this relation for different values of $A_{\rm FB}$ are shown in Figs. 4.3 and 4.4. Similar constraints are obtained in the low recoil region also. These constraints are shown in the Fig. 4.4. The significant change that is noticeable between large and low recoil is that at low recoil the predicted values of $F_\perp$ are smaller than that predicted in the large recoil region. At low recoil the shifts towards lower value of $F_\perp$ is shown in Fig. 4.4. It is interesting to note that irrespective of the value of R, in the limit $\mathsf{P}_1' \to \mathsf{P}_1$ one obtains $(1 - F_L)/F_\perp = 1 + 1/\mathsf{P}_1^2$. In the limit $m_B \to \infty$ and the energy of the K^*, $E_{K^*} \to \infty$, it is easy to see that $\mathsf{P}_1 = \mathsf{P}_1' \to -1$, and we find that $F_\parallel = F_\perp$. In this limit Eq. (3.30) will result in a constant distribution in ϕ. Since the values of P_1 and P_1' differ slightly we expect only a very small coefficient of $\cos\phi$. The relation similar to Eq. (4.80) can be derived from Eq. (4.76) where we can write $\sqrt{A_5}$ and $A_{\rm FB} + \sqrt{A_5}$ in terms of helicity fractions as,

$$\sqrt{2}A_5 = \frac{3(RX_2 - \sqrt{Y_2(\mathsf{P}_2 - \mathsf{P}_2')^2(1 + R^2) - X_2^2})}{4(\mathsf{P}_2 - \mathsf{P}_2')(1 + R^2)} \tag{4.82}$$

where,

$$\begin{aligned} X_2 &= 2(F_L \mathsf{P}_2 \mathsf{P}_2' - F_\perp) \\ Y_2 &= 4F_L F_\perp. \end{aligned}$$

The relation that follows from Eq. (4.77) is,

$$A_{\rm FB} + \sqrt{2}A_5 = \frac{3(RX_3 - \sqrt{Y_3(\mathsf{P}_3 - \mathsf{P}_3')^2(1+R^2) - X_3^2})}{4(\mathsf{P}_3 - \mathsf{P}_3')(1+R^2)} \tag{4.83}$$

where,

$$\begin{aligned} X_3 &= 2((F_L + F_\parallel + \sqrt{2}\pi A_4)\mathsf{P}_3\mathsf{P}_3' - F_\perp) \\ Y_3 &= 4(F_L + F_\parallel + \sqrt{2}\pi A_4)F_\perp. \end{aligned}$$

Since the form factor ratios $\mathsf{P}_{2,3}$ and $\mathsf{P}'_{2,3}$ are not reliable theoretical inputs we refrain from deriving constraints on $F_L - F_\perp$ from these equations.

4.7 Bound on Form Factor Ratios.

As discussed before, even at leading order in $\Lambda_{\rm QCD}/m_b$ it is impossible to isolate the Wilson coefficient $C_7^{\rm eff}$ from the form factor $\widetilde{\mathcal{G}}_\lambda$ due to radiative and "non-factorizable" corrections. We therefore neglect the higher order corrections to form factors. Extremizing P_1^2 in terms of all the non observables in Eq. (4.62) we get following bounds on P_1^2,

$$\mathsf{P}_1^2 \lessgtr \frac{4F_\parallel F_\perp - \frac{16}{9}A_{\rm FB}^2}{F_\parallel^2} \quad \forall\, F_\parallel F_\perp \lessgtr \frac{2}{7}\Big(\frac{4A_{\rm FB}}{3}\Big)^2. \tag{4.84}$$

For $A_{\rm FB} = 0$, we have already noted the exact equality $\mathsf{P}_1^2 = F_\perp/F_\parallel$. Analytical bound on P_1' is also possible, but is harder to obtain. Similar straightforward extrimization with respect to all the non observables in Eq. (4.67) gives the following bounds on the form factor ratios P_2,

$$\mathsf{P}_2^2 \lessgtr \frac{4F_L F_\perp - \frac{32}{9}A_5^2}{F_L^2} \quad \forall\, F_L F_\perp \lessgtr \frac{2}{7}(\frac{4\sqrt{2}A_5}{3})^2. \tag{4.85}$$

And straightforward extrimization with respect to all the non observables in Eq (4.70) results in the following bounds on the form factor ratio P_3,

$$\begin{aligned} \mathsf{P}_3^2 \;&\leqslant\; \frac{4(F_L + F_\parallel + \sqrt{2}\pi A_4)F_\perp - \frac{16}{9}(A_{\rm FB} + \sqrt{2}A_5)^2}{(F_L + F_\parallel + \sqrt{2}\pi A_4)^2} \\ \forall \qquad &(F_L + F_\parallel + \sqrt{2}\pi A_4)F_\perp \leqslant \frac{2}{7}\Big(\frac{4(A_{\rm FB} + \sqrt{2}A_5)}{3}\Big)^2. \end{aligned} \tag{4.86}$$

4.8 Sign of $C_7^{\rm eff}$.

We will now discuss a few important relations that involve the Wilson coefficient $C_7^{\rm eff}$. It can be separated from the form factor only when the higher order corrections including the "non-factorizable" corrections are neglected. Hence all the results that we will discuss now are valid only at the leading order and the tilde from the form factors $\mathcal{G}_\lambda$ are removed. At leading order we can write the Eq. (4.64) as,

$$C_7^{\rm eff} = \frac{\sqrt{\Gamma_f}}{\sqrt{2}\mathcal{G}_\parallel} \frac{(\mathsf{P}_1^2 F_\parallel - F_\perp)}{\Big[\pm(\mathsf{P}_1 - \mathsf{P}_1')\sqrt{\mathsf{P}_1^2 F_\parallel + F_\perp + \mathsf{P}_1 Z_1}\Big]}. \tag{4.87}$$

Using the above expression and the Eq. (4.62) we can write,

$$\frac{C_7^{\rm eff}}{C_{10}} = \frac{3}{2}\frac{\mathcal{F}_\parallel}{\mathcal{G}_\parallel}\frac{(\mathsf{P}_1^2 F_\parallel - F_\perp)}{A_{\rm FB}(\mathsf{P}_1 - \mathsf{P}_1')}. \tag{4.88}$$

Since both the form factors $\mathcal{F}_\parallel$ and $\mathcal{G}_\parallel$ appear in the above equation, the ratio $C_7^{\rm eff}/C_{10}$ can not be determined without theoretical uncertainties. However the Eq. (4.88) imply certain constraints on the ratio $C_7^{\rm eff}/C_{10}$. The sign of the ratio $\mathcal{F}_\parallel/\mathcal{G}_\parallel$ can be very accurately determined from the following equation,

$$\frac{\mathcal{F}_\parallel}{\mathcal{G}_\parallel} = -\frac{q^2 A_1(q^2)}{2(m_B - m_{K^*})m_b T_2(q^2)}.$$

where both $A_1(q^2)$ and $T_2(q^2)$ are both are positive. It is easy to conclude that,

$$\frac{C_7^{\rm eff}}{C_{10}} A_{\rm FB} \gtrless 0, \quad \text{only if} \quad \mathsf{P}_1^2 \lesseqgtr F_\perp/F_\parallel, \quad \text{when} \quad \mathsf{P}_1 - \mathsf{P}_1' > 0 \tag{4.89}$$

Eq. (4.84) together with Eq. (4.88) can be used to obtain more useful bounds that are purely in terms of observables alone, albeit they are not completely exhaustive. Eq. (4.84) implies:

$$\mathsf{P}_1^2 F_\parallel - F_\perp \lesseqgtr \frac{Z_1 - F_\parallel F_\perp}{F_\parallel} \quad \forall\, F_\parallel F_\perp \lesseqgtr \frac{2}{7}\Big(\frac{4A_{\rm FB}}{3}\Big)^2, \tag{4.90}$$

which in turn implies for $(\mathsf{P}_1^2 F_\parallel - F_\perp) < 0$ that,

$$\frac{C_7^{\rm eff}}{C_{10}} A_{\rm FB} > 0 \qquad \forall \quad F_\parallel F_\perp < \frac{32}{63} A_{\rm FB}^2 \,. \tag{4.91}$$

If, however, $(\mathsf{P}_1^2 F_\parallel - F_\perp) > 0$ we obtain an analogous condition

$$\frac{C_7^{\rm eff}}{C_{10}} A_{\rm FB} < 0 \qquad \forall \quad F_\parallel F_\perp > \frac{16}{27} A_{\rm FB}^2 \,. \tag{4.92}$$

The above bounds have nothing to say on the sign of $C_7^{\rm eff}/C_{10}$ in the region,

$$\frac{32}{63} A_{\rm FB}^2 \le F_\parallel F_\perp \le \frac{16}{27} A_{\rm FB}^2 \tag{4.93}$$

and may not be particularly useful in general. One can nevertheless draw conclusions on the signs of the Wilson coefficients by combining Eq. (4.73) together with Eq. (4.88) to write:

$$\begin{aligned} \Big(\frac{2}{3}\frac{C_9}{C_{10}}\mathsf{P}_1'' - \frac{4}{3}\frac{C_7^{\rm eff}}{C_{10}}\mathsf{P}_1\Big) A_{\rm FB} &= (\mathsf{P}_1{}^2 F_\parallel + F_\perp + \mathsf{P}_1 Z_1) \\ &> 0, \end{aligned} \tag{4.94}$$

where, $\mathsf{P}_1'' = (\mathcal{G}_\parallel/\mathcal{F}_\parallel)(\mathsf{P}_1 + \mathsf{P}_1') > 0$ since each of $(\mathcal{G}_\parallel/\mathcal{F}_\parallel)$, P_1 and P_1' are always negative. Defining,

$$E_1 \equiv \frac{C_9}{C_{10}} A_{\rm FB}, \qquad E_2 \equiv \frac{C_7^{\rm eff}}{C_{10}} A_{\rm FB}, \tag{4.95}$$

for convenience, Eq. (4.94) reads

$$\frac{2}{3}\mathsf{P}_1^{''}E_1 - \frac{4}{3}\mathsf{P}_1 E_2 > 0 \tag{4.96}$$

In SM, $C_7^{\rm eff}/C_{10} > 0$ and $C_9/C_{10} < 0$, hence the sign of E_2 (E_1) will be same (opposite) to that observed for $A_{\rm FB}$. If, for any q^2, we find $A_{\rm FB} > 0$, Eq. (4.96) cannot be satisfied unless the contribution from the E_2 term exceeds the E_1 term, or the sign of the E_2 term is wrong in SM. In the SM the E_2 term dominates at large recoil i.e. small q^2, hence, $A_{\rm FB}$ must be positive at small q^2 to be consistent with SM. If $A_{\rm FB} < 0$ is observed for all q^2 i.e. no zero crossing of $A_{\rm FB}$ is seen, one can convincingly conclude that $C_7^{\rm eff}/C_{10} < 0$ in contradiction to SM. However, if zero crossing of $A_{\rm FB}$ is confirmed with $A_{\rm FB} > 0$ at small q^2, it is possible to conclude that the signs $C_7^{\rm eff}/C_{10} > 0$ and $C_9/C_{10} < 0$ are in conformity with SM, as long as other constraints like $Z_1^2 > 0$ hold. In Fig.4.2 we have shown how the $A_{\rm FB} = 0$ distinguishes the two regions. In Ref. [114] the zero crossing is indeed seen. However, in the $2{\rm GeV}^2 \le q^2 \le 4.3{\rm GeV}^2$ bin, $Z_1^2 > 0$ is only marginally satisfied. We emphasize that these conclusions drawn from Eq. (4.94) are exact and not altered by any hadronic uncertainties. We can write equations similar to Eq. (4.88) by using Eqs. (4.67), (4.68) and Eqs. (4.70), (4.71). These equations which are valid only at leading order are written below as,

$$\frac{C_7^{\rm eff}}{C_{10}} = \frac{3}{2}\frac{\mathcal{F}_0}{\mathcal{G}_0}\frac{(\mathsf{P}_2^2 F_L - F_\perp)}{\sqrt{2}A_5(\mathsf{P}_2 - \mathsf{P}_2')}, \tag{4.97}$$

$$\frac{C_7^{\rm eff}}{C_{10}} = \frac{3}{2}\frac{(\mathcal{F}_\parallel + \mathcal{F}_0)}{\mathcal{G}_\parallel + \mathcal{G}_0}\frac{(\mathsf{P}_3^2(F_L + F_\parallel + \sqrt{2}\pi A_4) - F_\perp)}{(A_{\rm FB} + \sqrt{2}A_5)(\mathsf{P}_3 - \mathsf{P}_3')}\,. \tag{4.98}$$

The above two equations are not as important to determine the $C_7^{\rm eff}/C_{10}$ ratio. But they will be very useful as shown later. Eqs. (4.76) and (4.97) can be combined to obtain

$$\begin{aligned}(\frac{2}{3}\frac{C_7^{\rm eff}}{C_{10}}\mathsf{P}_2^{''} - \frac{4}{3}\frac{C_9}{C_{10}}\mathsf{P}_2)A_5 &= \frac{(\mathsf{P}_2^2 F_L + F_\perp + \mathsf{P}_2 Z_2)}{\sqrt{2}} \\ &> 0\end{aligned} \tag{4.99}$$

$\mathsf{P}_2'' = (\mathcal{G}_0/\mathcal{F}_0)(\mathsf{P}_2 + \mathsf{P}_2') > 0$, since $\mathcal{G}_0/\mathcal{F}_0$, P_2 and P_2' are all negative. While this is not easily seen as in the case of P_1'' we have numerically verified at leading order that this is true for the entire q^2 domain. We have shown earlier, by doing a power expansion in $A_{\rm FB}$, that $(\mathsf{P}_1^2 F_\parallel + F_\perp + \mathsf{P}_1 Z_1)$ is always positive. It is easy to see that similar arguments can be made for the positivity of $(\mathsf{P}_2^2 F_L + F_\perp + \mathsf{P}_2 Z_2)$ by considering expansions in A_5. Hence if the term in the bracket must be positive A_5 must be positive. At large recoil the term in the bracket is expected to be positive. From Eqs. (4.77) and (4.98) we can obtain yet another important relation, which is of the same kind as we obtained earlier in Eqs. (4.94) and (4.99)

$$\begin{aligned}(\frac{2}{3}\frac{C_7^{\rm eff}}{C_{10}}\mathsf{P}_3'' - \frac{4}{3}\frac{C_9}{C_{10}}\mathsf{P}_3)(A_{\rm FB} + \sqrt{2}A_5) &= \left[(\mathsf{P}_3^2(F_L + F_\parallel + \sqrt{2}\pi A_4) + F_\perp + \mathsf{P}_3 Z_3\right] \\ &> 0 \end{aligned} \tag{4.100}$$

where $\mathsf{P}_3'' = (\mathcal{G}_0 + \mathcal{G}_\parallel)/(\mathcal{F}_0 + \mathcal{F}_\parallel)(\mathsf{P}_3 + \mathsf{P}_3') > 0$. This is easily verified to be true at leading order for the entire q^2 domain. We have shown earlier by doing a power expansion in $A_{\rm FB}$ and A_5 , that respectively $(\mathsf{P}_1^2 F_\parallel + F_\perp + \mathsf{P}_1 Z_1)$ and $(\mathsf{P}_2^2 F_L + F_\perp + \mathsf{P}_2 Z_2)$ are always positive. It is easy to see that similar arguments can be made for the positivity of $(\mathsf{P}_3^2(F_L + F_\parallel + 2\sqrt{2}\pi A_4) + F_\perp + \mathsf{P}_3 Z_3)$ by considering expansions in $A_{\rm FB} + \sqrt{2}A_5$. These equations are equally useful to determine the sign of $C_7^{\rm eff}$ as discussed earlier. However, the form factors involved are not completely free from HQET form factor.

4.9 Form Factor Ratios in Terms of Observables.

In Sec. 4.1 we have defined several form factor ratios in terms of $\mathcal{F}_\lambda$ and $\widetilde{\mathcal{G}}_\lambda$. These ratios enter as inputs in the solutions of Wilson coefficients and effective photon vertices. Except for the ratios P_1 and P_1', the rest of the ratios are polluted by hadronic uncertainties. In this section we derive many important relations that relate the form factor ratios to the observables. From Eq. (4.32) we see that at the forward-backward zero crossing $A_{\rm FB} = 0$, $r_\parallel + r_\perp = 0$. At the

forward-backward zero crossing point we can write from Eq. (4.33),

$$\begin{aligned} r_{\parallel} + r_{\perp}\Big|_{A_{\rm FB}=0} &= \pm\frac{\sqrt{\Gamma_f}}{\sqrt{2}\mathcal{F}_{\perp}}\Big[\mathsf{P}_1^2 F_{\parallel} + F_{\perp} + \mathsf{P}_1 Z_1\Big]^{1/2} \\ &= \pm\frac{\sqrt{\Gamma_f}}{\sqrt{2}\mathcal{F}_{\perp}}\Big[\mathsf{P}_1^2 F_{\parallel} + F_{\perp} + \mathsf{P}_1 2\sqrt{F_{\parallel}F_{\perp}}\Big]^{1/2} \\ &= \pm\frac{\sqrt{\Gamma_f}}{\sqrt{2}\mathcal{F}_{\perp}}\Big[\sqrt{F_{\perp}} + \mathsf{P}_1\sqrt{F_{\parallel}}\Big] = 0. \end{aligned}$$

Since both $\sqrt{F_{\perp}}$ and $\sqrt{F_{\parallel}}$ are positive quantities and the ratio P_1 is negative the relation $\sqrt{F_{\perp}} + \mathsf{P}_1\sqrt{F_{\parallel}} = 0$ imply [121, 122],

$$\mathsf{P}_1 = -\frac{\sqrt{F_{\perp}}}{\sqrt{F_{\parallel}}}\Big|_{A_{\rm FB}=0}. \tag{4.101}$$

This equation enables the measurement of P_1 in terms of the ratio of helicity fractions. If zero crossing occurs it would provide an interesting test of our understanding of form factors. Very recently LHCb has confirmed [114] zero crossing of $A_{\rm FB}$ for the first time. The zero crossing is observed at $q^2 = 4.9^{+1.1}_{-1.3}\text{GeV}^2$, which is consistent with the predictions of the standard model and lies in the large recoil region. Eq. (4.101) can hence be used to measure P_1 at the zero crossing of $A_{\rm FB}$. A confirmation of the estimate of P_1 with direct helicity measurements would leave no doubt of the reliable predictability of HQET in the large recoil region.

The ratios P_2 and P_3 can also be written in terms observables. Using Eq. (4.46) we can similarly derive the relation,

$$\mathsf{P}_2 = -\frac{\sqrt{F_{\perp}}}{\sqrt{F_L}}\Big|_{A_5=0} \tag{4.102}$$

enabling measurements of form the factor ratio P_2 in terms of observables at the zero crossing of A_5. We can similarly use Eq. (4.48) to express P_3 in terms of the helicity fractions and A_4 at the zero crossing point of the observable $A_{\rm FB} + \sqrt{2}A_5$ as,

$$\mathsf{P}_3 = -\frac{\sqrt{F_{\perp}}}{\sqrt{F_L + F_{\perp} + \sqrt{2}\pi A_4}}\Big|_{A_{\rm FB}+\sqrt{2}A_5=0}. \tag{4.103}$$

Hence, the zero crossing of $A_{\rm FB} + \sqrt{2}A_5$ enables the measurement of form factor ratio P_3 as

well, in terms of observables. Next we derive several relations that express the four form factor ratios P_2, P_2' and P_3, P_3' in terms of observables and P_1 and P_1'. These relations are valid up to leading order in α_s in perturbation series and leading order in $\Lambda_{\rm QCD}/m_b$ in heavy quark expansion. Since we have already defined three sets of C_9/C_{10} and $C_7^{\rm eff}/C_{10}$ ratios, equating Eq. (4.97) and Eq. (4.98) with Eq. (4.88) we get the expressions of P_2' and P_3' in terms of observables and P_1 and P_1'.

$$\mathsf{P}_2' = \frac{\sqrt{2}A_5\Big(F_\perp - F_\parallel \mathsf{P}_1^2\Big)\mathsf{P}_2^2\mathsf{P}_1'}{A_{\rm FB}T_2(\mathsf{P}_1 - \mathsf{P}_1') + \sqrt{2}A_5\Big(F_\perp - F_\parallel \mathsf{P}_1^2\Big)\mathsf{P}_2\mathsf{P}_1'} \tag{4.104}$$

$$\mathsf{P}_3' = \frac{(A_{\rm FB} + \sqrt{2}A_5)(F_\perp - F_\parallel \mathsf{P}_1^2)\mathsf{P}_3^2\mathsf{P}_1'}{A_{\rm FB}T_3(\mathsf{P}_1 - \mathsf{P}_1') + \sqrt{2}A_5(F_\perp - F_\parallel \mathsf{P}_1^2)\mathsf{P}_3^2\mathsf{P}_1'}, \tag{4.105}$$

where,

$$T_2 = \mathsf{P}_1(F_\perp - F_L\mathsf{P}_2^2) \tag{4.106}$$

$$T_3 = \mathsf{P}_1\Big[F_\perp(1+\mathsf{P}_3^2) - \mathsf{P}_3^2(1+\sqrt{2}\pi A_4)\Big]. \tag{4.107}$$

Similarly equating Eq. (4.76) and Eq. (4.77) with Eq. (4.73) and using the Eqs. (4.104) and (4.105) we get the following expressions of P_2 and P_3 in terms of observables and form factor ratios P_1 and P_1'.

$$\mathsf{P}_2 = \frac{2\mathsf{P}_1 A_{\rm FB}F_\perp}{\sqrt{2}A_5(2F_\perp + Z_1\mathsf{P}_1) - Z_2\mathsf{P}_1A_{\rm FB}} \tag{4.108}$$

$$\mathsf{P}_3 = \frac{2\mathsf{P}_1 A_{\rm FB}F_\perp}{(A_{\rm FB} + \sqrt{2}A_5)(2F_\perp + Z_1\mathsf{P}_1) - Z_3\mathsf{P}_1A_{\rm FB}}. \tag{4.109}$$

If all the observables are measured from the full angular analysis then the form factor ratios P_2 and P_3 can be measured using Eqs. (4.108) and (4.109). These values can be used in Eqs. (4.104) and (4.105) to measure the values of P_2' and P_3'.

4.10 Model Independent Constraints between Observables.

In this section we discuss a few important relations and constraints among observables that have no dependence on the hadronic form factors and hence are clean probes of new physics. Some of these relations are derived from the fact that in the standard model the tiny *CP* violation [74] in the $B \to K^* \ell^+ \ell^-$ decay mode can be neglected. Hence all the Wilson coefficients are real. This implies that, in the denominator of Eq. (4.62), the term under the square root $\mathsf{P}_1^2 F_\parallel + F_\perp + \mathsf{P}_1 Z_1$ must be real. This is only possible as long as Z_1 is real i.e, as long as $4F_\parallel F_\perp \geq \frac{16}{9} A_{\rm FB}^2$ which is seen by an (infinite) series expansion in $A_{\rm FB}$:

$$\begin{aligned} \mathsf{P}_1^2 F_\parallel + F_\perp + \mathsf{P}_1 Z_1 &= (\mathsf{P}_1 \sqrt{F_\parallel} + \sqrt{F_\perp})^2 \\ &- \frac{4A_{\rm FB}^2 \mathsf{P}_1}{9\sqrt{F_\parallel F_\perp}} - \frac{4A_{\rm FB}^4 \mathsf{P}_1}{81(F_\parallel F_\perp)^{3/2}} + O(A_{\rm FB}^6) \geq 0, \end{aligned} \tag{4.110}$$

where every terms is positive since P_1 is negative. The condition that Z_1 must be real thus leads to a relation restricting the observables $F_\parallel$, $F_\perp$ and $A_{\rm FB}$ such that [121, 122]:

$$4F_\parallel F_\perp \geq \frac{16}{9} A_{FB}^2. \tag{4.111}$$

The above relation is purely in terms of observables and does not depend on any theoretical parameters and hence is a clean probe of new physics. The violation of this condition will be a clear signal of new physics. On the other hand, if the experiments find a real value that does not agree with the C_{10} estimates of standard model value, it could either be a signal of new physics or of the uncertainties in form factor estimations. We have two more such relations. These relations follow from Eq. (4.67) and Eq. (4.70). In Eq. (4.67) the term term $\mathsf{P}_2^2 F_L + F_\perp + \mathsf{P}_2 Z_2$ will be positive only if Z_2 is real. This can be shown by doing a power expansion in A_5. So the condition that Z_2 is real implies that,

$$4F_L F_\perp \geq \frac{16}{9} (\sqrt{2} A_5)^2 \,. \tag{4.112}$$

Similarly Z_3 should also be real in Eq. (4.70) which implies,

$$4(F_L + F_\parallel + \sqrt{2}\pi A_4)F_\perp \geq \frac{16}{9}(A_{FB} + \sqrt{2}A_5)^2. \tag{4.113}$$

The combination of bounds in Eqs. (4.111) and (4.112) results in yet another interesting bound among observables alone but involving only $A_{\rm FB}^2$, A_5^2 and $F_\perp$:

$$4(1 - F_\perp)F_\perp \geq \frac{16}{9}(A_{\rm FB}^2 + 2A_5^2). \tag{4.114}$$

The violation of any of these relations will be a signal new physics. With the help of the observables $A_{\rm FB}$ and $F_\perp$ we can measure the observable A_5 using Eq. (4.114). For a given value of $F_\perp$ (or $1 - F_\perp$) the Eq. (4.114) imply a constraint between the observables $A_{\rm FB}$ and A_5 shown in the Fig. 4.6 by different colored lines. In Chapter 5 we have discussed in details about the constraints coming from the Eqs.(4.111), (4.112) and (4.113). In the remainder of this section we derive a very important relation that involves all the three helicity fractions and the angular asymmetries $A_{\rm FB}$, A_4 and A_5 and does not depend on any hadronic quantities. The relations follows from Eq. (4.52) which can be rewritten as,

$$\mathsf{P}_1\mathsf{P}_2 = \mathsf{P}_3\mathsf{P}_1 + \mathsf{P}_3\mathsf{P}_2$$

Substituting the expressions of P_2 and P_3 interms of P_1 and observables from Eq. (4.108) and Eq. (4.109) we get,

$$Z_3 \;=\; Z_1 + Z_2.$$

which can be written in terms of observables only as,

$$\sqrt{4(F_L + F_\parallel \sqrt{2}\pi A_4) - \frac{16}{9}(A_{\rm FB} + \sqrt{2}A_5)^2} = \sqrt{4F_\parallel F_\perp - \frac{16}{9}A_{\rm FB}^2} + \sqrt{4F_L F_\perp - \frac{32}{9}A_5^2} \tag{4.115}$$

We use this relation to solve for A_4 leading to [121, 122],

$$A_4 = \frac{8A_5A_{\rm FB}}{9\pi F_\perp} + \sqrt{2}\,\frac{\sqrt{F_LF_\perp - \frac{8}{9}A_5^2}\,\sqrt{F_\parallel F_\perp - \frac{4}{9}A_{\rm FB}^2}}{\pi F_\perp}. \tag{4.116}$$

It should be noted that Eq. (4.115) is a quadratic equation in A_4. Hence there are two solutions for A_4 out of which only one is correct. The correct solution is chosen by substituting the observables in terms of the form factors and Wilson coefficients. Since $F_\perp$ is already predicted in Eq. (4.74) in terms of the already measured observables F_L and $A_{\rm FB}$ and P_1, P_1' and R, we can estimate A_4 in terms of A_5. The correlations predicted by Eq. (4.116) should hold unless NP contributes. For a given value of A_5 the A_4 can be completely predicted in terms of F_L and $A_{\rm FB}$. This is shown in Fig. 4.5. We have predicted the values of $F_\perp$ from Eq. (4.74) in terms of $F_L, A_{\rm FB}, \mathsf{P}_1, \mathsf{P}_1'$ and R. The values of P_1 and P_1' are averaged over $1\ {\rm GeV}^2 \le q^2 \le 6\ {\rm GeV}^2$ and the value of the ratio $R = -1$. The solid blue line correspond to the predicted values of A_4 as a function of F_L and $A_{\rm FB}$ for a given value of A_5. The lines are constrained to stay within the shaded region which results from the conditions $(F_LF_\perp - (8/9)A_5^2) \ge 0$ and $(F_\parallel F_\perp - (4/9)A_{\rm FB}^2) \ge 0$. As can be seen from the different panels of Fig. 4.5, the region shrinks with the increasing values of A_5. In the Fig. 4.7 we have studied the dependence of the input R on the predicted values of A_4. It should be noted that the dependence of R enters through $F_\perp$ which is predicted from Eq. (4.74). Our prediction is shown for three values of R. The prediction for $R = -1$, $R = -10$ and $R = 10$ are shown by solid black, dashed blue and dashed green lines respectively. It can be noticed that the value of A_4 is not much sensitive to the values of R. The Eq. (4.116) is a relation involving only observables without any assumptions of hadronic form factors, hence its violation must be an unambiguous signal of NP. In addition the constraints Eqs. (4.111), (4.112), (4.113) and Eq. (4.114) are also model independent constraints among observables. These constraints need to be tested experimentally before ruling out the presence of new physics.

4.11 Low recoil limit.

So far we have discussed many relations and constraints among observables for new physics tests, as well a few relations that can be used to measure hadronic form factor ratios in experiments. In this section we discuss in detail about the low recoil limit approximation of these results. These relations will allow us not only to test the validity of the low recoil approximation but also the presence of new physics. In the large recoil limit we had six observables: the decay width Γ_f, the helicity fractions F_L and $F_\perp$ and the angular asymmetries $A_{\rm FB}$, A_4 and A_5. These six observables are expressed in terms of eight independent theoretical parameters. The parameters being the six effective form factors $\mathcal{F}_0$, $\mathcal{F}_\parallel$, $\mathcal{F}_\perp$, $\widetilde{\mathcal{G}}_0$, $\widetilde{\mathcal{G}}_\parallel$ and $\widetilde{\mathcal{G}}_\perp$ and the two Wilson coefficients C_9 and C_{10}. We can hence solve the theoretical parameters in terms of observables if we take two theoretical inputs which happens to be the two ratios of form factors. In the low recoil due to various simplifications the number of independent observables as well as number of independent theoretical parameters are different. Hence the solutions of theoretical parameters in terms of observables and the important results that follow therefrom needs to treated more carefully.

We have discussed in Sec 2.4 that in the low recoil limit the long distance contributions to the $B \to K^* \ell^+ \ell^-$ hadronic matrix elements can be computed as the short distance effects using simultaneous heavy quark and operator product expansion $1/Q$ with $Q = \{m_b, \sqrt{q^2}\}$. In this limit the sub-leading m_{K^*}/m_b as well as the non-factorizable corrections can be ignored so that the Wilson coefficient $C_7^{\rm eff}$ is distinguishable from the form factor $\widetilde{\mathcal{G}}_\lambda$. Hence the variables $r_\parallel, r_\perp, r_0$ and $r_\wedge$ are now defined as

$$\begin{aligned} r_\parallel &= C_7^{\rm eff}\frac{\mathcal{G}_\parallel}{\mathcal{F}_\parallel} - C_9 \\ r_\perp &= C_7^{\rm eff}\frac{\mathcal{G}_\perp}{\mathcal{F}_\perp} - C_9 \\ r_0 &= C_7^{\rm eff}\frac{\mathcal{G}_0}{\mathcal{F}_0} - C_9 \\ r_\wedge &= C_7^{\rm eff}\frac{\mathcal{G}_\wedge}{\mathcal{F}_\wedge} - C_9 \end{aligned}$$

Since the $C_7^{\rm eff}$ is distinguished from $\widetilde{\mathcal{G}}_\lambda$ we have removed the tilde. We also derived in Sec 2.4 that the form factors $\mathcal{F}_\lambda$ and $\mathcal{G}_\lambda$ satisfy the following relations,

$$\frac{\mathcal{G}_\parallel}{\mathcal{F}_\parallel} = \frac{\mathcal{G}_\perp}{\mathcal{F}_\perp} = \frac{\mathcal{G}_0}{\mathcal{F}_0} = \hat{\kappa}, \tag{4.117}$$

which implies that

$$r_\parallel = r_\perp = r_0 = r_\wedge \equiv r. \tag{4.118}$$

The above relation imply that the Eqs. (4.22)–(4.24) are modified as the following equations,

$$r^2 + C_{10}^2 = \frac{\Gamma_f F_\parallel}{2\mathcal{F}_\parallel^2} = \frac{\Gamma_f F_\perp}{2\mathcal{F}_\perp^2} \equiv \frac{\hat{F}\Gamma_f}{2} \tag{4.119}$$

$$4rC_{10} = \frac{2A_{\rm FB}\Gamma_f}{3\mathcal{F}_\parallel\mathcal{F}_\perp} \equiv \frac{4A_{\rm FB}}{3\sqrt{F_\parallel F_\perp}}\frac{\hat{F}\Gamma_f}{2}, \tag{4.120}$$

where

$$\hat{F} \equiv \frac{F_\parallel}{\mathcal{F}_\parallel^2} = \frac{F_\perp}{\mathcal{F}_\perp^2}. \tag{4.121}$$

Using the above equation and the definition of P_1 from Eq. (4.29) we can write,

$$\mathsf{P}_1^2 = \frac{\mathcal{F}_\perp^2}{\mathcal{F}_\parallel^2} = \frac{F_\perp}{F_\parallel}$$

The relation among the form factors Eq. (4.117) imply,

$$\frac{\mathcal{F}_\perp^2}{\mathcal{F}_\parallel^2} = \frac{\mathcal{G}_\perp^2}{\mathcal{G}_\parallel^2}$$

Hence we can write,

$$\mathsf{P}_1^2 = {\mathsf{P}'_1}^2 = \frac{F_\perp}{F_\parallel} = \frac{\mathcal{F}_\perp^2}{\mathcal{F}_\parallel^2}. \tag{4.122}$$

From Eqs. (4.119) and (4.120) that we can solve for r^2 and C_{10}^2:

$$r^2 = \frac{\hat{F}\Gamma_f}{4}\Big(1 + \frac{Z_1}{2\sqrt{F_\parallel F_\perp}}\Big) \tag{4.123}$$

$$C_{10}^2 = \frac{\hat{F}\Gamma_f}{4}\Big(1 - \frac{Z_1}{2\sqrt{F_\parallel F_\perp}}\Big). \tag{4.124}$$

The sign of r/C_{10} is fixed such that,

$$\frac{r}{C_{10}} = \frac{3}{4}\frac{2\sqrt{F_\perp F_\parallel} + Z_1}{A_{\rm FB}}, \tag{4.125}$$

in order to satisfy the limit derived by appropriate combination of Eqs. (4.64) and (4.65). In the low recoil limit "r" is same not just for $\parallel$ and $\perp$ helicities but for all three helicities. This requires in analogy with Eq. (4.122) that,

$$\mathsf{P}_2^2 = \mathsf{P}_2'^{\,2} = \frac{F_\perp}{F_L} = \frac{\mathcal{F}_\perp^2}{\mathcal{F}_0^2}, \tag{4.126}$$

$$\mathsf{P}_3^2 = \mathsf{P}_3'^{\,2} = \frac{F_\perp}{(F_L + F_\parallel)} = \frac{\mathcal{F}_\perp^2}{(\mathcal{F}_0^2 + \mathcal{F}_\parallel^2)}. \tag{4.127}$$

One can hence measure P_1, P_2 and P_3 in the low recoil region in terms of the ratio of helicity fractions. Hence, the value $C_{10}^2\mathcal{F}_\parallel^2$ can be expressed in terms of observables alone. In the large recoil case $C_{10}^2\mathcal{F}_\parallel^2$ depended on P_1 and P_2. The form factor $\mathsf{P}_1 = \mathsf{P}_1'$ can be measured, enabling a possibility of verifying the estimate of presented in Table 4.2. To derive a relation between observables that is valid at low recoil and tests the validity of the approximation, we note Eq. (4.119) leads to the generalized relation

$$\begin{aligned}\frac{r^2 + C_{10}^2}{2rC_{10}} &= \frac{3}{2}\frac{\sqrt{F_\parallel F_\perp}}{A_{\rm FB}} \\ &= \frac{3}{2}\frac{\sqrt{F_L F_\perp}}{\sqrt{2}A_5} \\ &= \frac{3}{2}\frac{\sqrt{(1 - F_\perp + \sqrt{2}\pi A_4)F_\perp}}{(A_{\rm FB} + \sqrt{2}A_5)}.\end{aligned} \tag{4.128}$$

The equalities on the left side of the above equation yields two interesting relations

$$\sqrt{2}A_5 = A_{\rm FB}\frac{\sqrt{F_L}}{\sqrt{F_\parallel}} \tag{4.129}$$

$$A_4 \;=\; \frac{\sqrt{2}}{\pi}\sqrt{F_L F_\parallel}. \tag{4.130}$$

It is easily seen by direct substitution of Eq. (4.129) in Eq. (4.116) that it reduces to Eq. (4.130), hence it is not independent. It is emphasized that a reasonable validity of the low recoil approximation requires large q^2 and not the exact equality of form factors as derived Eq. (4.126). Even though the values of the form factors depicted in Table 4.2 are not exactly equal, the low recoil approximation works well. This is demonstrated in Fig. 4.8 where we have plotted the left hand and right hand of Eqs. (4.129) and (4.130). These figures demonstrate that the equality of both sides of Eqs. (4.129) and (4.130) holds at the low recoil region. The values of observables are estimated using the form factors given in Sec 2.4. We emphasize that the relation derived in Eqs. (4.129) and (4.130) are extremely important both in testing the validity of the low recoil approximation and the presence of New Physics. The value of A_5 predicted by these relations tests the validity of the low recoil approximation, whereas the value of A_4 verifies the validity of SM. If both the relations are found to be valid it would prove both the validity of the low recoil limit and the absence of New Physics. On the other hand if both the relations fail we must conclude that low recoil limit is not valid. The presence of New Physics could still be tested by the validity Eq. (4.116) even in this large q^2 domain. The remaining meaningful possibility is that Eq. (4.129) holds and (4.130) is violated. This would imply validity of low recoil limit but signal the presence of New Physics. It is interesting to note that one should expect from Eqs. (4.129) and (4.130) a very tiny product of asymmetries A_4 and A_5.

$$A_4 A_5 = \frac{A_{\rm FB} F_L}{\pi} \tag{4.131}$$

since the right hand side $A_{\rm FB}$ and F_L have already been measured. *We emphasize that even in the low recoil limit, C_9/C_{10} and all the expressions independent of Wilson coefficients are independent of the universal form factors $\xi_\parallel$ and $\xi_\perp$.*

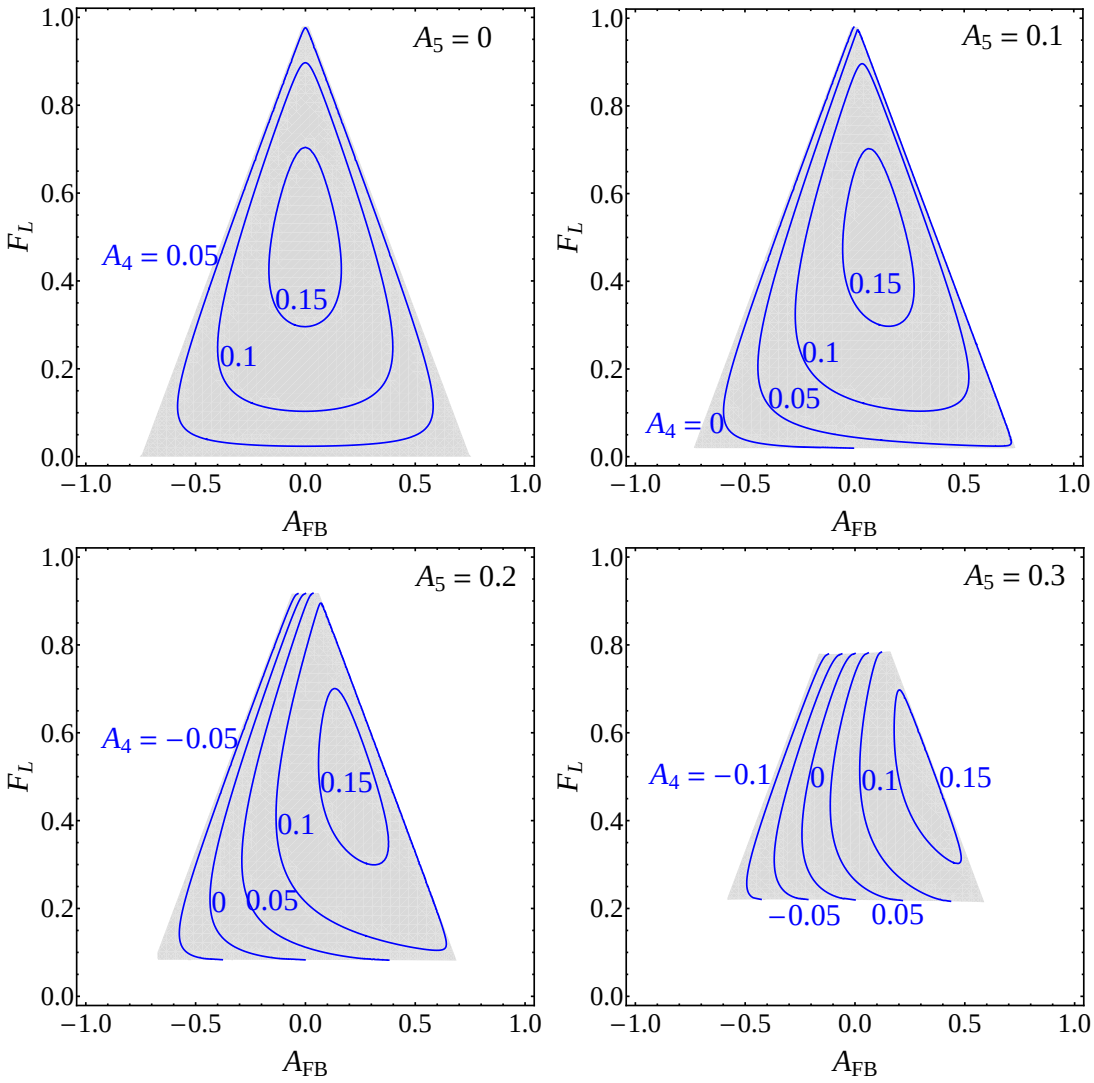

Figure 4.5: The blue curves correspond to the value of A_4 that is estimated using Eq. (4.116) for different values of A_5 as shown in different panels. The perpendicular helicity fraction $F_\perp$ is predicted in terms of F_L and A_{FB} from Eq. (4.74). The values of P_1 and P'_1 are averaged over $1\ \text{GeV}^2 \leq q^2 \leq 6\ \text{GeV}^2$ and we have chosen $R = -1$.

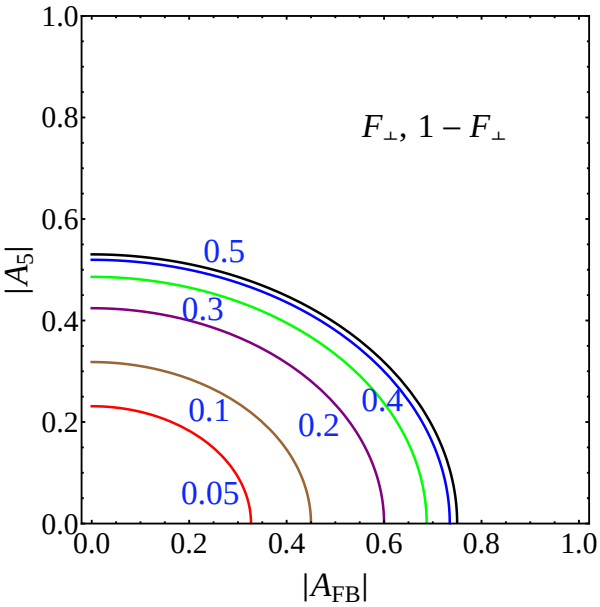

Figure 4.6: The Eq. (4.114) implies that the values of $|A_{FB}|$ and $|A_5|$ are constrained to stay within the different colored lines corresponding to the different values of $F_\perp$.

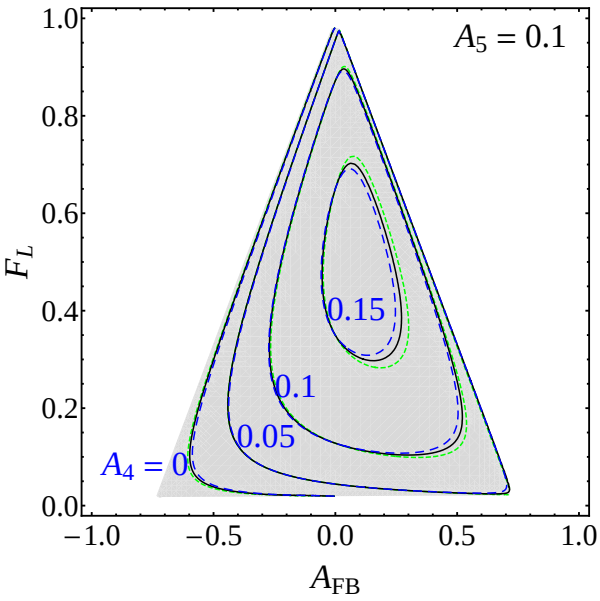

Figure 4.7: The same as Fig. 4.5 but the sensitivity of R on the predicted values of A_4 is studied. The small dashed (green) curves are for the case $R = 10$ while the big dashed (blue) curve correspond to $R = -10$. The solid black curves are for standard model value of $R = -1$.

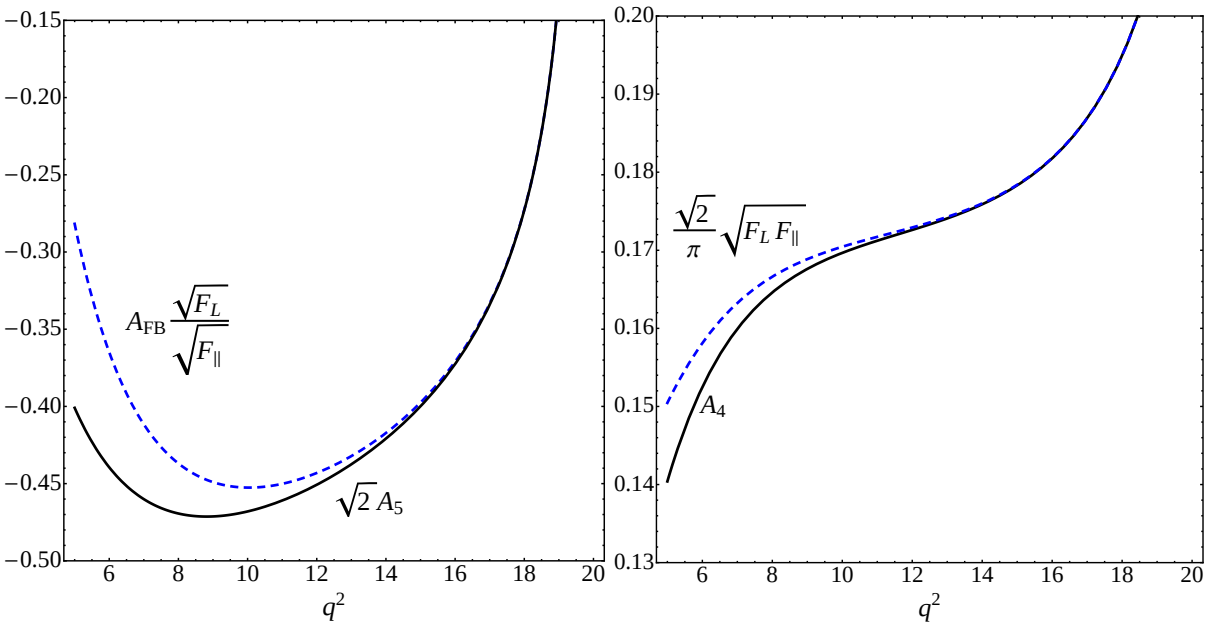

Figure 4.8: In the figure to the left two sides of equation Eq. (4.129) are plotted. The left hand side is depicted by solid black curve and right hand side by dashed blue curve. In the figure to the right both sides of Eq. (4.130) are plotted. Here also the left hand side is depicted by solid black curve and right hand side by dashed blue curve. These figures demonstrate the domain of validity in q^2 for the low recoil approximation and the region where new physics can be tested.

Chapter 5

Implications of Experimental Measurements.

In Chapter 4 we have derived the expression of Wilson coefficient C_{10} in terms of observables. In this section we use the experimental data and calculate the value of C_{10}. We also calculate the value of $F_\perp$ from Eq (4.74) using experimental data on F_L and $A_{\rm FB}$, assuming that in the standard model $R = -1$. Moreover, we also study in detail the constraints on $F_L - A_{\rm FB}$ arising from Eq (4.78). We show that the constraints are consistent with the one presented by LHCb in Ref. [126]. We also show that the constraints Eqs. (4.111), (4.112) and (4.113) which are completely free from any hadronic form factor imply rigorous constraint on the allowed $F_L - F_\perp$ region.

5.1 Numerical estimates of C_{10} and $F_\perp$.

In Eq. (4.62) the Wilson coefficient C_{10} is expressed in terms of two helicity fractions F_L and $F_\perp$, the forward-backward asymmetry $A_{\rm FB}$, one form factor $\mathcal{F}_\parallel$ and the theoretically reliably calculated form factor ratio P_1. The helicity fraction $F_\perp$ is predicted in Eq (4.74) in terms forward-backward asymmetry $A_{\rm FB}$, helicity fraction F_L, two theoretically reliably calculated form factor ratios P_1 and P'_1 and the ratio R. Assuming that in the standard model $R = -1$

and using the measured values of $A_{\rm FB}$ and F_L from Ref. [113], we have calculated the Wilson coefficient $|C_{10}|$ and the perpendicular helicity fraction $F_\perp$ (denoted by "(T)") in Table 5.1 in different dilepton invariant mass squared bins. The form factor $\mathcal{F}_\parallel$ and the ratios P_1 and P'_1 are calculated using heavy-to-light form factors at large recoil region (between 0.10 GeV^2 $\leq q^2 \leq$ 12.86GeV^2) and is averaged over each of the q^2 bins. In the low recoil region these quantities are calculated using heavy-to-light form factor at low recoil and is averaged over each of the q^2 bins. The bin 14.18 GeV^2 $\leq q^2 \leq$ 16GeV^2 is neglected as the the form factors are not reliably evaluated in this region. There is a unusually large value of $|C_{10}|$ in the 0.10 GeV^2 $\leq q^2 \leq$ 2 GeV^2 bin. It is unlikely [123, 124, 125] that such a large effect can be due to the contributions from low lying resonances in the experimental data. It could be due to failure in estimating $\mathcal{F}_\parallel$ or perhaps be a signal of new physics. In the first bin the $A_{\rm FB}$ approaches zero in which case our method is no longer valid. Therefore the values of C_{10} in the first bin should not be taken too seriously. In the 1 GeV^2 $\leq q^2 \leq$ 6 GeV^2 bin the value of $|C_{10}|$ is 3.81±0.58. It may be noted that estimate of $F_\perp$ does not depend on universal form factors and is clean in the low recoil limit. Using Eq. 3.30 LHCb has measured the observable

q^2(GeV^2)	0.10-2.00	2.00-4.30	4.30-8.68	10.09-12.86	16.00-19.00	1-6
$F_\perp$ (T)	0.44±0.01	0.14±0.06	0.19±0.03	0.25±0.04	0.14±0.016	0.21±0.05
$\lvert C_{10}\rvert$ (T)	14.36±1.68	2.81±0.78	3.00±0.38	2.34±0.37	3.11±0.39	3.81±0.58

Table 5.1: The predictions for $F_\perp$ (Eq. (4.74)) and $|C_{10}|$ (Eq. (4.62)) using 0.37 fb^{-1} LHCb [113] data for F_L, $A_{\rm FB}$ and $d\Gamma/dq^2$. "(T)" in the first column indicates that the values quoted are theoretical estimates. The form factor $\mathcal{F}_\parallel$ and the ratios P_1 and P'_1 are averaged over each q^2 bin using heavy-to-light form factor at large recoil (for 0.10 GeV^2 $\leq q^2 \leq$ 12.86GeV^2) and heavy-to-light form factor at low recoil (for 16 GeV^2 $\leq q^2 \leq$ 19 GeV^2). The region 14.18 GeV^2 $\leq q^2 \leq$ 16 GeV^2 is neglected as the form factors can not be calculated reliably in this region. It should be noted that in the first bin the $A_{\rm FB}$ approaches zero in which case the solution of C_{10} and $F_\perp$ can no longer be derived. Therefore the values of C_{10} in the first bin should not be taken too seriously.

$F_\perp$ in Ref. [114]. The measured $F_\perp$ are tabulated for each dilepton invariant mass squared bins in Table 5.2 and denoted by"(E)". We compare the measured values with the theoretically predicted values ("(T)") from Eq (4.74). Also tabulated are the predicted values of C_{10} which are denoted by "(T)". To tabulate the predicted values we have used the measured values of F_L

$q^2(\text{GeV}^2)$	$4m_\mu^2$-2.00	2.00-4.30	4.30-8.68	10.09-12.86	16.00-19.00	1-6
$F_\perp$ (E)	$0.36^{+0.14}_{-0.11}$	$0.11^{+0.09}_{-0.15}$	0.31 ± 0.09	$0.15^{+0.12}_{-0.13}$	$0.08^{+0.13}_{-0.14}$	$0.22^{+0.10}_{-0.11}$
$F_\perp$ (T)	0.31±0.03	0.15±0.04	0.20±0.03	0.22±0.03	0.12±0.01	0.17±0.03
$\|C_{10}\|$ (T)	12.91±1.07	2.60±0.78	2.88±0.32	2.0±0.25	2.55±0.29	3.26±0.45

Table 5.2: The same as Table 5.1 but with 1.0 fb^{-1} LHCb data [114]. "(E)" in the first column indicates that the values quoted are experimental estimates. $F_\perp$ (E) is computed directly from data using Eq. (3.30) and the value of S_3 quoted in Ref. [114]. The values of $|C_{10}|$ seem to decrease with the larger data set used and are marginally lower than theoretical estimates. Unfortunately, the cause of discrepancy in $|C_{10}|$ can not be fixed, it could either be due to failure in estimating $\mathcal{F}_\parallel$ or perhaps be a signal new physics. Note that in the 0.10 $\text{GeV}^2 \leq q^2 \leq 2$ GeV^2 region $|C_{10}|$ is still large even with improved statistics. We emphasize that the two values of $F_\perp$ are in good agreement almost throughout the q^2 region. It should be noted that in the first bin the A_{FB} approaches zero in which case the solution of $|C_{10}|$ and $F_\perp$ can no longer be derived. Therefore the values of $|C_{10}|$ in the first bin should not be taken too seriously.

and A_{FB} from Ref [114]. The form factor $\mathcal{F}_\parallel$ and the form factor ratios P_1 and P'_1 are calculated in the same way as for the Table 5.1. The 14.18 $\text{GeV}^2 \leq q^2 \leq 16\text{GeV}^2$ bin is neglected as the the form factors are not reliably evaluated in this region. The standard model estimate of C_{10} is perturbative calculation. However, our expression of C_{10} (see Eq-(4.62)) incorporates both the perturbative and the nonperturbative physics. Therefore, our estimate of C_{10} is not directly comparable to the standard model estimate.

5.2 The $F_L - A_{\text{FB}}$ region.

The observables F_L and A_{FB} are constrained by Eq (4.78). As shown in Fig. 5.1, the allowed values of F_L and A_{FB} are constrained within the solid blue triangle. The LHCb has recently performed in Ref. [126], a log-likelihood fit to the A_{FB} and F_L data in the different q^2 bins. The fits are shown in Fig. 5.4. We emphasize that the data [126] is consistent with the allowed domain in Fig. 5.1. If the measured F_L and A_{FB} in a given q^2 bin are outside the triangle then that is a clear signal of new physics. We note that since the Eq (4.78) does not involve any hadronic form factor, the violation of the constraint is a clean signal of new physics. The other details in the Fig. 5.1 correspond to the values of $|C_{10}|$ which are shown by the dashed lines. The values of $|C_{10}|$ are calculated from Eq. (4.62) using experimental data for F_L, A_{FB}

and branching fractions from Ref [113]. Using the same experimental data, the values of $F_\perp$ are calculated using Eq (4.74) and are plotted by dashed lines in Fig.5.2. The different panels correspond to different dilepton invariant mass squared q^2 bins. The form factor $\mathcal{F}_\parallel$ and the form factor ratios P_1 and P'_1 are calculated using heavy-to-light form factor at large recoil ($0.10\ \text{GeV}^2 \leq q^2 \leq 12.86\text{GeV}^2$) and is averaged over each bin. In the low recoil region these quantities are calculated using heavy-to-light form factor at low recoil and is averaged over each of the q^2 bin. The $14.18\ \text{GeV}^2 \leq q^2 \leq 16\text{GeV}^2$ bin is neglected due to the reasons mentioned before. In Fig. 5.1 and Fig.5.2 we have assumed that $R = -1$. The sensitivity of the triangular region on R is shown in Fig. 5.3 for three choices of R: $R = -10, -1, 10$. As mentioned in the caption the dashed blue line corresponds to $R = -10$, the solid black line corresponds to $R = -1$ and the $R = 10$ case is shown by large-dashed red line. The triangular region is sensitive to the value of R in the large q^2 bins and not significantly sensitive in the low q^2 bins. The lines inside the triangles correspond to the values of $F_\perp$.

5.3 Model independent bound on F_L and $F_\parallel$.

In Sec. 4.10 we derived relations among observables that are free from any hadronic form factors. The relations are in terms of inequality and are given in Eqs. (4.111), (4.112) and (4.113). Moreover, in Eq. (4.116) the observable A_4 is expressed in terms of the three helicity fractions and angular asymmetries A_5 and A_{FB}. One can hence eliminate the A_4 observables from Eq. (4.113) and obtain constraints involving three helicity fractions, A_{FB} and A_5. The consequences of these constrained relations can be studied as bound on two helicity fractions F_L and $F_\perp$. In Fig 5.5 we have assumed different values of A_{FB} and A_5 and shown the allowed regions of F_L and $F_\perp$. In the first panel of Fig 5.5 we assume $|A_{\text{FB}}| = 0$ and if $A_5 = 0$ then allowed values of F_L and $F_\perp$ are constrained between the two solid (black) lines. With the increasing values of A_5 the allowed region is constrained from the left. This is shown by the dot-dashed (red), dashed (purple) and dotted (blue) lines. These three lines correspond to

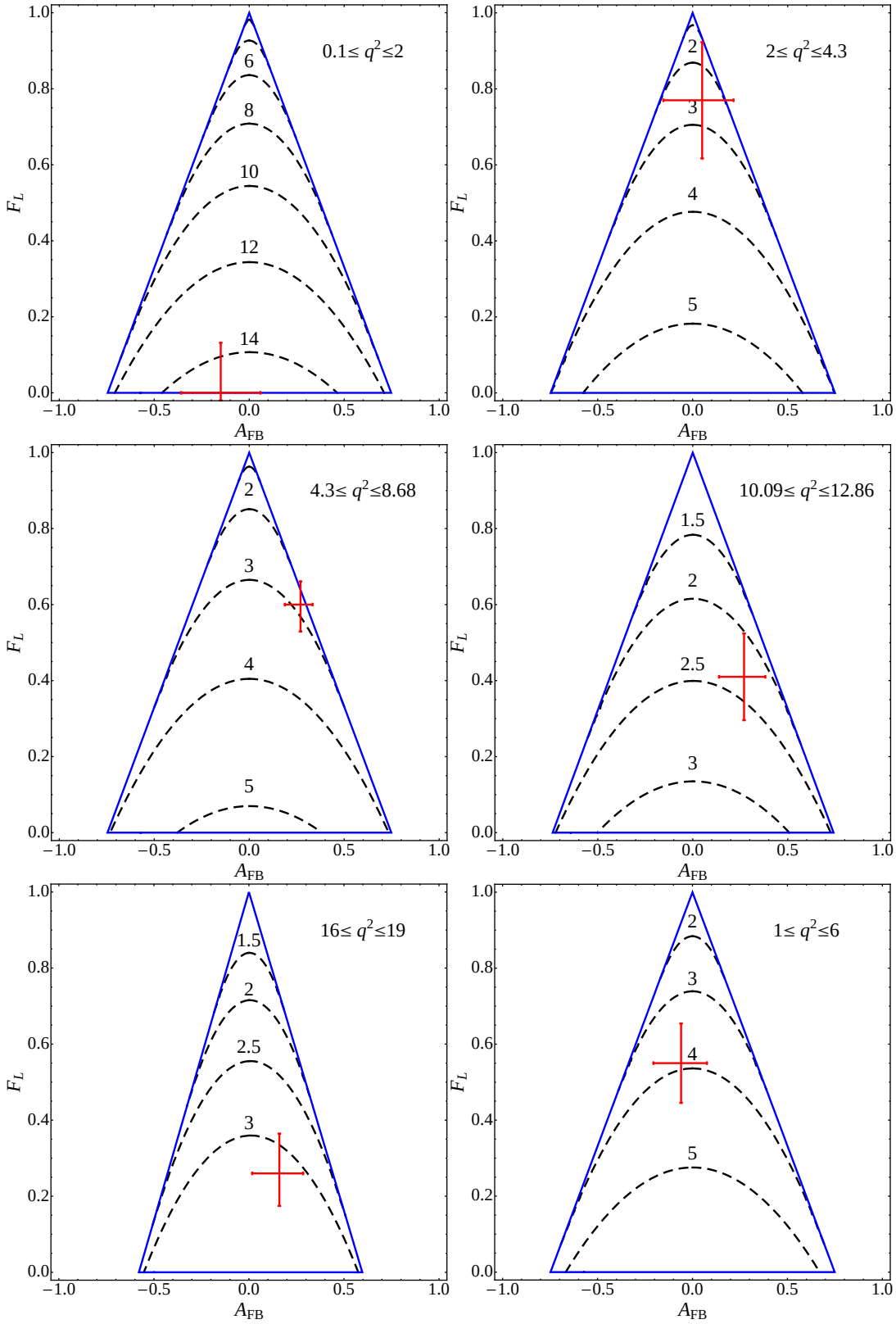

Figure 5.1: The allowed $F_L - A_{\rm FB}$ region is constrained by Eq (4.78) within the solid blue triangle. The ratio R is assumed to be -1. The different panels correspond to the different dilepton invariant mass squared bins. The values of the form factor ratios P_1 and P_1' are appropriately averaged in different q^2 bins. Inside the triangles, the solid (black dashed) lines correspond to the values of $|C_{10}|$ calculated from Eq. (4.62). The red cross correspond to the LHCb data [113].

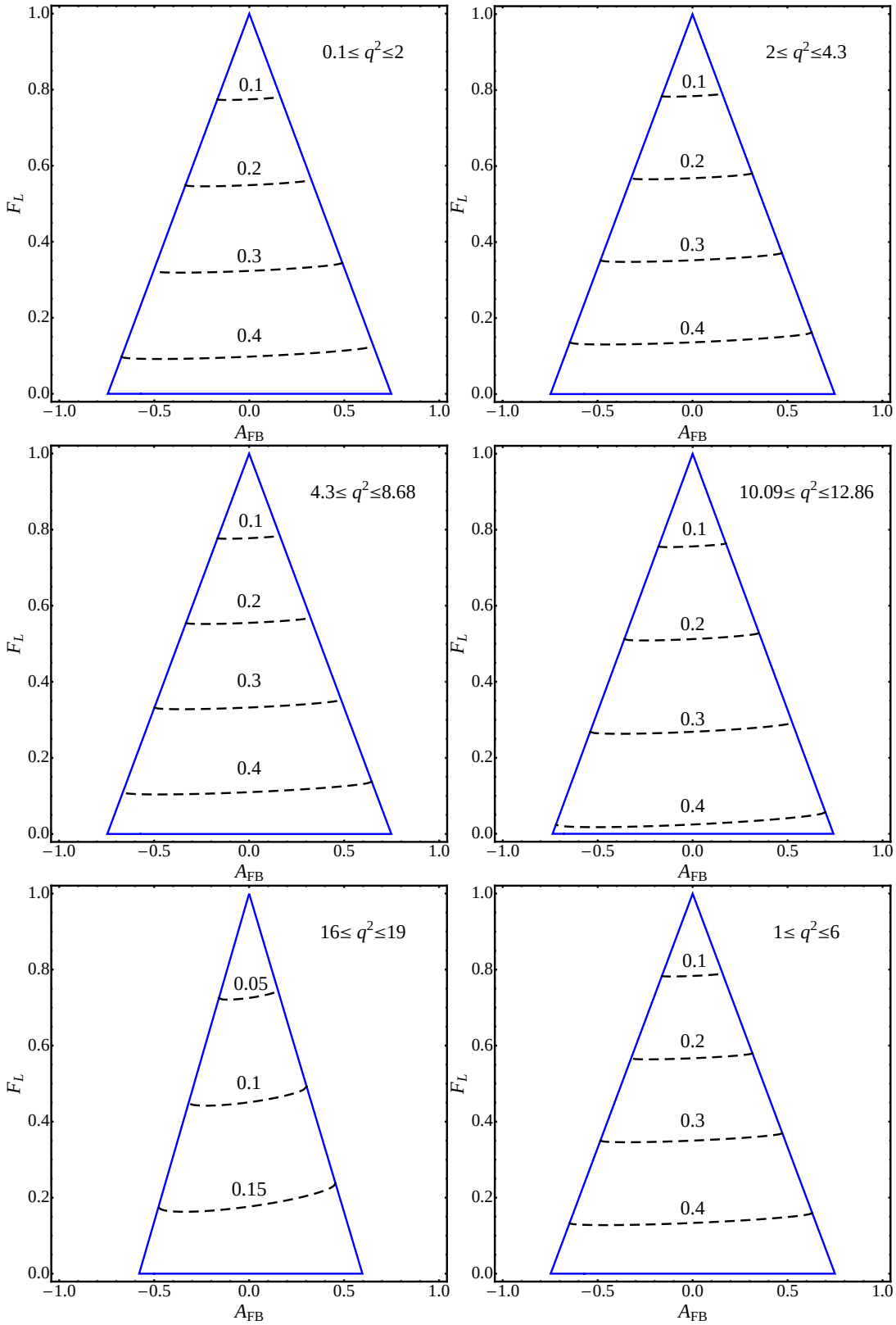

Figure 5.2: The same as Fig. 5.1 but the black dashed lines correspond to the values of $F_\perp$ calculated using Eq (4.74).

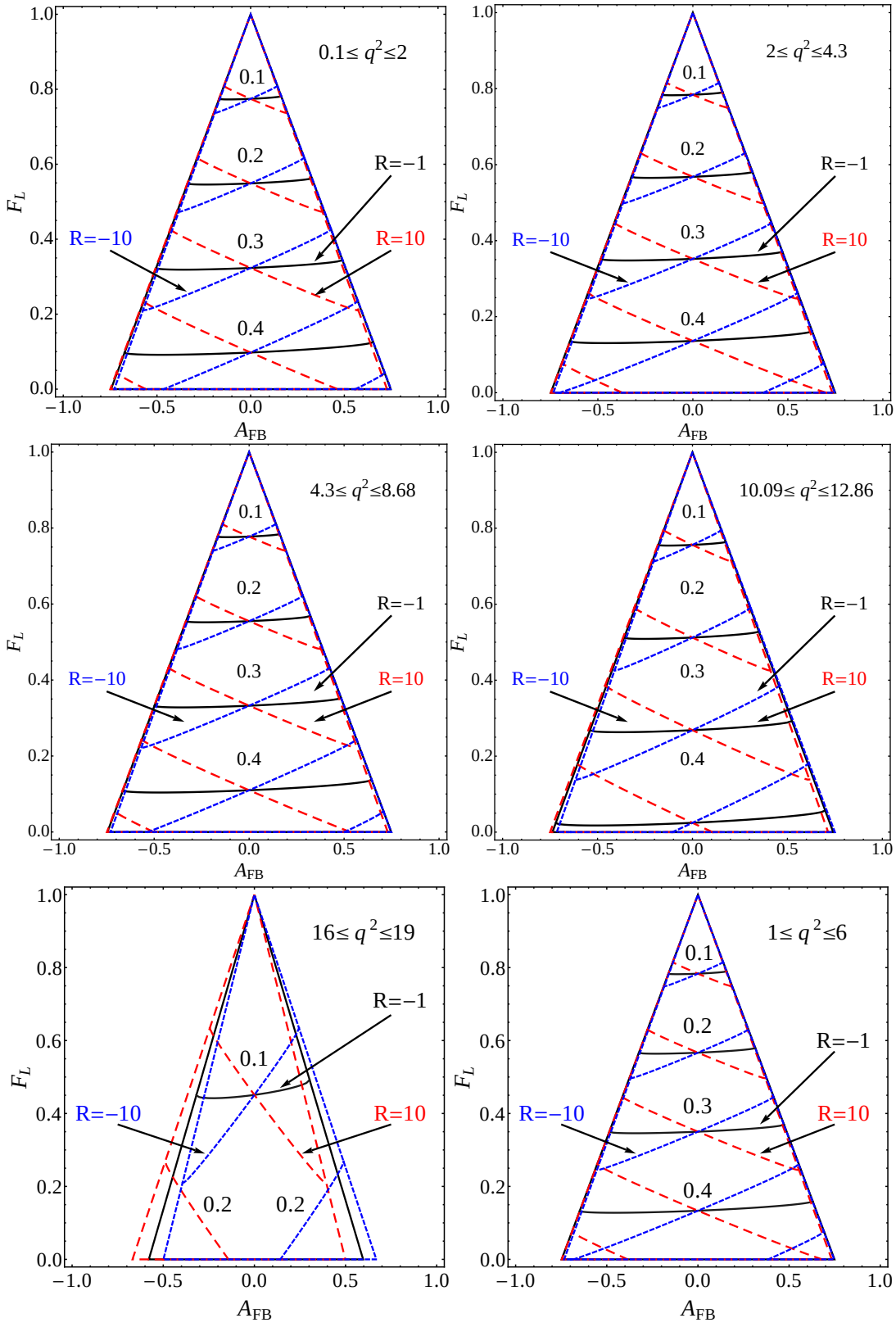

Figure 5.3: The same as Fig. 5.2. The sensitivity of the triangular region to R is studied for three choices of R. The triangle in blue (small dashed), black (solid) and red (large dashed) correspond to $R = -10$, $R = -1$ and $R = 10$ respectively. The lines inside the triangles are the values of $F_\perp$.

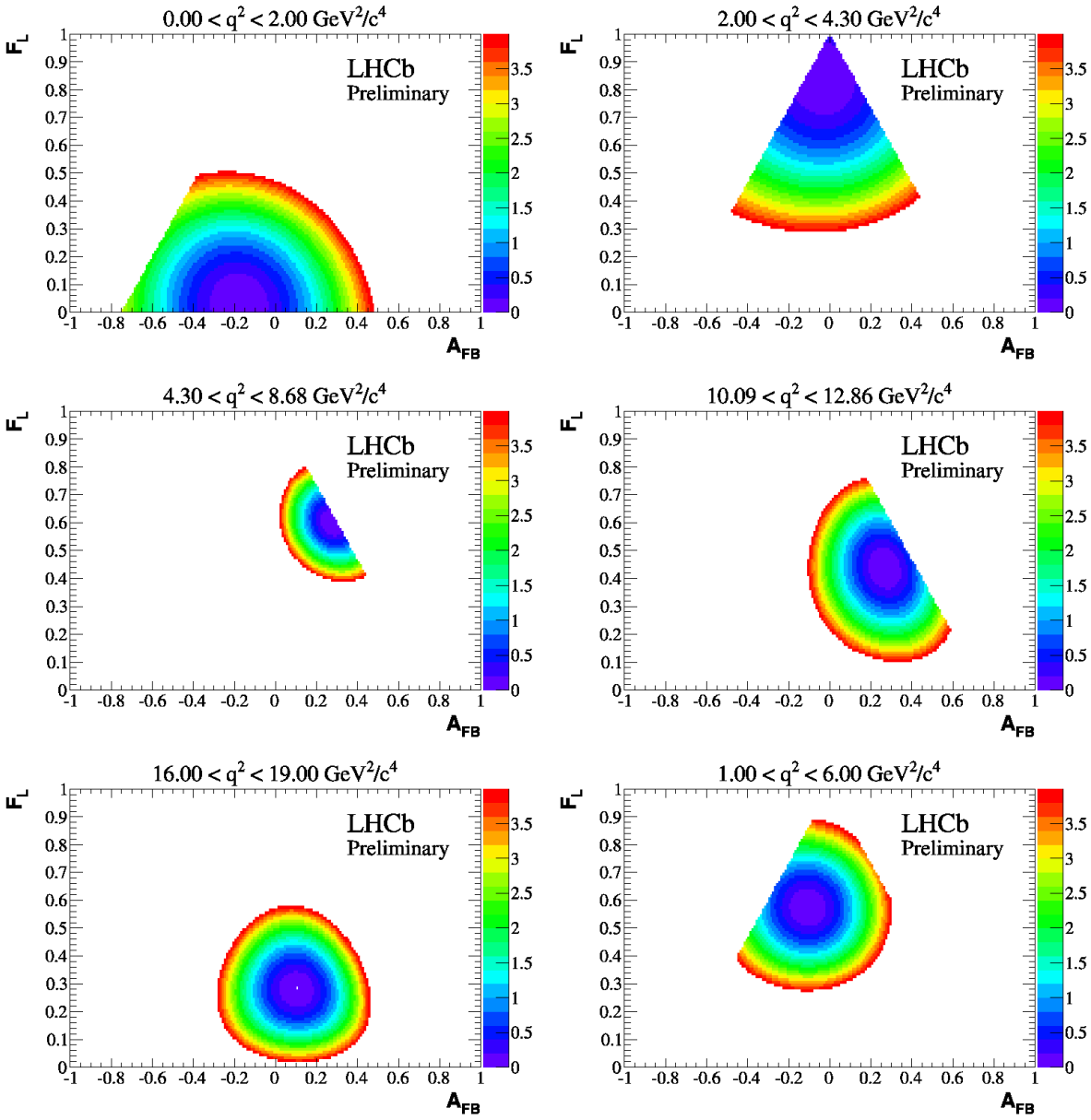

Figure 5.4: Log-likelihood fit the values of $A_{\rm FB}$ and F_L performed by LHCb [126] indicating a triangular boundary. We emphasize that these triangular domains are consistent with the regions shown in Figs. 5.1, 5.2 and 5.3.

$|A_5| = 0.15$, $|A_5| = 0.30$ and $|A_5| = 0.45$ respectively. If the value of $|A_{\rm FB}|$ is increased then both the solid (black) lines move towards the left constraining the region from the right. This is shown in the second panel of Fig 5.5 for $|A_{\rm FB}| = 0.15$ and in the subsequent panels. These figures illustrate the fact that the observables F_L, $F_\perp$, $A_{\rm FB}$ and A_5 are correlated with each other and such correlations are independent of any hadronic uncertainties, the violation of which is a clean signal of new physics. As an example we refer to the fourth panel of Fig 5.5. Here $|A_{\rm FB}| = 0.45$ and the dotted (blue) line for $|A_5| = 0.45$ is outside the allowed region (between the two solid black lines) of F_L and $F_\perp$. This is a violation of the relations given by Eqs. (4.111), (4.112) and (4.113).

In Fig. 5.6 we have shown the F_L-$F_\perp$ regions which are similar to Fig 5.5. However, we have used the values of $|A_{\rm FB}|$ given in each q^2 bins from Ref. [114]. The solid lines (in blue) correspond to the central value of $A_{\rm FB}$ and the dot-dashed (in red) and dotted (in black) lines correspond to the experimental error in $A_{\rm FB}$. Since A_5 has not been measured yet we have assumed $|A_5| = 0$. The experimental values of F_L and $F_\perp$ Ref. [114] are shown by black cross. In the first bin ($4m_\mu^2 \leq q^2 \leq 2$ GeV^2) the measured value of F_L and $F_\perp$ is at the boundary of the allowed region for $A_{\rm FB} = 0.00^{+0.08+0.01}_{-0.07-0.01}$. However for a non-zero value of A_5 the boundary line in the left will be shifted towards right and the $F_L - F_\perp$ point will be outside the region. In the third bin $4.30 \leq q^2 \leq 8.68$ GeV^2 (see the third panel of Fig. 5.6) the $F_L - F_\perp$ point is inside the allowed $F_L - F_\perp$ region and in the rest of the bins the $F_L - F_\perp$ points are at the boundary. As noted in all these plots the A_5 is assumed to be zero. So to see if the Eqs. (4.111), (4.112) and (4.113) are violated or not the observable A_5 has to be measured. As noted in Sec. 4.6, the Eq. 4.81 imply constraint on $F_L - F_\perp$ in terms of P_1, P'_1 and R. As shown in Fig.4.2 such constraints for $R = -1$ is well approximated by a line. These constraints are again shown in Fig. 5.6 by long dashed lines. In the third bin the measured value of $F_L - F_\perp$ is not consistent with the bound. In the rest of the bins the consistency holds within the measured error band of F_L and $F_\perp$.

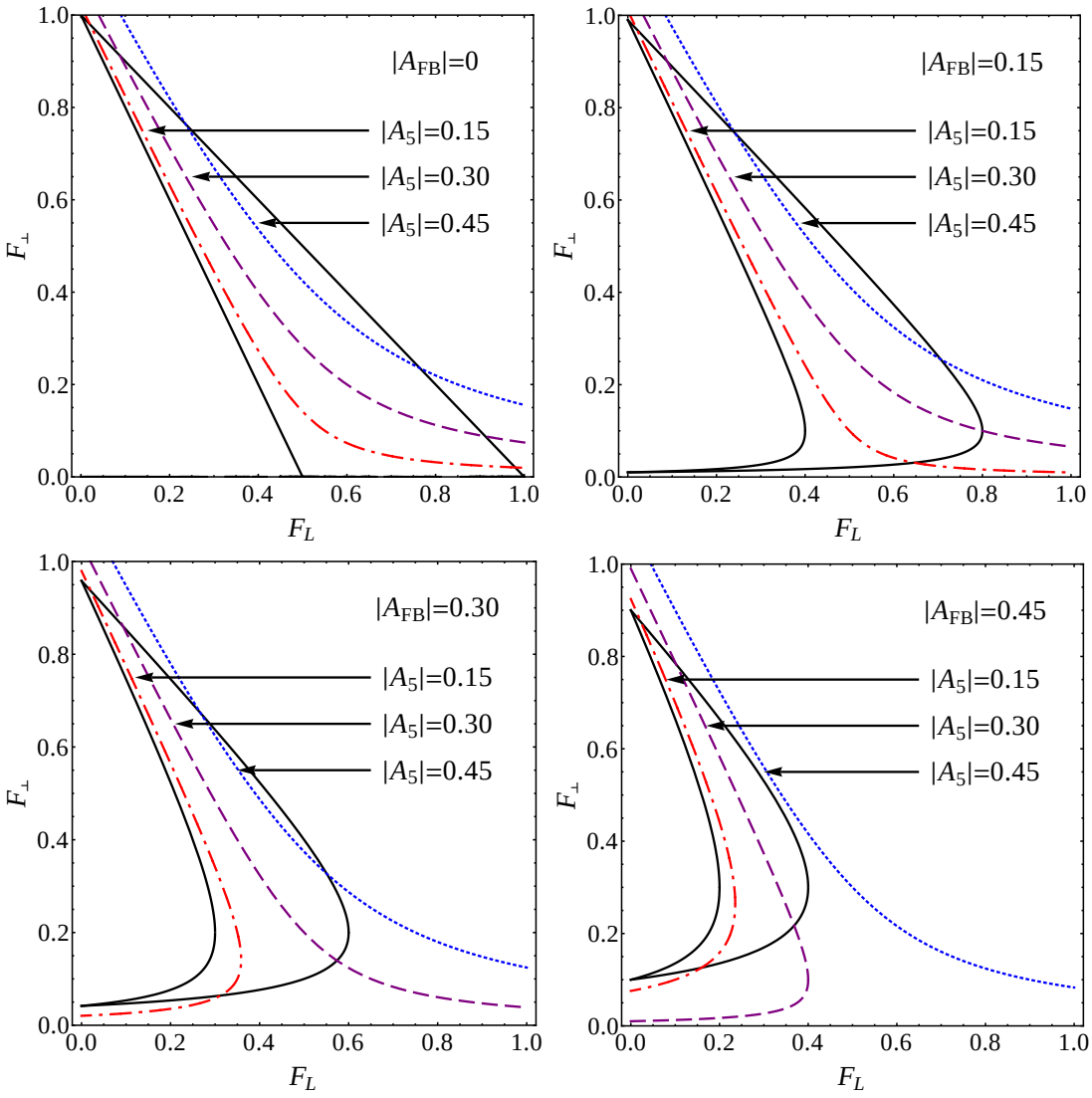

Figure 5.5: The requirement that Z_1, Z_2, Z_3 must be real, for any consistent set of independent observables $A_{\rm FB}$, F_L, $F_\perp$ and A_5 constrains the allowed F_L-$F_\perp$ parameter space to lie only within the solid black lines. A_4 is given by Eq. (4.116). Even within the allowed F_L-$F_\perp$ domain only the region on the right is allowed depending on the values of $A_{\rm FB}$ and A_5. In the four figures we have sampled values of $A_{\rm FB}$ and A_5 are as depicted. *There is no hadronic assumption made in obtaining the constraints depicted in these plots.*

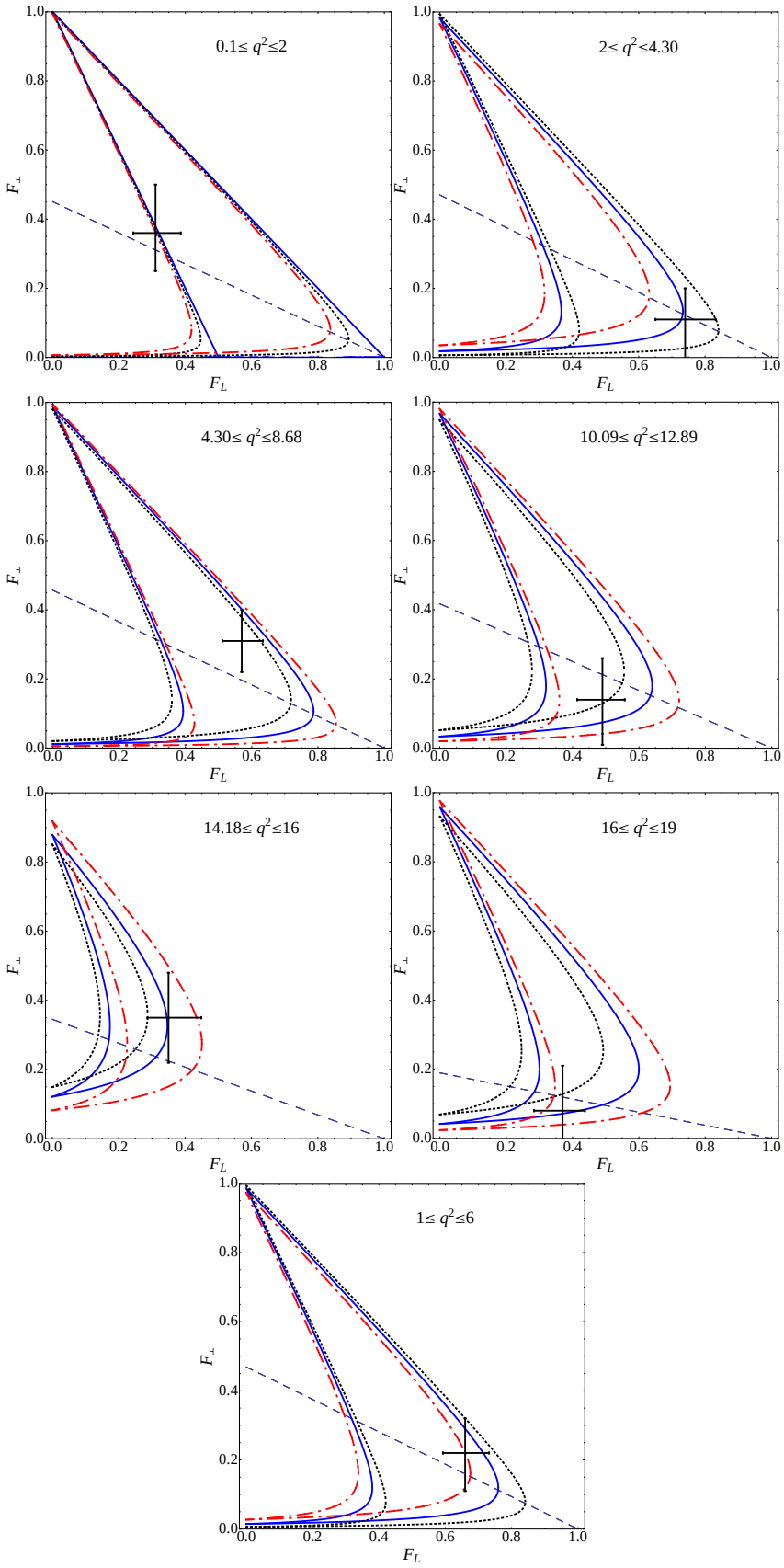

Figure 5.6: Same as in Fig. 5.5, but the values of $A_{\rm FB}$ are taken from Ref. [114]. The values of A_5 are assumed to be zero and the values of F_L and $F_\perp$ as measured in Ref. [114] is shown by black crosses.

Chapter 6

Summary and Conclusion.

In this thesis we have derived several important new results. After a brief introduction to the standard model in Chapter 1, we have discussed the theoretical framework in Chapter 2, followed by the differential decay distribution of $B \to K^* \ell^+ \ell^-$ in Chapter 3. In Chapter 3 we have introduced the observables Γ_f, F_L, $F_\perp$, $A_{\rm FB}$, A_4 and A_5 that can be extracted from angular analysis. While the partial decay rate Γ_f can be measured by angular integration, the other observables require a study of angular distributions. We showed how uni-angular distributions in the azimuthal angle ϕ can be used to measure the helicity fraction $F_\perp$. F_L and $A_{\rm FB}$ have already been measured by studying the uni-angular distribution in θ_ℓ. A_4 and A_5 can only be measured by a complete angular analysis involving θ_ℓ and ϕ requiring higher statistics. The main results of the thesis are derived and discussed in Chapter 4 and Chapter 5. In Chapter 4, after setting up our notation and defining the observables in terms of form factors, we expressed the amplitude in the most general form within the Standard Model as $\mathcal{A}_\lambda^{L,R} = C_{L,R}\mathcal{F}_\lambda - \widetilde{\mathcal{G}}_\lambda$, where $\lambda = \{0, \perp, \|\}$ is the helicity of the K^*, $C_{L,R} = C_9^{\rm eff} \mp C_{10}$ and L, R define the chirality of the ℓ^-. The form factors $\mathcal{F}_\lambda$ and $\widetilde{\mathcal{G}}_\lambda$ are expressed in terms of conventional $B \to K^*$ form factors $V, A_{1,2}$ and $T_{1,2,3}$. To be exact $\widetilde{\mathcal{G}}_\lambda \equiv C_7^{\rm eff}\mathcal{G}_\lambda + \cdots$ with the dots representing the higher order and "non-factorizable" contributions and only at leading order $\mathcal{G}_\lambda$'s are related to $T_{1,2,3}$. It may be noted that even at leading order $C_7^{\rm eff}$ and $\mathcal{G}_\lambda$ cannot be separated and $C_7^{\rm eff}$ can only be defined at leading order on assuming $\mathcal{G}_\lambda$. The six observables are thus defined in terms eight parameters, the six

form factors $\mathcal{F}_\lambda$, $\widetilde{\mathcal{G}}_\lambda$ and two Wilson Coefficients $C_{9,10}$. Hence only six theoretical parameters can be eliminated in terms of observables and a minimum of two reliable theoretical inputs are needed, to resolve between new physics and hadronic contributions. This is made possible by the significant advances in our understanding of form-factors that permit us to make truly these reliable inputs. One of our achievement are derivation of "clean relations" that permit the verifications of these hadronic inputs.

The $B \to K^*$ form factors are estimated using heavy quark effective theory and the treatment varies depending on the recoil energy of the K^*. At large recoil the ratio of the form factors $\mathsf{P}_1 = \mathcal{F}_\perp/\mathcal{F}_\parallel$ and $\mathsf{P}'_1 = \widetilde{\mathcal{G}}_\perp/\widetilde{\mathcal{G}}_\parallel$ are reliably evaluated at $\mathcal{O}(\Lambda_{\rm QCD}/m_b)$ to be free from universal wave functions and are unaltered by "non-factorizable" contributions and higher order corrections in α_s. In the large recoil limit we therefore choose P_1 and P'_1 as the two inputs in addition to observables. In the low recoil limit, the relation $\mathsf{P}_1 = \mathsf{P}'_1$ between the form factors serves as an additional input.

We summarize briefly a few significant new results derived in Chapter 4. The simple analytic derivation and solutions to the Wilson coefficients in terms of the observables and "clean" form factors were achieved by defining new variables $r_\lambda = \widetilde{\mathcal{G}}_\lambda/\mathcal{F}_\lambda - C_9$. These enable solutions to C_9 and C_{10} in terms of observables, P_1, P'_1 and the form factor $\mathcal{F}_\parallel$ to be

$$C_9 = \frac{\sqrt{\Gamma_f}}{\sqrt{2}\mathcal{F}_\parallel} \frac{(F_\parallel \mathsf{P}_1 \mathsf{P}'_1 - F_\perp) - \frac{1}{2}(\mathsf{P}_1 - \mathsf{P}'_1)Z_1}{\left[\pm (\mathsf{P}_1 - \mathsf{P}'_1) \sqrt{\mathsf{P}_1^2 F_\parallel + F_\perp + \mathsf{P}_1 Z_1} \right]}, \tag{6.1}$$

$$C_{10} = \frac{\sqrt{\Gamma_f}}{\sqrt{2}\mathcal{F}_\parallel} \frac{2}{3} \frac{A_{\rm FB}}{\left[\pm \sqrt{\mathsf{P}_1^2 F_\parallel + F_\perp + \mathsf{P}_1 Z_1} \right]}. \tag{6.2}$$

where Z_1 is expressed in terms of observables in Eq. (4.28). Two additional solutions for C_9 and C_{10} can be obtained in terms of different observables. These are obtained by the replacements

- $F_\parallel \to F_L$, $A_{\rm FB} \to \sqrt{2}A_5$, $\mathcal{F}_\parallel \to \mathcal{F}_0$, $\mathcal{G}_\parallel \to \mathcal{G}_0$, which also imply that $r_\parallel \to r_0$, $\mathsf{P}_1 \to \mathsf{P}_2$ and $\mathsf{P}'_1 \to \mathsf{P}'_2$.

- $F_\parallel \to F_L + F_\parallel + \sqrt{2}\pi A_4$, $A_{\rm FB} \to A_{\rm FB} + \sqrt{2}A_5$, $\mathcal{F}_\parallel \to \mathcal{F}_\parallel + \mathcal{F}_0$, $\mathcal{G}_\parallel \to \mathcal{G}_\parallel + \mathcal{G}_0$, which also imply $r_\parallel \to r_\wedge$, $\mathsf{P}_1 \to \mathsf{P}_3$ and $\mathsf{P}'_1 \to \mathsf{P}'_3$.

We found that the form factor ratios P_1, P_2 and P_3 can be directly measured in terms of the ratio of helicity fractions at q^2 corresponding to the zero crossings of asymmetries $A_{\rm FB}$, A_5 and $A_{\rm FB} + \sqrt{2}A_5$ respectively by the relations:

$$\mathsf{P}_1 = -\frac{\sqrt{F_\perp}}{\sqrt{F_\parallel}}\Big|_{A_{\rm FB}=0} \qquad \mathsf{P}_2 = -\frac{\sqrt{F_\perp}}{\sqrt{F_L}}\Big|_{A_5=0} \tag{6.3}$$

$$\mathsf{P}_3 = -\frac{\sqrt{F_\perp}}{\sqrt{F_L + F_\perp + \sqrt{2}\pi A_4}}\Big|_{A_{\rm FB}+\sqrt{2}A_5=0} \tag{6.4}$$

Since we have neglected the tiny CP violation in the standard model, we find that the observables must satisfy the following inequalities which are completely free from any hadronic uncertainties and hence clean. These relations are,

$$4F_\parallel F_\perp \geq \frac{16}{9}A_{\rm FB}^2 \tag{6.5}$$

$$4F_L F_\perp \geq \frac{16}{9}(\sqrt{2}A_5)^2\ . \tag{6.6}$$

$$4(1-F_\perp)F_\perp \geq \frac{16}{9}(A_{\rm FB}^2 + 2A_5^2), \tag{6.7}$$

$$4(F_L + F_\parallel + \sqrt{2}\pi A_4)F_\perp \geq \frac{16}{9}(A_{FB} + \sqrt{2}A_5)^2. \tag{6.8}$$

In Figs. 5.5 and 5.6 we have plotted the constraints on $F_L - F_\perp$ that depends only on observables. The condition $4F_\parallel F_\perp \geq 16/9A_{\rm FB}^2$ implies that if $|A_{\rm FB}|$ is large, F_L must be small so that $4F_\parallel F_\perp$ can be sufficiently large. Our approach is sensitive enough to already show tensions in the data [114].

The first set of solutions of Wilson coefficients C_{10} and C_9 (see Eqs.(4.65) and (4.62)) are not "clean". This set however leads some very important results including the constraints among the standard model observables. For example, the ratio C_9/C_{10} is obtained as a "clean expression". Assuming the theoretical estimate of C_9/C_{10} which is reliably evaluated at NNLL in standard model we have "cleanly" predicted $F_\perp$ in Eq. (4.74). Requiring that the observable $F_\perp$ is real

we showed that the valid domain of $A_{\rm FB}$ is constrained in terms of F_L as follows:

$$\frac{-3(1-F_L)}{4}T_- \leq A_{FB} \leq \frac{3(1-F_L)}{4}T_+, \tag{6.9}$$

where $T_\pm$ is given in terms of P_1, P_1' and R in Eq. (4.78). The above equation constrains the values of F_L and $A_{\rm FB}$ within a triangular region shown in Figs. 5.1, 5.2 and 5.3. The existence of such a triangular bound is already hinted in Ref. [126]. In Eq. (4.80) we have expressed the forward backward asymmetry $A_{\rm FB}$ in terms of the two helicity fractions F_L and $F_\perp$. Since the $A_{\rm FB}$ has to be real there exist a constraint between the two helicity fractions F_L and $F_\perp$ which we have derived in Eq. (4.81)). It is interesting to note *that F_L and $F_\perp$ are constrained in the Standard Model to lie in a very narrow region, well approximated by a line* as shown in Fig. 4.2 and 4.4.

The C_9/C_{10} and $C_7^{\rm eff}/C_{10}$ ratios in Eqs. (4.73) ratio in (4.88) were combined to obtain

$$\Big(\frac{2}{3}\frac{C_9}{C_{10}}\mathsf{P}_1'' - \frac{4}{3}\frac{C_7^{\rm eff}}{C_{10}}\mathsf{P}_1\Big)A_{\rm FB} = (\mathsf{P}_1{}^2 F_\parallel + F_\perp + \mathsf{P}_1 Z) > 0. \tag{6.10}$$

If the $A_{\rm FB}$ zero crossing is confirmed [114] with $A_{\rm FB} > 0$ at small q^2, then based on the signs of the from factors it is unambiguously concluded that the signs of C_7/C_{10} and C_9/C_{10} are in agreement with the Standard Model, i.e. $C_7^{\rm eff}/C_{10} > 0$ and $C_9/C_{10} > 0$ as long as other constraints like $Z_1^2 > 0$ hold. In Ref. [114] the zero crossing is indeed seen. However, in the $2{\rm GeV}^2 \leq q^2 \leq 4.3{\rm GeV}^2$ bin $Z_1^2 > 0$ is only marginally satisfied. These conclusions are exact and not altered by any hadronic uncertainties.

We have obtained three sets of C_9/C_{10} and $C_7^{\rm eff}/C_{10}$ solutions involving difference observables and form factor ratios. Since, the form factor ratios P_1 and P_1' are the ones that are most reliably estimated in both large recoil and low recoil limits, we obtain relations for P_2, P_2' and P_3, P_3' in terms of P_1, P_1' and observables. Equating the relations obtained for C_9/C_{10} and $C_7^{\rm eff}/C_{10}$ in Eqs. (4.73), (4.88) with those in Eqs. (4.76), (4.97) and Eqs. (4.77), (4.98) we get:

$$\mathsf{P}_2 \;=\; \frac{2\mathsf{P}_1 A_{\rm FB} F_\perp}{\sqrt{2}A_5(2F_\perp + Z_1\mathsf{P}_1) - Z_2\mathsf{P}_1 A_{\rm FB}}$$

$$
\begin{aligned}
\mathsf{P}_2' &= \frac{\sqrt{2}A_5\Big(F_\perp - F_\parallel \mathsf{P}_1^2\Big)\mathsf{P}_2^2\mathsf{P}_1'}{A_{\rm FB}T_2(\mathsf{P}_1 - \mathsf{P}_1') + \sqrt{2}A_5\Big(F_\perp - F_\parallel \mathsf{P}_1^2\Big)\mathsf{P}_2\mathsf{P}_1'} \\
\mathsf{P}_3 &= \frac{2\mathsf{P}_1 A_{\rm FB}F_\perp}{(A_{\rm FB} + \sqrt{2}A_5)(2F_\perp + Z_1\mathsf{P}_1) - Z_3\mathsf{P}_1 A_{\rm FB}}, \\
\mathsf{P}_3' &= \frac{(A_{\rm FB} + \sqrt{2}A_5)(F_\perp - F_\parallel \mathsf{P}_1^2)\mathsf{P}_3^2\mathsf{P}_1'}{A_{\rm FB}T_3(\mathsf{P}_1 - \mathsf{P}_1') + \sqrt{2}A_5(F_\perp - F_\parallel \mathsf{P}_1^2)\mathsf{P}_3^2\mathsf{P}_1'},
\end{aligned}
$$

where $T_2 = \mathsf{P}_1(F_\perp - F_L\mathsf{P}_2^2)$ and $T_3 = \mathsf{P}_1[F_\perp(1+\mathsf{P}_3^2) - \mathsf{P}_3^2(1+\sqrt{2}\pi A_4)]$. Even though P_2, P_2' and P_3, P_3' inherently depend on $\xi_\parallel$ and $\xi_\perp$ we have expressed them in terms of "clean relations" above. *Hence, in our approach, all the expressions for observables are "clean," with only the Wilson coefficients C_7^{eff}, C_9 and C_{10} being expressed in terms of only one form factor $\mathcal{G}_\parallel$ or $\mathcal{F}_\parallel$.*

We have derived significant constraints between observables that can be used to test for new physics. The constraint purely in terms of observables arises since P_2 and P_3 are expressed in terms of observables and P_1 while P_3 itself is related in Eq. (4.52) to P_1 and P_2. We obtain the interesting constraint (4.116) among observables:

$$
A_4 = \frac{8A_5A_{\rm FB}}{9\pi F_\perp} + \sqrt{2}\,\frac{\sqrt{F_LF_\perp - \frac{8}{9}A_5^2}\,\sqrt{F_\parallel F_\perp - \frac{4}{9}A_{\rm FB}^2}}{\pi F_\perp}. \tag{6.11}
$$

In Fig. 4.5 we plotted A_4 as function of F_L and $A_{\rm FB}$ where the values of A_5 has been assumed.

We have paid special attention to the low recoil limit and derive two new relations

$$
\sqrt{2}A_5 = A_{\rm FB}\frac{\sqrt{F_L}}{\sqrt{F_\parallel}} \tag{6.12}
$$

$$
A_4 = \frac{\sqrt{2}}{\pi}\sqrt{F_LF_\parallel} \tag{6.13}
$$

in terms of observables alone. These two relations allow us to test not only the validity of the low recoil approximation but also the presence of New Physics. The value of A_5 predicted by these relations tests the validity of the low recoil approximation, whereas the value of A_4 verifies the validity of SM. If both relations hold we verify that the low recoil approximation is correct and that no new physics can exist. If both relation fail we can conclude that the low

recoil approximation fails but *one can never-the-less still test for new physics* by Eq. (4.116), which is valid in general. If A_5 is accurately predicted but A_4 does not have the value given by these two relations one can conclude that there is new physics and that the low recoil limit is accurate.

In this thesis we re-examined the new physics discovery potential of the mode $B \to K^* \ell^+ \ell^-$. This mode has an advantage as a multitude of observables can be measured via angular analysis. We showed how the multitude of related observables obtained from $B \to K^* \ell^+ \ell^-$ can provide many new clean tests of the Standard Model and discriminate new physics contributions from hadronic effects. The hallmark of these tests is that most of them are independent of the unknown form factors $\xi_\parallel$ and $\xi_\perp$ in heavy quark effective theory. In the large recoil limit (at $O(\Lambda_{\rm QCD}/m_b)$) these relations are valid to all orders in α_s. We derive a relation between observables that is free of form factors and Wilson coefficients, the violation of which will be an unambiguous signal of New Physics. We also obtained for the first time relations between observables and form factors that are independent of Wilson coefficients and enable verification of hadronic estimates. We show how form factor ratios can be measured directly from helicity fractions without any assumptions what so ever. We find that the allowed parameter space for observables is very tightly constrained in Standard Model, thereby providing clean signals of New Physics. We examine in detail both the large-recoil and low-recoil regions of the K^* meson and probe special features valid in these two limits. Another new relation involving only observables that would verify the validity of the relations between form-factors assumed in the low-recoil region was also derived. The several relations and constraints derived will provide unambiguous signals of New Physics if it contributes to these decays. *We emphasize that in our approach, C_9/C_{10} and all the expressions independent of Wilson coefficients are "clean" in the large recoil limit and in the low recoil limit they are reliably calculated as they do not depend on the universal form factors $\xi_\parallel$ and $\xi_\perp$.*

Bibliography

[1] S. L. Glashow, Nucl. Phys. **22**, 579 (1961).

[2] S. Weinberg, Phys. Rev. Lett. **19**, 1264 (1967).

[3] A. Salam, in *Elementary Particle Theory*, ed. N. Svartholm (Almquist and Wiksells, Stockholm, 1969), p. 367.

[4] S. L. Glashow, J. Iliopoulos and L. Maiani, Phys. Rev. D **2**, 1285 (1970).

[5] T. D. Lee and C. -N. Yang, Phys. Rev. **104**, 254 (1956).

[6] C. S. Wu, E. Ambler, R. W. Hayward, D. D. Hoppes and R. P. Hudson, Phys. Rev. **105**, 1413 (1957).

[7] R. L. Garwin, L. M. Lederman and M. Weinrich, Phys. Rev. **105**, 1415 (1957).

[8] J. I. Friedman and V. L. Telegdi, Phys. Rev. **106**, 1290 (1957).

[9] F. Englert and R. Brout, Phys. Rev. Lett. **13**, 321 (1964).

[10] P. W. Higgs, Phys. Rev. Lett. **13**, 508 (1964).

[11] P. W. Higgs, Phys. Lett. **12**, 132 (1964).

[12] G. S. Guralnik, C. R. Hagen and T. W. B. Kibble, Phys. Rev. Lett. **13**, 585 (1964).

[13] N. Cabibbo, Phys. Rev. Lett. **10**, 531 (1963).

[14] M. Kobayashi and T. Maskawa, Prog. Theor. Phys. **49**, 652 (1973).

[15] C. Dib, I. Dunietz, F. J. Gilman and Y. Nir, Phys. Rev. D **41**, 1522 (1990).

[16] L. -L. Chau and W. -Y. Keung, Phys. Rev. Lett. **53**, 1802 (1984).

[17] L. Wolfenstein, Phys. Rev. Lett. **51**, 1945 (1983).

[18] A. J. Buras, M. E. Lautenbacher and G. Ostermaier, Phys. Rev. D **50**, 3433 (1994) [hep-ph/9403384].

[19] J. Charles *et al.* [CKMfitter Group Collaboration], Eur. Phys. J. C **41**, 1 (2005) [hep-ph/0406184].

[20] S. Weinberg, Phys. Rev. D **13**, 974 (1976).

[21] L. Susskind, Phys. Rev. D **20**, 2619 (1979).

[22] K. G. Wilson, Phys. Rev. D **3**, 1818 (1971).

[23] Gerard ’t Hooft,NATO Adv. Study Inst. Ser. B Phys. **volume 59**, 135 (1980)

[24] V. M. Abazov *et al.* [D0 Collaboration], Phys. Rev. D **84**, 052007 (2011) [arXiv:1106.6308 [hep-ex]].

[25] A. Lenz and U. Nierste, JHEP **0706**, 072 (2007) [hep-ph/0612167].

[26] V. M. Abazov *et al.* [D0 Collaboration], arXiv:1207.1769 [hep-ex].

[27] The LHCb collaboration, LHCb-CONF-2012-022

[28] B. Aubert *et al.* [BABAR Collaboration], Phys. Rev. Lett. **98**, 211802 (2007) [hep-ex/0703020 [HEP-EX]].

[29] M. Staric *et al.* [Belle Collaboration], Phys. Rev. Lett. **98**, 211803 (2007) [hep-ex/0703036].

[30] Y. Amhis *et al.* [Heavy Flavor Averaging Group Collaboration], arXiv:1207.1158 [hep-ex].

[31] A. Abashian *et al.* [BELLE Collaboration], Phys. Rev. Lett. **86**, 2509 (2001) [hep-ex/0102018].

[32] K. Abe *et al.* [Belle Collaboration], Phys. Rev. Lett. **87**, 091802 (2001) [hep-ex/0107061].

[33] K. Abe *et al.* [Belle Collaboration], Phys. Rev. D **66**, 032007 (2002) [hep-ex/0202027].

[34] K. Abe *et al.* [Belle Collaboration], Phys. Rev. D **66**, 071102 (2002) [hep-ex/0208025].

[35] B. Aubert *et al.* [BABAR Collaboration], Phys. Rev. Lett. **86**, 2515 (2001) [hep-ex/0102030].

[36] B. Aubert *et al.* [BABAR Collaboration], Phys. Rev. D **66**, 032003 (2002) [hep-ex/0201020].

[37] B. Aubert *et al.* [BABAR Collaboration], Phys. Rev. Lett. **87**, 091801 (2001) [hep-ex/0107013].

[38] B. Aubert *et al.* [BABAR Collaboration], Phys. Rev. Lett. **89**, 201802 (2002) [hep-ex/0207042].

[39] RAaij *et al.* [LHCb Collaboration], JHEP **1207**, 133 (2012) [arXiv:1205.3422 [hep-ex]].

[40] T. Feldmann and J. Matias, JHEP **0301**, 074 (2003) [hep-ph/0212158].

[41] I. Adachi *et al.* [Belle Collaboration], Phys. Rev. Lett. **110**, 131801 (2013) [arXiv:1208.4678 [hep-ex]].

[42] **LHCb** Collaboration, "Measurement of the flavour-specific CP violating asymmetry a^s_{sl} in B_s decays," LHCb-CONF-2012-022.

[43] **CDF** Collaboration, "Search for $B_s \to \mu^+\mu^-$ and $B_d \to \mu^+\mu^-$ Decays with CDF II," Phys. Rev. Lett. **107**, 239903 (2011) [Phys. Rev. Lett. **107**, 191801 (2011)] [arXiv:1107.2304 [hep-ex]].

[44] **CMS** Collaboration, S. Chatrchyan *et al.*, "Search for $B_s^0 \to \mu^+\mu^-$ and $B^0 \to \mu^+\mu^-$ decays," JHEP **1204**, 033 (2012) [arXiv:1203.3976 [hep-ex]].

[45] **ATLAS** Collaboration, G. Aad *et al.*, "Search for the decay $B_s^0 \to \mu^+\mu^-$ with the ATLAS detector," Phys. Lett. B **713**, 387 (2012) [arXiv:1204.0735 [hep-ex]].

[46] **LHCb** Collaboration, "First evidence for the decay Bs -> mu+ mu-," Phys. Rev. Lett. **110**, 021801 (2013) [arXiv:1211.2674 [Unknown]].

[47] A. J. Buras, J. Girrbach, D. Guadagnoli and G. Isidori, "On the Standard Model prediction for BR(Bs,d to mu+ mu-)," Eur. Phys. J. C **72**, 2172 (2012) [arXiv:1208.0934 [hep-ph]].

[48] C. Hamzaoui, M. Pospelov and M. Toharia, Phys. Rev. D **59**, 095005 (1999) [hep-ph/9807350].

[49] S. R. Choudhury and N. Gaur, Phys. Lett. B **451**, 86 (1999) [hep-ph/9810307].

[50] K. S. Babu and C. F. Kolda, Phys. Rev. Lett. **84**, 228 (2000) [hep-ph/9909476].

[51] J. P. Lees *et al.* [BaBar Collaboration], Phys. Rev. Lett. **109**, 101802 (2012) [arXiv:1205.5442 [hep-ex]].

[52] S. Fajfer, J. F. Kamenik and I. Nisandzic, Phys. Rev. D **85**, 094025 (2012) [arXiv:1203.2654 [hep-ph]].

[53] K. G. Wilson, Phys. Rev. **179**, 1499 (1969);

[54] K. G. Wilson and W. Zimmermann, Commun. Math. Phys. **24**, 87 (1972);

[55] W. Zimmermann, Annals Phys. **77**, 570 (1973) [Lect. Notes Phys. **558**, 278 (2000)].

[56] H. Georgi, Phys. Lett. B **240**, 447 (1990).

[57] A. F. Falk, H. Georgi, B. Grinstein and M. B. Wise, Nucl. Phys. B **343**, 1 (1990).

[58] N. Isgur and M. B. Wise, Phys. Lett. B **232**, 113 (1989).

[59] N. Isgur and M. B. Wise, Phys. Lett. B **237**, 527 (1990).

[60] A. J. Buras and M. Munz, Phys. Rev. D **52**, 186 (1995) [hep-ph/9501281].

[61] M. Misiak, Nucl. Phys. B **393**, 23 (1993) [Erratum-ibid. B **439**, 461 (1995)].

[62] G. Buchalla, A. J. Buras and M. E. Lautenbacher, Rev. Mod. Phys. **68**, 1125 (1996) [hep-ph/9512380].

[63] C. Bobeth, M. Misiak and J. Urban, Nucl. Phys. B **574**, 291 (2000) [hep-ph/9910220].

[64] K. Adel and Y. -P. Yao, Phys. Rev. D **49**, 4945 (1994) [hep-ph/9308349].

[65] C. Greub and T. Hurth, Phys. Rev. D **56**, 2934 (1997) [hep-ph/9703349].

[66] A. J. Buras, A. Kwiatkowski and N. Pott, Nucl. Phys. B **517**, 353 (1998) [hep-ph/9710336].

[67] M. Ciuchini, G. Degrassi, P. Gambino and G. F. Giudice, Nucl. Phys. B **527**, 21 (1998) [hep-ph/9710335].

[68] P. Gambino, M. Gorbahn and U. Haisch, Nucl. Phys. B **673**, 238 (2003) [hep-ph/0306079].

[69] M. Gorbahn and U. Haisch, Nucl. Phys. B **713**, 291 (2005) [hep-ph/0411071].

[70] M. Gorbahn, U. Haisch and M. Misiak, Phys. Rev. Lett. **95**, 102004 (2005) [hep-ph/0504194].

[71] W. Altmannshofer, P. Ball, A. Bharucha *et al.*, JHEP **0901**, 019 (2009). [arXiv:0811.1214 [hep-ph]].

[72] A. J. Buras, M. Misiak, M. Munz and S. Pokorski, Nucl. Phys. B **424**, 374 (1994) [hep-ph/9311345].

[73] M. Beneke, T. Feldmann, D. Seidel, Nucl. Phys. **B612**, 25-58 (2001). [hep-ph/0106067].

[74] F. Kruger, L. M. Sehgal, N. Sinha, R. Sinha, Phys. Rev. **D61**, 114028 (2000). [hep-ph/9907386].

[75] N. G. Deshpande and J. Trampetic, Phys. Rev. Lett. **60**, 2583 (1988).

[76] P. Ball and V. M. Braun, Phys. Rev. D **58** (1998) 094016 [arXiv:hep-ph/9805422].

[77] P. Ball and R. Zwicky, Phys. Rev. D **71** (2005) 014029 [arXiv:hep-ph/0412079].

[78] V. L. Chernyak and A. R. Zhitnitsky, JETP Lett. **25** (1977) 510 [Pisma Zh. Eksp. Teor. Fiz. **25** (1977) 544];

[79] V. L. Chernyak and A. R. Zhitnitsky, Sov. J. Nucl. Phys. **31** (1980) 544 [Yad. Fiz. **31** (1980) 1053];

[80] A.V. Efremov and A.V. Radyushkin, Phys. Lett. B **94** (1980) 245; Theor. Math. Phys. **42** (1980) 97 [Teor. Mat. Fiz. **42** (1980) 147];

[81] G.P. Lepage and S.J. Brodsky, Phys. Lett. B **87** (1979) 359; Phys. Rev. D **22** (1980) 2157;

[82] V.L. Chernyak, A.R. Zhitnitsky and V.G. Serbo, JETP Lett. **26** (1977) 594 [Pisma Zh. Eksp. Teor. Fiz. **26** (1977) 760];

[83] V.L. Chernyak, A.R. Zhitnitsky and V.G. Serbo, Sov. J. Nucl. Phys. **31** (1980) 552 [Yad. Fiz. **31** (1980) 1069].

[84] P. Colangelo and A. Khodjamirian, hep-ph/0010175;

[85] A. Khodjamirian, AIP Conf. Proc. **602** (2001) 194 [arXiv:hep-ph/0108205].

[86] A. Ali, P. Ball, L. T. Handoko *et al.*, Phys. Rev. **D61**, 074024 (2000). [hep-ph/9910221].

[87] C. Bobeth, G. Hiller and G. Piranishvili, JHEP **0807**, 106 (2008) [arXiv:0805.2525 [hep-ph]].

[88] U. Egede, T. Hurth, J. Matias, M. Ramon and W. Reece, JHEP **0811**, 032 (2008) [arXiv:0807.2589 [hep-ph]];

[89] M. Beneke, G. Buchalla, M. Neubert and C. T. Sachrajda, Phys. Rev. Lett. **83**, 1914 (1999) [hep-ph/9905312].

[90] M. Beneke, G. Buchalla, M. Neubert and C. T. Sachrajda, Nucl. Phys. B **591**, 313 (2000) [hep-ph/0006124].

[91] M. Beneke, T. .Feldmann and D. Seidel, Eur. Phys. J. C **41**, 173 (2005) [hep-ph/0412400].

[92] C. W. Bauer, S. Fleming and M. E. Luke, Phys. Rev. D **63**, 014006 (2000) [hep-ph/0005275].

[93] C. W. Bauer, S. Fleming, D. Pirjol and I. W. Stewart, Phys. Rev. D **63**, 114020 (2001) [hep-ph/0011336].

[94] C. W. Bauer and I. W. Stewart, Phys. Lett. B **516**, 134 (2001) [hep-ph/0107001].

[95] M. Beneke, A. P. Chapovsky, M. Diehl and T. Feldmann, Nucl. Phys. B **643**, 431 (2002) [hep-ph/0206152].

[96] R. J. Hill and M. Neubert, Nucl. Phys. B **657**, 229 (2003) [hep-ph/0211018].

[97] A. Ali, G. Kramer and G. H. Zhu, Eur. Phys. J. C **47** (2006) 625 [arXiv:hep-ph/0601034].

[98] B. Grinstein and D. Pirjol, Phys. Rev. D **70**, 114005 (2004) [hep-ph/0404250].

[99] M. A. Shifman and M. B. Voloshin, Sov. J. Nucl. Phys. **45**, 292 (1987) [Yad. Fiz. **45**, 463 (1987)].

[100] J. Charles, A. Le Yaouanc, L. Oliver, O. Pene and J. C. Raynal, Phys. Rev. D **60**, 014001 (1999) [hep-ph/9812358].

[101] M. Beneke and T. Feldmann, Nucl. Phys. B **592** (2001) 3 [arXiv:hep-ph/0008255].

[102] G. Burdman and G. Hiller, Phys. Rev. D **63**, 113008 (2001) [hep-ph/0011266].

[103] F. Kruger and J. Matias, Phys. Rev. D **71**, 094009 (2005) [arXiv:hep-ph/0502060].

[104] C. Bobeth, G. Hiller and D. van Dyk, JHEP **1007**, 098 (2010) [arXiv:1006.5013 [hep-ph]].

[105] P. Ball and R. Zwicky, Phys. Rev. D **71**, 014015 (2005) [hep-ph/0406232].

[106] P. Ball and R. Zwicky, Phys. Rev. D **71**, 014029 (2005) [hep-ph/0412079].

[107] J. T. Wei *et al.* [BELLE Collaboration], Phys. Rev. Lett. **103**, 171801 (2009) [arXiv:0904.0770 [hep-ex]].

[108] B. Aubert *et al.* [BABAR Collaboration], Phys. Rev. D **73**, 092001 (2006) [hep-ex/0604007].

[109] B. Aubert *et al.* [BABAR Collaboration], Phys. Rev. D **79**, 031102 (2009) [arXiv:0804.4412 [hep-ex]].

[110] CDF Public Note 10047

[111] T. Aaltonen *et al.* [CDF Collaboration], Phys. Rev. Lett. **107**, 201802 (2011) [arXiv:1107.3753 [hep-ex]].

[112] T. Aaltonen *et al.* [CDF Collaboration], Phys. Rev. Lett. **108**, 081807 (2012) [arXiv:1108.0695 [hep-ex]].

[113] R. Aaij, C. Abellan Beteta, B. Adeva, M. Adinolfi, C. Adrover, A. Affolder, Z. Ajaltouni and J. Albrecht *et al.*, arXiv:1112.3515 [hep-ex].

[114] Rare beauty and charm decays at LHCb, by Chris Parkinson, 47th Rencontres de Moriond on QCD and High Energy Interactions, La Thuile, Italy, 10 - 17 Mar 2012. Report No LHCb-TALK-2012-040.

[115] R. Sinha, [hep-ph/9608314].

[116] G. Hiller and F. Kruger, Phys. Rev. D **69**, 074020 (2004) [hep-ph/0310219].

[117] C. S. Kim, Y. G. Kim, C. -D. Lu and T. Morozumi, Phys. Rev. D **62**, 034013 (2000) [hep-ph/0001151].

[118] A. Faessler, T. Gutsche, M. A. Ivanov, J. G. Korner and V. E. Lyubovitskij, Eur. Phys. J. direct C **4**, 18 (2002) [hep-ph/0205287].

[119] U. Egede, T. Hurth, J. Matias, M. Ramon and W. Reece, JHEP **1010**, 056 (2010) [arXiv:1005.0571 [hep-ph]].

[120] D. Becirevic and E. Schneider, Nucl. Phys. B **854**, 321 (2012) [arXiv:1106.3283 [hep-ph]].

[121] D. Das and R. Sinha, arXiv:1202.5105 [hep-ph].

[122] D. Das and R. Sinha, Phys. Rev. D **86**, 056006 (2012) [arXiv:1205.1438 [hep-ph]].

[123] A. Y. .Korchin and V. A. Kovalchuk, Phys. Rev. D **82**, 034013 (2010) [arXiv:1004.3647 [hep-ph]].

[124] A. Y. .Korchin and V. A. Kovalchuk, arXiv:1111.4093 [hep-ph].

[125] A. Y. .Korchin and V. A. Kovalchuk, Eur. Phys. J. C **72**, 2155 (2012) [arXiv:1205.3683 [hep-ph]].

[126] The LHCb collaboration, LHCb-CONF-2011-038